

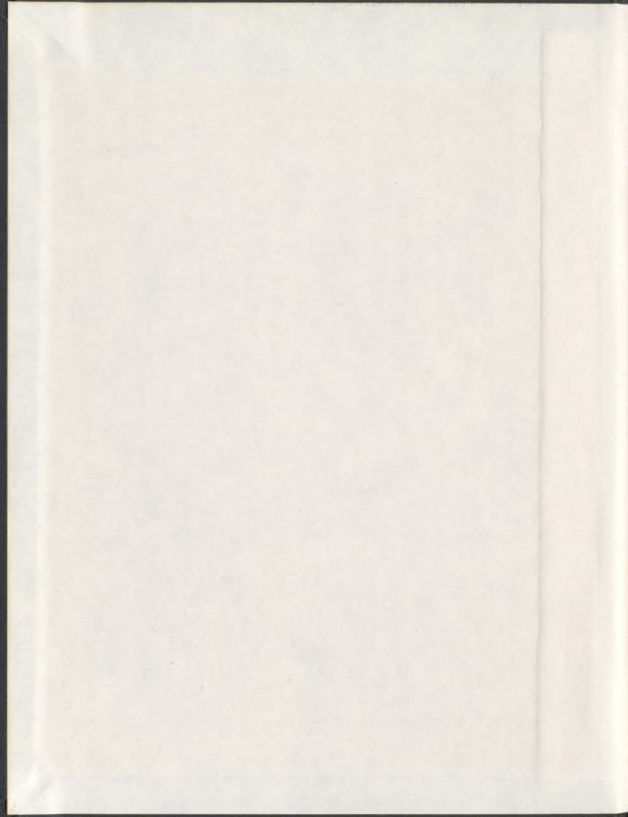
COMPLEXATION STUDIES OF CALIXNAPHTHALENES
AND HEXAHOMOTRIOXACALIXNAPHTHALENES
WITH [60] FULLERENE

CENTRE FOR NEWFOUNDLAND STUDIES

**TOTAL OF 10 PAGES ONLY
MAY BE XEROXED**

(Without Author's Permission)

SHEHADEH A. MIZYED



001311



INFORMATION TO USERS

This manuscript has been reproduced from the microfilm master. UMI films the text directly from the original or copy submitted. Thus, some thesis and dissertation copies are in typewriter face, while others may be from any type of computer printer.

The quality of this reproduction is dependent upon the quality of the copy submitted. Broken or indistinct print, colored or poor quality illustrations and photographs, print bleedthrough, substandard margins, and improper alignment can adversely affect reproduction.

In the unlikely event that the author did not send UMI a complete manuscript and there are missing pages, these will be noted. Also, if unauthorized copyright material had to be removed, a note will indicate the deletion.

Oversize materials (e.g., maps, drawings, charts) are reproduced by sectioning the original, beginning at the upper left-hand corner and continuing from left to right in equal sections with small overlaps.

ProQuest Information and Learning
300 North Zeeb Road, Ann Arbor, MI 48106-1346 USA
800-521-0600

UMI[®]

**Complexation Studies of Calixnaphthalenes and
Hexahomotrioxacalixnaphthalenes with [60]Fullerene**

by

Shehadeh A. Mizyed
(B.Sc., M.Sc.) Yarmouk University
Irbid-Jordan

A thesis submitted to the School of Graduate Studies in partial fulfilment of the
requirements for the degree of Doctor of Philosophy

Department of Chemistry
Memorial University of Newfoundland
St John's, Newfoundland, Canada
November, 2001

Acknowledgments

I would like to express my deep appreciation to Dr. Paris Georghiou for his guidance, encouragement and friendly advice during the course of this research and during the writing of this thesis.

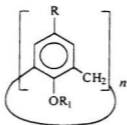
My appreciation is also extended to my supervising committee; Dr. G. Bodwell and Dr. B. Gregory for their helpful discussions which were essential for the success of this work. I am also grateful to Mr. D. Miller for NMR spectra and X-ray structures, to Dr. B. Gregory and M. Baggs for mass spectra and Dr. P. Tremaine for using his laboratory to carry out the volumetric measurements. My thanks are also extended to my friend Dr. M. Ashram for his collaboration during the synthesis of oxacalixnaphthalenes.

My special thanks and appreciation are also extended to my parents, wife, children and sisters for their patience and encouragement. Thanks are also extended to the organic group (present and former members) for the valuable meetings and discussions. Also my thanks to the Staff in the Chemistry Department for their help and friendship. Financial support from N.S.E.R.C., The Chemistry Department and The School of Graduate Studies is also acknowledged.

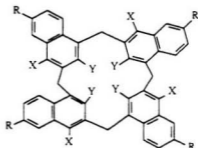
Abstract

Calixarenes **1-3** are cyclic oligomers of *p*-substituted phenols and formaldehyde which have been used as hosts in supramolecular chemistry. A related group of molecules are the naphthalene ring-based calixnaphthalenes *e.g.* (**8** and **9**) and hexahomotrioxacalix[3]arene *e.g.* **19**

This thesis describes the ability of calixnaphthalenes to form complexes with C_{60} in



- 1 $n = 4$, R = *tert*-butyl, $R_1 = H$
- 2 $n = 6$, R = *tert*-butyl, $R_1 = H$
- 3 $n = 8$, R = *tert*-butyl, $R_1 = H$



- 8 R = X = H, Y = OH
- 9 R = *tert*-butyl, X = H, Y = OH

different solvents using different methods. It also describes the first synthesis of hexahomotrioxacalix[3]naphthalenes and their complexation properties

Calix[4]naphthalenes **8** and **9** have deeper cavities than those of the analogous calix[4]arenes and our physicochemical data confirm they do form complexes with C_{60} . Results obtained for the complexation of C_{60} with the C_2 -symmetrical *endo*-calix[4]naphthalene **8** and its *tert*-butyl-substituted derivative **9** using uv-vis spectrophotometry show that they form relatively stable supramolecular 1:1 complexes with

C_{60} in toluene, benzene and CS_2 solution. Thermodynamic parameters have also been determined for the complexation of **8** and **9** with C_{60} and show that both a solvophobic effect and π - π interactions are major driving forces for the complexation process.

The symmetrical hexahomotrioxacalix[3]naphthalene **26** and its *tert*-butyl-substituted derivative **26a** were synthesized via either the cyclization of the linear precursors **48** or **48a** respectively, or by the direct cyclization of the monomers **46** or **46a** respectively. The unsymmetrical hexahomotrioxacalix[3]naphthalene **27** was also obtained from the cyclization of the linear precursor **48**. Complexation studies showed that the ability of **26** and **26a** to bind alkali metal cations was not significant. However, as shown by 1H NMR studies they do form stable 1:1 complexes with C_{60} in solution. A crystalline 2:1 complex of **26a** with C_{60} was isolated and its X-ray structure was successfully determined.

Using densitometry, partial molar volume changes were determined for the complexation of **8**, **9**, **26**, or **26a** with C_{60} in toluene, benzene or CS_2 solution. The results are consistent with a solvophobic effect, and some other additional factors which are discussed.

Ester derivatives of hexahomotrioxacalix[3]naphthalenes in both the "cone" **49** (or **50**) and the "partial-cone" **49a** (or **50a**) conformations were synthesized and the X-ray crystal structure of **49a** was determined. The ability of these esters to bind with alkali metal cations using standard extraction experiments is described.

Table of Contents

	page
Acknowledgments	ii
Abstract	iii
Table of Contents	v
List of Figures	viii
List of Schemes	xvi
List of Tables	xvii
List of Symbols and Abbreviations	xix
Dedication	xxii
Chapter 1. Introduction	
1.1. Calix[n]arenes.....	1
1.2. Calixarene Derivatives.....	3
1.3. Calixnaphthalenes.....	4
1.4. Supramolecular Chemistry.....	10
1.5. [60]Fullerene, C ₆₀	13
1.6. Complexes of Calix[n]arenes with C ₆₀	17
1.7. Conclusion.....	25

Chapter 2. Complexation Study of Calix[4]naphthalenes with C₆₀	
2.1. Introduction.....	27
2.2. Calix[4]naphthalene Complexes with C ₆₀	29
2.3. Thermodynamic Study of the Complexes of calix[4]naphthalenes with C ₆₀	49
2.4. Experimental.....	59
Chapter 3. Synthesis of Hexahomotrioxacalix[3]naphthalenes and Their Binding Properties	
3.1. Introduction	62
3.2. Synthesis Strategy.....	67
3.3. Binding of 26 and 26a with metal ions	75
3.4. Complexes of hexahomotrioxacalix[3]naphthalenes with C ₆₀	76
3.5. Experimental.....	90
Chapter 4. Volumetric Study of the Complexation of Calix[4]naphthalenes with C₆₀	
4.1. Introduction.....	107
4.2. Volumetric Study of 8 and 9 with C ₆₀	110
4.3. Volumetric Study of hexahomotrioxacalix[3]naphthalenes	

	26 and 26a with C₆₀	126
4.4.	Experimental.....	141
4.5.	Vibrating Tube Densimeter.....	142
Chapter 5.	Ester Derivatives of Hexahomotrioxacalix[3]naphthalenes and Their Binding Properties	
5.1.	Introduction.....	145
5.2.	Ester Derivatives of Calixnaphthalenes.....	146
5.3.	Binding properties of 49 and 59 with metal ions.....	152
5.4.	Experimental.....	156
References		160
Appendix A.	Absorbance Data for 8 C ₆₀ and 9 C ₆₀ Complexes.....	174
Appendix B.	$\Delta\delta_{\text{H}}$ values for the complexes 26 , and 26a with C ₆₀	180
Appendix C.	Volumetric Data for 8 , 9 , 26 , 26a , C ₆₀ and their Complexes.....	184
Appendix D.	X-Ray Data of Compounds.....	189
Appendix E.	¹ H NMR, ¹³ C NMR spectra.....	204

List of Figures

	Page
Fig. 1.1. Calix[<i>n</i>]arenes and some derivatives.....	1
Fig. 1.2. Conformational isomers of calix[4]arenes.....	2
Fig. 1.3. Calix[4]naphthalenes.....	5
Fig. 1.4. Depth and width of a calix[4]arene as compared with a calix[4]naphthalene.....	8
Fig. 1.5. The electrostatic potential maps on the surface of (a)calix[4]naphthalene 8 and (b) calix[4]arene 1	9
Fig. 1.6. Three different types of electrostatic interactions.....	11
Fig. 1.7. The π - π interactions.....	12
Fig. 1.8. The solvophobic effect during typical host-guest complexation.....	13
Fig. 1.9. X-Ray structure of the CTV- C_{60} complex.....	16
Fig. 1.10. Structure of (BEDT-TTF).....	17
Fig. 1.11. Double "cone" conformation of calixarene 2	21
Fig. 1.12. Calix[5]arene and some derivatives.....	21
Fig. 1.13. Packing diagrams viewed along (a)looking down the linear columns of calixarene- C_{60} , (b) showing a side view of the columns.....	23
Fig. 1.14. Family of resorc[4]arenes.....	24

Fig. 2.1.	Complex formation during spectrophotometric titration (a) a very stable complex, (b) and (c) complexes of decreasing stability.....	28
Fig. 2.2	Absorption spectra of C_{60} and 8 in toluene at 25 °C.....	32
Fig. 2.3	Absorption spectra of C_{60} and 8 in benzene at 25 °C.....	32
Fig. 2.4	Absorption spectra of C_{60} and 8 in CS_2 at 25 °C.....	33
Fig. 2.5	Absorption spectra of C_{60} and 9 in toluene at 25 °C.....	33
Fig. 2.6	Absorption spectra of C_{60} and 9 in benzene at 25 °C.....	34
Fig. 2.7	Absorption spectra of C_{60} and 9 in CS_2 at 25 °C.....	34
Fig. 2.8.	Continuous variation plot (Job plot) for the 8 C_{60} complex in toluene at 25 °C.....	36
Fig. 2.9	Continuous variation plot (Job plot) for the 8 C_{60} complex in benzene at 25 °C.....	36
Fig. 2.10.	Continuous variation plot (Job plot) for the 8 C_{60} complex in CS_2 at 25 °C.....	37
Fig. 2.11.	Continuous variation plot (Job plot) for the 9 C_{60} complex in Toluene at 25 °C.....	37
Fig. 2.12.	Continuous variation plot (Job plot) for the 9 C_{60} complex in benzene at 25 °C.....	38

Fig. 2.13.	Continous variation plot (Job plot) for the 9 : C_{60} complex in CS_2 at 25 °C.....	38
Fig. 2.14.	Mole ratio plot for the 8 C_{60} complex in toluene at 25 °C	39
Fig. 2.15.	Mole ratio plot for the 8 C_{60} complex in benzene at 25 °C	39
Fig. 2.16.	Mole ratio plot for the 8 C_{60} complex in CS_2 at 25 °C	40
Fig. 2.17.	Mole ratio plot for the 9 C_{60} complex in toluene at 25 °C	40
Fig. 2.18.	Mole ratio plot for the 9 C_{60} complex in benzene at 25 °C	41
Fig. 2.19.	Mole ratio plot for the 9 C_{60} complex in CS_2 at 25 °C.	41
Fig. 2.20.	Double reciprocal plot for the 8 C_{60} complex in toluene	43
Fig. 2.21.	Double reciprocal plot for the 8 C_{60} complex in benzene	43
Fig. 2.22.	Double reciprocal plot for the 8 C_{60} complex in CS_2	44
Fig. 2.23.	Double reciprocal plot for the 9 C_{60} complex in toluene	44
Fig. 2.24.	Double reciprocal plot for the 9 C_{60} complex in benzene	45
Fig. 2.25.	Double reciprocal plot for the 9 C_{60} complex in CS_2	45
Fig. 2.26.	Van't Hoff plot for the 8 C_{60} complex in toluene	51
Fig. 2.27.	Van't Hoff plot for the 8 C_{60} complex in benzene	51
Fig. 2.28.	Van't Hoff plot for the 8 C_{60} complex in CS_2	52
Fig. 2.29.	Van't Hoff plot for the 9 C_{60} complex in toluene	52
Fig. 2.30.	Van't Hoff plot for the 9 C_{60} complex in benzene	53
Fig. 2.31.	Van't Hoff plot for the 9 C_{60} complex in CS_2	53

Fig. 2.32.	The enthalpy-entropy compensation plot for the complexes of 8 and 9 with C_{60}	58
Fig. 3.1.	Octahomotetraoxacalix[4]arene 24	64
Fig. 3.2.	C_2 - and C_1 -symmetrical hexahomotrioxacalix[3]naphthalenes.....	66
Fig. 3.3.	1H NMR spectrum ($CDCl_3$) of 26	74
Fig. 3.4.	Double reciprocal plot for the 26a : C_{60} complex in toluene- d_6	79
Fig. 3.5.	Double reciprocal plot for the 26 : C_{60} complex in toluene- d_6	79
Fig. 3.6.	Double reciprocal plot for the 26a : C_{60} complex in benzene- d_6	80
Fig. 3.7.	Double reciprocal plot for the 26 : C_{60} complex in benzene- d_6	80
Fig. 3.8.	Assignment of protons in 26 and (for 26a , $H_d = tert$ -butyl protons).....	82
Fig. 3.9.	Continuous variation plot (Job plot) for the 26a : C_{60} complex in toluene- d_6 at 25 °C.....	83
Fig. 3.10.	Continuous variation plot (Job plot) for the 26 : C_{60} complex in toluene- d_6 at 25 °C.....	83
Fig. 3.11.	Continuous variation plot (Job plot) for the 26a : C_{60} complex in benzene- d_6 at 25 °C.....	84
Fig. 3.12.	Continuous variation plot (Job plot) for the 26 : C_{60} complex in benzene- d_6 at 25 °C.....	84
Fig. 3.13.	Plot of chemical shift changes $\Delta\delta$ vs $[C_{60}]$ for 26a protons in	

	toluene- d_6	85
Fig. 3.14.	Plot of chemical shift changes $\Delta\delta$ vs $[C_{60}]$ for 26 protons in toluene- d_6	85
Fig. 3.15.	Plot of chemical shift changes $\Delta\delta$ vs $[C_{60}]$ for 26a protons in benzene- d_6	86
Fig. 3.16.	Plot of chemical shift changes $\Delta\delta$ vs $[C_{60}]$ for 26 protons in benzene- d_6	86
Fig. 3.17.	Absorption spectra of mixtures of C_{60} and 26a in toluene at 25 °C.....	87
Fig. 3.18.	X-ray partial packing diagram for $(\mathbf{26a})_2 C_{60}$ in which the other molecules have been removed for clarity.....	88
Fig. 4.1.	D- α -manno-naphtho-18-crown-6.....	108
Fig. 4.2.	Apparent molar volume ($V\phi$) of (8 C_{60} , 8 and C_{60}) vs molality in toluene.....	112
Fig. 4.3.	Apparent molar volume ($V\phi$) of (8 C_{60} , 8 and C_{60}) vs molality in benzene.....	112
Fig. 4.4.	Apparent molar volume ($V\phi$) of (8 C_{60} , 8 and C_{60}) vs molality in CS_2	113
Fig. 4.5.	Apparent molar volume ($V\phi$) of (9 C_{60} , 9 and C_{60}) vs molality in toluene.....	113
Fig. 4.6.	Apparent molar volume ($V\phi$) of (9 C_{60} , 9 and C_{60}) vs	

Fig. 4.7.	Apparent molar volume (V^{ϕ}) of (9- C_{60} , 9 and C_{60}) vs molality in CS_2	114
Fig. 4.8.	Specific volume (V_s) of (8- C_{60} , 8 and C_{60}) vs mass fraction in toluene.....	120
Fig. 4.9.	Specific volume (V_s) of (8- C_{60} , 8 and C_{60}) vs mass fraction in benzene.....	120
Fig. 4.10.	Specific volume (V_s) of (8- C_{60} , 8 and C_{60}) vs mass fraction in CS_2	121
Fig. 4.11.	Specific volume (V_s) of (9- C_{60} , 9 and C_{60}) vs mass fraction in toluene.....	121
Fig. 4.12.	Specific volume (V_s) of (9- C_{60} , 9 and C_{60}) vs mass fraction in benzene.....	122
Fig. 4.13.	Specific volume (V_s) of (9- C_{60} , 9 and C_{60}) vs mass fraction in CS_2	122
Fig. 4.14.	Apparent molar volume (V^{ϕ}) of (26- C_{60} , 26 and C_{60}) vs molality in toluene.....	128
Fig. 4.15.	Apparent molar volume (V^{ϕ}) of (26- C_{60} , 26 and C_{60}) vs molality in benzene.....	128
Fig. 4.16.	Apparent molar volume (V^{ϕ}) of (26- C_{60} , 26 and C_{60}) vs molality in CS_2	129
Fig. 4.17.	Apparent molar volume (V^{ϕ}) of (26a- C_{60} , 26a and C_{60}) vs	

	molality in toluene.....	129
Fig. 4.18.	Apparent molar volume (V^{ϕ}) of (26a C ₆₀ , 26a and C ₆₀) vs molality in benzene.....	130
Fig. 4.19.	Apparent molar volume (V^{ϕ}) of (26a C ₆₀ , 26a and C ₆₀) vs molality in CS ₂	130
Fig. 4.20.	Specific volume (V^{ρ}) of (26 C ₆₀ , 26 and C ₆₀) vs mass fraction in toluene.....	131
Fig. 4.21.	Specific volume (V^{ρ}) of (26 C ₆₀ , 26 and C ₆₀) vs mass fraction in benzene.....	131
Fig. 4.22.	Specific volume (V^{ρ}) of (26 C ₆₀ , 26 and C ₆₀) vs mass fraction in CS ₂	132
Fig. 4.23.	Specific volume (V^{ρ}) of (26a C ₆₀ , 26a and C ₆₀) vs mass fraction in toluene.....	132
Fig. 4.24.	Specific volume (V^{ρ}) of (26a C ₆₀ , 26a and C ₆₀) vs mass fraction in benzene.....	133
Fig. 4.25.	Specific volume (V^{ρ}) of (26a C ₆₀ , 26a and C ₆₀) vs mass fraction in CS ₂	133
Fig. 4.26.	Schematic representation for the Picker-type densitometer (Sodev Model D03).....	143
Fig 5.1.	¹ H NMR spectrum of 49 in CDCl ₃	150
Fig 5.2.	¹ H NMR spectrum of 49a in CDCl ₃	151

Fig. 5.3.	Stereoviews of the X-ray structure for compound 49	153
Fig. 5.4.	%E of 49 and 50 for metal picrate in CHCl ₃	155

List of Schemes

	Page
Scheme 1.1. 1-Naphthol-derived calix[4]naphthalenes.....	5
Scheme 1.2. Convergent synthetic route for the <i>exo</i> -type calix[4]naphthalenes.....	6
Scheme 1.3. Synthetic route for the <i>endo</i> -type calix[4]naphthalenes.....	7
Scheme 1.4. Purification of fullerene mixture using calix[8]arenes.....	18
Scheme 3.1. Synthesis of oxacalixarenes.....	63
Scheme 3.2. Attempted synthesis of oxacalixarenes by reductive homocoupling.....	65
Scheme 3.3. Attempted synthesis of oxacalixnaphthalenes from 28	67
Scheme 3.4. Attempts at the synthesis of 28	68
Scheme 3.5. Intermolecular hetero-Diels-Alder reaction of 38	70
Scheme 3.6. Synthesis of hexahomotrioxacalix[3]arenes.....	71
Scheme 3.7. Synthesis of hexahomotrioxacalix[3]naphthalenes.....	72
Scheme 5.1. Alkylation of calix[4]naphthalenes.....	146
Scheme 5.2. Alkylation of hexahomotrioxacalix[3]naphthalenes.....	147

List of Tables

	Page
Table 1.1. K_{assoc} values for C_{60} and C_{70} with calix[5]arene compounds in toluene.....	22
Table 2.1. Log K_{assoc} values for C_{60} with 8 in toluene, benzene and CS_2 , at different temperatures.....	47
Table 2.2. Log K_{assoc} values for C_{60} with 9 in toluene, benzene and CS_2 , at different temperatures.....	48
Table 2.3. Thermodynamic values for C_{60} complexes with 8 and 9 in toluene, benzene and CS_2 at 25°C.....	55
Table 2.4. The slope (α) and intercept ($T\Delta S$) of the ΔH - ΔS plot for 1:1 host-guest complexation by various host molecules.....	58
Table 3.1. Percentage extractability (%E) of metal picrates into $CHCl_3$ at 25°C.....	76
Table 3.2. K_{assoc} values for C_{60} complexes with 26 and 26a in toluene- d_6 and benzene- d_6	81
Table 4.1. Partial molar volumes of C_{60} , 8 , and of the 8 : C_{60} complex in different solvents.....	116
Table 4.2. Partial molar volumes of C_{60} , 9 , and of the 9 : C_{60} complex in different solvents.....	118
Table 4.3. Partial molar volumes of C_{60} , 26a , and of the 26a : C_{60} complex	

	in different solvents.....	134
Table 4.4.	Partial molar volumes of C_{60} , 26 , and of the 26 : C_{60} complex in different solvents.....	136
Table 5.1.	Distribution of the products of alkylation of 26 and 26a between cone and partial-cone conformations.....	148
Table 5.2.	%E values for metal picrates with 49 and 50 triesters into $CHCl_3$ at 25 °C.....	154

List of Symbols, Abbreviations

Å	angstrom units
Ac	acetyl
BEDT-TTF	bis(ethylenedithio)tetrathiafulvalene
CPK	Corey-Pauling-Koltum
ΔH	enthalpy change
ΔS	entropy change
DMF	<i>N,N</i> -dimethylformamide
DNA	deoxyribonucleic acid
ESI	electrospray ionization
equiv.	equivalent(s)
FAB	fast atom bombardment
h	hour(s)
HIV	human immunodeficiency virus
HOMO	highest occupied molecular orbital
HRMS	high resolution mass spectrometry
INS	inelastic neutron scattering
IR	infrared spectroscopy
kJ	kilojoules
LAH	lithium aluminum hydride

LUMO	lowest unoccupied molecular orbital
Me	methyl
min	minute(s)
MOM	methoxymethyl
m.p.	melting point
MS	mass spectrometry
NMR	nuclear magnetic resonance
NOBA	3-nitrobenzylalcohol
<i>p</i> -	para
PLC	preparative thin layer chromatography
Ph	phenyl
rt	room temperature
<i>tert</i>	tertiary
THF	tetrahydrofuran
Tf	trifluoromethanesulfonyl
TFA	trifluoroacetic acid
tlc	thin-layer chromatography
TMS	trimethylsilyl
TsOH	toluenesulfonic acid
UV	ultraviolet
vis	visible

vis

visible

VT

variable temperature

χ

mole fraction

To the memory of my father, my mother, lovely sons, beautiful daughter, wife and sisters

Chapter One Introduction

1.1. Calix[n]arenes

Calixarenes are cavity-containing cyclic molecules which consist of aryl groups linked by methylene groups. These molecules can be synthesized from the acid or base-

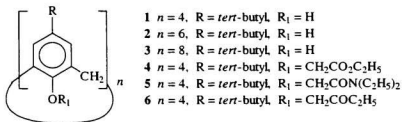


Figure 1.1 Calix[n]arenes and some derivatives.

catalyzed condensation of *para*-substituted phenols with formaldehyde.¹ The most common calixarenes (1-3) respectively have either four, six or eight aryl groups joined by the same number of methylene groups in a cyclic array (Figure 1.1). One of the most fascinating aspects of calixarenes is the variety of conformations which they can assume. This is as a result of the flipping of the aryl groups to be above or below the molecular plane which is defined by the intraannular macrocycle which includes the methylene bridges. The phenolic hydroxyl groups are situated on what is referred to as the “lower rim”, and the *para*-alkyl substituents on the aryl groups (or naphthyl groups of the calixnaphthalenes) are usually located on what is referred to as the “upper rim”. At room temperature, *tert*-

butylcalix[4]arene **1**, for example, can exist in at least four clearly defined different conformational isomers (or conformers) which were recognized as early as 1955 by Cornforth and his co-workers.² Gutsche³ later designated these conformers shown in Figures 1.2 a-d respectively as:

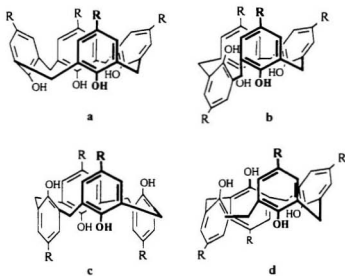


Figure 1.2 Conformational isomers of calix[4]arenes.

- a. The “*cone*” or “*crown*” conformer, in which all the aryl groups are *syn* to one another.
- b. The “*partial-cone*” or “*partial-crown*” conformer, in which three aryl groups are *syn* to one another and one is *anti* to the other three.
- c. The “*1,3-alternate*” conformer, in which adjacent aryl groups are *anti* to each other,

but the opposite aryl groups are *syn*.

- d. The "*1,2-alternate*" conformer, in which adjacent pairs of aryl groups are *syn* and *anti*.

In solution and in the solid state, *tert*-butylcalix[4]arene **1** always exists in the "*cone*" conformation.³ In this "*cone*" conformation, calixarenes possess cavities or bowl-like shapes, which are defined by the aryl groups and their dimensions are expected to increase as the number of the aryl groups increases.

Another important property of calixarenes and their derivatives is their ability to include smaller "guest" molecules or ions within their cavities to form inclusion compounds or complexes. Various inclusion compounds of **1** in the solid state ("clathrates") with different guests such as benzene, anisole, pyridine, acetone, chloroform, acetonitrile, methanol and water have been reported.⁴ Other complexes with metal ions, in which the calixarene derivatives behave as ionophores⁵ to transport alkali metals (especially Cs⁺) through organic membranes have also been reported. Calix[*n*]arenes, where *n* = 5, 6 and 8, are also able to include larger neutral molecules, in particular [60]- and [70]fullerenes (C₆₀ and C₇₀).^{6,7} As a result of some of these properties, calixarenes are important molecules for supramolecular (for a definition of "supramolecular", see Section 1.4) chemistry studies.

1.2. Calixarene Derivatives

The ability of a calix[4]arene to form complexes with metal cations can be enhanced by modifying its lower rim to prepare corresponding tetraesters such as **4**, tetraamides such as **5**, or tetraketones such as **6**. Several studies^{8a-f} in this area have been reported and the

following rules can be formulated:

- a. The tetraester **4** and tetraketone **6**, can selectively form complexes with alkali metal cations rather than with alkaline earth metal cations.
- b. The particular conformation of the calixarene derivative has a great effect on the selectivity towards the metal cations: the “*cone*” conformation selectively binds Na⁺ while the other conformations selectively bind K⁺.
- c. Tetraamides bind alkali metal cations more strongly than do the corresponding tetraesters.
- d. The lower rim functionality (“podand”) controls the calixarene conformation by hindering conformational inversion, since the larger groups are unable to pass through the macrocyclic annulus. In general, *O*-tetraallyl and *O*-tetrabenzyl ethers lock the calixarene into the “*cone*” conformation while the tetraacetyl and smaller *p*-tetraalkyl groups favor the “*partial-cone*” conformation.³
- e. Tetraesters and tetraamides are more soluble than the parent calixarenes in organic solvents.⁹

1.3. Calixnaphthalenes

In 1993 our group reported the first syntheses of a group of novel naphthalene ring containing cyclic compounds, shown in Figure 1.3. These compounds are analogous to the calix[4]arenes, and were thus named as “calix[4]naphthalenes”.^{10a,b} Compound **7** and its isomers were prepared from the base-mediated condensation of 1-naphthol with formaldehyde (Scheme 1.1) in DMF,^{10a} or via convergent synthetic routes (Scheme 1.2).¹¹

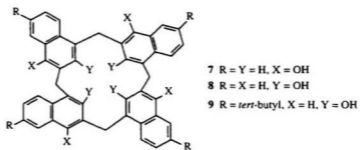
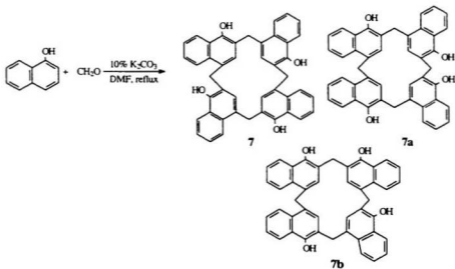
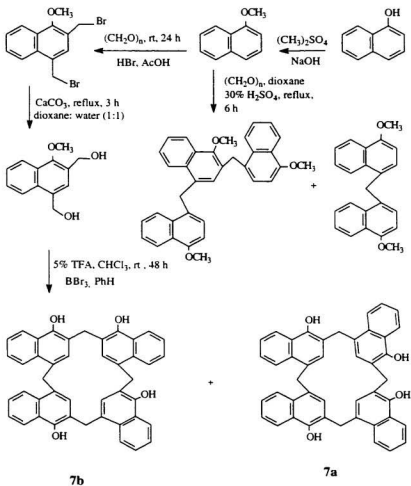


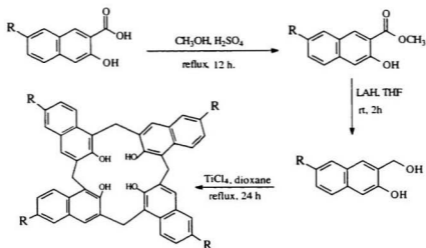
Figure 1.3 Calix[4]naphthalenes.



Scheme 1.1 1-Naphthol-derived calix[4]naphthalenes.



Scheme 1.2 Convergent synthetic route for the *exo*-type calix[4]naphthalenes.



8 R = H, **9** R = *tert*-butyl

Scheme 1.3 Synthetic route for the *endo*-type calix[4]naphthalenes.

The major difference between calix[4]arenes and the calix[4]naphthalenes derived from 1-naphthol is that the former compounds have their hydroxyl groups at the lower rim (*endo*-type) and the latter have their hydroxyl groups outside the intraannular ring (*exo*-type). As a result of intramolecular hydrogen bonding which can occur in the *endo*-type calixarenes, their conformations can be locked in “*cone*” conformations. The *exo*-type calix[4]naphthalenes are conformationally more flexible. In order to prepare the *endo*-type calix[4]naphthalenes such as **8** (or **9**), in which the hydroxyl groups are located at the lower rim, a different synthetic route was required (Scheme 1.3).¹¹

Calix[4]naphthalenes,^{10, 11} like the calix[4]arenes, can also exist in the four major different conformations described previously and depicted in Figure 1.2. Molecular modeling

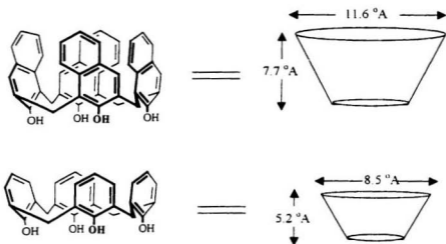
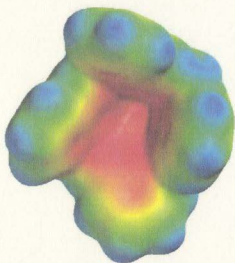
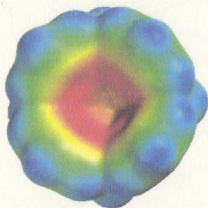


Figure 1.4 Depth and width of a calix[4]arene as compared with a calix[4]naphthalene.

of calix[4]naphthalenes using CPK models and PC SPARTAN¹² indicates clearly that they have deeper cavities than calix[4]arenes. Figure 1.4 shows the depth and diameters as measured between the most distal (carbons) of calix[4]arenes and calix[4]naphthalenes calculated using PC SPARTAN.¹² Calix[4]naphthalenes can also be π -electron richer than the corresponding calix[4]arenes. Figure 1.5 shows the electrostatic potential maps on the surfaces of calix[4]naphthalene **8** and calix[4]arene **1** (density functional theory: BP/DN***)¹² which predicts that the cavities of calix[4]naphthalenes are indeed more electron rich (cover a larger surface area) than the cavities of calix[4]arenes. These factors should enable these



(a)



(b)

Figure 1.5. The electrostatic potential maps on the surfaces of (a) calix[4]naphthalene 8 and (b) calix[4]arene 1

compounds to serve as potentially effective receptors for supramolecular or host-guest chemistry, and molecular recognition.

1.4. Supramolecular Chemistry

Supramolecular chemistry¹³ deals with non-covalent bonding interactions that can be utilized to construct units or adducts which may associate with one another to form larger species, with a high degree of control and efficiency. It has also been defined as “chemistry beyond the molecule”^{13a} The non-covalent, or “supramolecular” interactions between organic/inorganic ions or molecules, and macrocyclic receptors have been described in many papers.¹⁴ An important branch of investigation within supramolecular chemistry is the molecular recognition of biologically-relevant chiral compounds. The importance of these types of molecular recognitions have been appreciated in biomimetic systems, and in the chiral resolutions of racemates. Effective recognition requires complementarity between the host and guest. For example, an enzyme may catalyze a single reaction with high specificity if the active site of the enzyme is complementary with the substrate *i.e.* the shapes and the arrangements of binding sites in enzyme and substrate fit each other. In order to have good complementarity, the effective receptor sites of enzymes usually have at least a single cavity in which the substrate binds, to form an enzyme-substrate (or “host- guest”) complex.

Hosts are typically organic molecules that have convergent binding sites (their binding sites converge in the complex, such as a cavity) and guests are molecules or ions that have divergent binding sites (its binding sites diverge in the complex), while complexes are comprised of hosts and guests held together by non-covalent bonding.¹⁵ Such complexes

are characterized by the spatial arrangement of their components, and the nature of the intermolecular interactions that hold the species together. These intermolecular interactions differ in strength and directionality, and are therefore dependent on the distances and angles between host and guest. The non-covalent bonding could be any one of, or a combination of, the following interactions:¹³

a. *Hydrogen bonding*: These are probably the most important non-covalent interactions, and are found in many biological systems, such as in e.g. the DNA double-helix.⁹ This type of bonding is directional and selective. The directionality provides a control over the structure of the receptor-substrate complex.

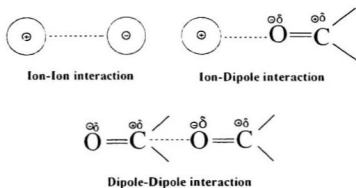


Figure 1.6 Three different types of electrostatic interactions

b. *Electrostatic interactions*: These include the interaction of all the permanent charges in molecules which can be point poles, dipoles, or multipoles. These interactions could be either attractive (ion-ion, ion-dipole and/or dipole-dipole) as shown in Figure 1.6 or

repulsive. Ion-ion interactions are non-directional, while ion-dipole and dipole-dipole interactions must be suitably aligned for maximum interaction. In this type of interaction, an electrically neutral molecule with an unsymmetrical charge distribution possesses a permanent dipole moment, which, when placed in the electrical field resulting from an ion or another dipole, will orient itself for maximum attraction or minimum repulsion.

c. *Dispersion forces:* Induced dipole-dipole attractions. These forces exist between induced dipoles. The attraction between molecules occurs when instantaneous dipoles in the electron clouds surrounding each molecule interact favorably with one another.¹¹⁴ Such interactions would provide an enthalpic stabilization to the system under investigation. Both types of interactions in (b) and (c) are considered to be van der Waals forces.

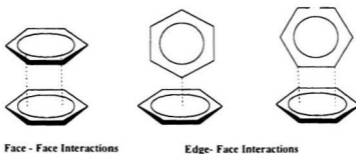


Figure 1.7 Types of π - π interactions.

d. *π - π Interactions:* These types of interactions occur between systems containing aromatic rings (Figure 1.7). Attraction could occur either in a “face-to-face” or “edge-to-face” manner. These types of interactions are frequently found in proteins and many cyclophane complexes.¹¹⁴

e. *Hydrophobic or solvophobic effects*: The hydrophobic effect ¹⁵ was first postulated by Frank and Evans in 1945, ¹⁶ when they found that solvent molecules, mainly in aqueous solutions, are more tightly packed around the dissolved solute molecules than they are in the pure solvent itself. If two solutions each containing a different solute e.g. a host molecule in one case, and a guest molecule in the other are mixed together, an inclusion complex is formed between the two solutes. Figure 1.8 shows a simple representation of this

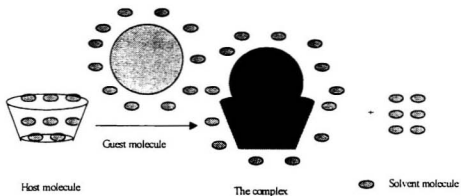


Figure 1.8 The solvophobic effect during typical host-guest complexation.

“solvophobic effect”^{17a} effect which is considered to be one of the driving forces for such associations (note this effect also plays an important role in biochemical enzyme-substrate complex formation.^{17b-d}). When alone in solution, the host molecule could have one or more solvent molecules contained within its cavity, in addition to those solvent molecules which are packed around the exterior “shell” of the molecule. When the two solutions are mixed and complex formation occurs, the result is that the entropy of the system increases since

there are now proportionately more unassociated solvent molecules in the resulting bulk solution.

f. *Charge-transfer*: These types of interactions occur between electron-donor molecules and electron-acceptor molecules. Electron transfer from the HOMO of the electron-rich compound (donor) into the LUMO of the electron-poor compound (acceptor) is known as a charge-transfer interaction¹⁸ and is recognized by the new band which appears in the long wavelength part of the UV-vis spectra. The complex formed between I₂ and benzene is an example of such a charge-transfer complex in which the new band is seen at $\lambda = 290$ nm.

When these non-covalent interactions are compared to typical covalent bonds, they are generally much weaker. The bond energy of a single covalent bond is around 350 kJ/mol, while the strengths of the non-covalent interaction in supramolecular complexes range from 2 kJ/mol for van der Waals forces, to 20 kJ/mol for hydrogen bonding and up to 250 kJ/mole for ion-ion interactions.¹³⁴ The combination of more than one of these types of interaction allows for strong and sometimes selective recognition of specific guests.

1.5. [60]Fullerene, C₆₀

Since its discovery in 1985, the electron-deficient C₆₀ has been widely studied.¹⁹ C₆₀ can undergo chemical modification by for example, the addition of *N,N'*-dimethylethylenediamine²⁰ across the 6,6'-position ring junction of two six-membered rings of the polyhedron. Exohedral metal complexes of C₆₀ are also known in which the metal-C₆₀ binding is usually associated with the same 6,6'-positions of C₆₀.²¹ Fullerenes can also undergo other reactions such as reduction to form fulleride salts, and can form solids in

which C_{60} and $PdCl_2$ co-crystallize in benzene.²² C_{60} has an interesting ability to co-crystallize with a variety of other molecules for example organic molecules, such as benzene,²³ organometallics such as ferrocene,²⁴ and inorganic species such as P_4 .²⁵ The shape of C_{60} , coupled with its distinct physical properties, such as the electronic absorption bands which are spread across the entire uv-vis spectrum, its efficient singlet oxygen sensitizing ability, its strong electron acceptor character, and its superconductivity properties upon doping with alkali metals,²⁶ makes it an attractive candidate for construction of larger supramolecular compounds. To our knowledge, the first example of a C_{60} supramolecular array was reported in 1991, in which hydroquinone and C_{60} were mixed in benzene in a 3:1 ratio to form black crystals when the solvent evaporated.²⁷ The X-ray structure of this complex shows the formation of a 3:1 complex. The driving force for this complexation process is the weak charge-transfer interaction between the π -electron deficient C_{60} and the π -electron-rich hydroquinone.

The geometries and stoichiometries of complexes of C_{60} in the solid state are largely determined by van der Waals interactions in conjunction with crystal packing forces, in order to accommodate the convex surface of the C_{60} molecules and fill the voids between them. The early solid complexes showed that the electron-accepting C_{60} prefers to be surrounded by electron-rich, rather than electron-poor π -systems. C_{60} has been shown to form supramolecular complexes with a variety of hydrophobic host systems, including calixarenes,²⁸ homooxalixarenes,²⁸ resorcinarenes,²⁸ and by ourselves with calix[4]naphthalene,^{29a} hexahomotrioxalix[3]naphthalenes^{29b} and substituted

corannulenes.^{29c} Other host systems such as cyclodextrins, and porphyrins have also been shown to form complexes with C_{60} .²⁸ The following section details some of these cases.

In 1992 C_{60} was reported to form complexes with γ -cyclodextrin. An attempt to increase the solubility of C_{60} in water led to the discovery that a boiling aqueous solution of γ -cyclodextrin in the presence of α - and β -cyclodextrins selectively forms complexes with C_{60} .³⁰ After verification of the complex on the basis of ^1H , ^{13}C NMR and elemental analysis, a 2:1 γ -cyclodextrin: C_{60} complex was proposed.

Cyclotrimeratrylene "CTV" is another host molecule for C_{60} which has been studied.³¹ It was found that CTV is able to form inclusion complexes with C_{60} in the solid state. Its *O*-methylated derivative also forms inclusion complexes with C_{60} in solution. The X-ray structure of the CTV: C_{60} complex (Figure 1.9) shows that C_{60} adopts a nesting position at the van der Waals contact distance above the concave surface of the CTV. The nine-membered intraannular ring in CTV lines up with a six-membered ring of the C_{60} , compelling three adjacent five-membered rings of the C_{60} to reside above the three electron-rich aryl groups of CTV. This explanation assumes that the relatively weak π - π interactions are contributing to the complex formation.

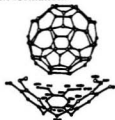


Figure 1.9 X-ray structure of the CTV: C_{60} complex.

Numerous charge-transfer complexes of C_{60} have been obtained using planar donors such as compounds of the tetrathiafulvalene and dithiaazafulvalene family.³² For example, Izuoka and his group obtained a black single crystal of the charge-transfer complex between C_{60} and 2-equivalents of bis(ethylenedithio)tetrathiafulvalene (BEDT-TTF) (Figure 1.10) by

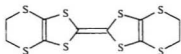


Figure 1.10 Structure of (BEDT-TTF).

co-crystallization from CS_2 solution. Its X-ray structure shows the C_{60} to be sandwiched between a pair of largely concave BEDT-TTF molecules.

The shape of C_{60} , coupled with its distinct physical properties have increasingly invited exploration of its physical and chemical properties. It has some biological applications, since for example it can act as a singlet oxygen photosensitizer to cleave DNA^{33, 34} and has been shown to be an inhibitor to suppress HIV protease activity.³⁵ The active site of the HIV protease is an open-ended cylindrical hydrophobic cavity containing two amino acids, where hydrolysis of the substrate is presumed to occur. Since it has a similar radius as that of the protease cavity and could bind strongly to the active site, it was proposed that C_{60} and its derivatives could potentially act as an HIV protease inhibitor.³⁵

1.6. Complexes of Calix[n]arenes with C_{60}

As discussed previously, calixarenes have conformations pre-organized or stabilized by intramolecular H-bonding between the phenolic groups at the lower rim. They also feature

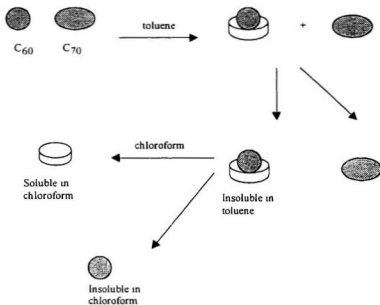
well-ordered macrocyclic arrays of aromatic rings and also possess enough flexibility to allow large guests such as C_{60} to be included within their cavities. The complexation of calixarenes with C_{60} has been extensively studied (*vide infra*).

In 1992 Verhoeven's group reported³⁶ that C_{60} can be solubilized in water by using a water-soluble calix[8]arene derivative. Changes in the UV-vis absorption spectrum relative to C_{60} in toluene were interpreted to be caused by charge-transfer interactions. The groups of Atwood⁶ and later, Shinkai⁷ discovered that solutions of C_{60} and *tert*-butylcalix[8]arene (**3**) in toluene, form a sparingly-soluble brown-yellow precipitate. This was identified as being a stable 1:1 complex of C_{60} :**3**. The complex decomposes in chloroform or dichloromethane, possibly due to the competitive CH- π interactions between the solvent and the aromatic rings of the calixarene taking precedence over the calixarene-fullerene interactions. A similar type of interaction has been found in the complex formed between calix[4]arene (**1**) with dichloromethane.³⁷ The complexation between **1** and C_{60} is proposed to be a monomeric 1:1 transient intermediate,³⁸ which distorts the electron cloud of C_{60} and in turn favors micelle-like formation featuring fullerene-fullerene interactions in the interior core, with C_{60} being encapsulated by the host calixarene molecules.

The vibrational spectrum of the **3**: C_{60} 1:1 complex has been studied by IR and Inelastic Neutron Scattering (INS) spectroscopy.³⁹ It was found that the interactions between C_{60} molecules are almost completely suppressed by the encapsulation of C_{60} in the cavities of the host calixarenes. Verhoeven and co-workers⁴⁰ carried out solid state ¹³C-NMR and IR spectroscopic studies to explore the nature of the complex between **3** and C_{60} . They found

that a complexation-induced conformational change of **3** took place, as indicated by the changes in the O-H stretching observed in the IR spectra and in the ^{13}C NMR CP-MAS (Cross Polarization Magnetic Angle Spinning) data. The NMR data led to the conclusion that complexed **3** does not have a pleated-loop conformation (in this conformation the eight OH groups lie in a circular array which is an undulating 'pleated loop'),¹ but instead, has a two-winged conformation (in this conformation two of the aryl groups are in 'out' alignments and the others are in non-equivalent 'up' and/or 'down' positions)¹ Shinkai's group reported a study on the electrochemical behaviour of the **3**: C_{60} complex in which the complex was found to dissociate upon reduction of the C_{60} center,²² this result showing that the π -electron sharing of the host-guest complex is weakened by the addition of an electron into the electron-poor C_{60} structure. To date, efforts to form a single crystal suitable for X-ray analysis of the **3**: C_{60} complex have failed. However, this complex and that of **3**: C_{70} was studied in toluene solution⁴¹ using uv-vis methods to determine their stability constants, K_{assoc} . The values of K_{assoc} were determined to be $381 \pm 4 \text{ M}^{-1}$ for **3**: C_{60} , and $179 \pm 6 \text{ M}^{-1}$ for **3**: C_{70} . The ability of **3** to form complexes with C_{60} has been successfully applied to water-solubilization of C_{60} ,³⁶ and also to the purification of C_{60} from a C_{60} and C_{70} fullerene mixture ("fullerite"). The selectivity of **3** to form complexes with C_{60} over C_{70} made it possible to obtain highly purified C_{60} from a fullerite mixture by using Atwood's⁶ procedure (Scheme 1.4) in which C_{60} -calixarene complex is insoluble in toluene and precipitates, and is isolated by filtration, while C_{70} and other impurities remain in solution. When the complex is suspended in chloroform it dissociates, the calixarene remains in solution while the C_{60}

precipitates and is isolated by filtration.



Scheme 1.4 Purification of fullerene mixture using calix[8]arenes.

Calix[6]arene **2** was found to form complexes in the solid state⁴² and in solution⁴¹ with both C₆₀ and C₇₀. It exists in a double cone conformation (Figure 1.11) and becomes associated with two C₆₀ molecules in its complex, the H-bonding network between the hydroxyl groups at the lower rim being fully retained after the complexation. The X-ray data revealed that both (2 C₆₀) and (2 C₇₀) complexes have 1:2 stoichiometries in the solid state.

The complexation study in solution showed that the complexes were formed with K_{assoc} values of $230 \pm 6 \text{ M}^{-1}$ for the 2:C₆₀ complex and $154 \pm 7 \text{ M}^{-1}$ for the 2:C₇₀ complex.⁴¹ Shinkai et al.^{43, 44} studied the complexation properties of C₆₀ with some derivatives of **2**.

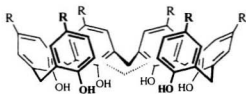
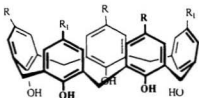


Figure 1.11 Double “cone” conformation of **2**.

They found that the *tert*-butylcalix[6]arene **2** was the only one among 13 other derivatives that induced a slight spectroscopic change in the C_{60} band at $\lambda = 420\text{--}440$ nm. They also reported that host molecules in which the donor groups such as *N,N*-dialkylaniline or *m*-phenylenediamine are pre-organized on an appropriate platform, form inclusion complexes with C_{60} in solution.

Both **2** and **3** require pre-organization of the cavity before complexing with C_{60} while calix[5]arene **10** (Figure 1.12) which has a smaller cavity with a cone conformation and C_5 -



- 10** R = R₁ = H
- 11** R = R₁ = CH₂C₆H₅
- 12** R = CH₃, R₁ = I
- 13** R = R₁ = *tert*-butyl
- 14** R = R₁ = *p*-allyl

Figure 1.12 Calix[5]arene and some derivatives.

symmetry as well, does not need pre-organization prior the complexation. The presence of a C_5 axis in the C_{60} molecule which aligns with the C_5 axis of **10** results in the maximization of the number of points of contact which will increase the van der Waals interactions and

give a maximum overlap of the π -cloud of the calixarene with C_{60} . Calix[5]arene **10** itself, forms a 1:1 complex with C_{60} in the solid state^{42,44} while its derivatives form either 1:1 or 2:1 complexes.⁴⁵ Atwood *et al.*⁴⁶ reported the formation of a toluene-solvated 1:1 species of C_{60} with p-benzylcalix[5]arene **11** and they also reported the structure of a 2:1 complex in the solid state. Fukazawa *et al.*⁴⁵ reported a solid state and solution study of the complexation of calix[5]arene derivatives in different solvents, such as CS_2 , toluene, benzene and CH_2Cl_2 . The stoichiometries of each of the complexes in solution are 1:1 as determined from Job Plots. The stability constants K_{assoc} for the complexes of diiodotrimethylcalix[5]arene **12** with C_{60} were determined using uv-vis data to be $308 \pm 41 M^{-1}$ in CH_2Cl_2 , $660 \pm 30 M^{-1}$ in CS_2 , $1840 \pm 130 M^{-1}$ in benzene and $2120 \pm 110 M^{-1}$ in toluene. Another solution study was conducted by Gutsche *et al.*⁴⁷ in which the stability constants of the C_{60} and C_{70} complexes with **10** and some of its derivatives in toluene were reported to be as shown in Table 1.1.

Table 1.1 K_{assoc} values (M^{-1}) for C_{60} and C_{70} with calix[5]arene compounds in toluene

	13	14	10	biscalix[5]arene	p-allylbiscalix[5]arene
C_{60}	9 ± 1	292 ± 15	30 ± 2	93 ± 5	1300 ± 65
C_{70}	n.a	141 ± 8	51 ± 3	119 ± 6	625 ± 32

They also reported²⁸ the X-ray structure for the C_{60} -5,5'-biscalix[5]arene complex together with the K_{assoc} values in CS_2 for C_{60} and C_{70} . Other solution studies have also been reported⁴⁸ including the electrochemical behavior of the complex of calix[5]arene. A densitometric study was conducted on the complexation of benzylcalix[5]arene with C_{60} in toluene.⁴⁹ On the basis of this study, it was found that two molecules of solvent were displaced upon

complexation.

Calix[4]arene itself showed little change in the electronic spectra⁴⁵ of C_{60} when treated with C_{60} in toluene, and thus there was no evidence for complexation. This could be due to the lack of complementarity between the cavity width (8.5 Å) of calix[4]arene and the outer diameter of C_{60} (10.2 Å),¹⁹ as well as due to a size constraint. Nevertheless, some calix[4]arene derivatives such as tetraphenylcalix[4]arene,⁵⁰ tetrabromocalix[4]arene-propylether⁵¹ and tetraiodocalix[4]arenebenzylether⁵² have shown an ability to complex with

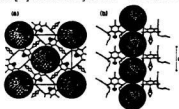


Figure 1.13 Packing diagrams viewed along (a) looking down the linear columns of calixarene and C_{60} ; (b) showing a side view of the columns.

C_{60} . A very close inter-fullerene contact in a columnar structure (Figure 1.13) was found in tetra bromocalix[4]arenepropylether-complex, while the C_{60} molecules were ordered without inter-fullerene interactions in tetraiodocalix[4]arenebenzylether complex.

Resorc[4]arenes or resorcinarenes are cyclic tetramers, e.g. **15** and **16** (Figure 1.14), which can be easily obtained by acid-catalyzed condensation of resorcinol with less reactive aldehydes (compared to formaldehyde) such as acetaldehyde and benzaldehyde.⁵³ Intramolecular H-bonding between adjacent hydroxyl groups of resorcinol units and the preferred axial arrangement of the R-groups⁵⁴ cause the formation of cyclic tetramers to adopt “cone” conformations.

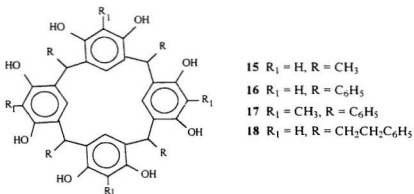


Figure 1.14 Family of resorc[4]arenes.

The inclusion complexes of these compounds could have π - π interactions, OH- π interactions, and/or CH- π interactions. In the case of C_{60} all of these types could exist.⁵⁵ Garcia *et al.*⁵⁵ reported that C_{60} and C_{70} form stable solid complexes with resorc[4]arene **17**. Atwood *et al.*⁵⁶ reported an X-ray structure for the complex of C_{60} with **18**. They found that **18** dimerizes, and that the dimers are stacked in columns involving alternating "head-to-head" and "head-to-tail" associations, while the C_{60} molecules are similarly arranged in columns and are not included inside the cavity of **18**.

1.7. Conclusions

One of the aims of supramolecular chemistry is to be able to imitate or duplicate structures of biological systems, in order to understand and explain the mechanisms by which these systems act or function. In living cells⁵⁷ for example, ions are absorbed or released, either by controlled opening of membrane channels or by transport using

ionophores in which the ionophores bind the ions in the cavity and create a lipid envelope around the ion, making the complex soluble in lipid solution.

One of the earliest examples of synthetic supramolecular compounds are the crown ethers ⁵⁶ which are a class of molecules that can act as ionophores, due to their complexing ability and selectivity towards alkali metal ions. They are considered to be effective receptors based on the requirements that Cram has summarized.¹⁵ Those requirements are that:

- a. The receptor should contain both polar and non-polar groups.
- b. The receptor should have a stable conformation that provides a cavity, surrounded by polar groups that are suitable for the uptake of cations, while the non-polar groups form a lipophilic shell around the coordination sphere.
- c. There should be preferably 5 to 8 coordination sites of the ligand sphere but not more than 12.
- d. There be a rigid arrangement around the cavity of the receptor to provide for high selectivity.
- e. The receptor should be flexible enough to allow a sufficiently fast ion exchange

E.g. are all or most these requirements fulfilled by calix[*n*]arenes and calix[4]naphthalenes, it will be easy to notice that they are therefore potentially useful supramolecular compounds. They are also suitable hosts to form inclusion complexes with many diverse guests including many neutral molecules, among them fullerenes.

In this thesis, the complexation properties of calix[4]naphthalenes **8** and **9** with C₆₀ have been studied by using uv-vis spectrophotometry and densitometry techniques. Chapter

Two of this thesis will discuss the results which were obtained from the uv-vis spectrophotometry of the complexes formed along with the thermodynamic parameters that were obtained using both **8** and **9** with C_{60} in different solvents.

Chapter Three will include the synthesis of hexahomotrioxacalix[3]naphthalenes as a new class of calixnaphthalene compounds. Their complexation properties of with C_{60} in toluene- d_6 or benzene- d_6 using an NMR method will be described. The ability of these compounds to extract alkali metal cations will also be discussed.

Chapter Four will describe the results of the volumetric study of both **8**, **9**, **26** and **26a** with C_{60} using densitometry, in different solvents. A full discussion that connects the volumetric results with the host-guest interactions will be included.

Chapter Five will include the synthesis of some ester derivatives of hexahomotrioxacalix[3]naphthalenes. The ability of these to extract alkali metal cations will also be discussed.

Chapter Two

Complexation Study of Calix[4]naphthalenes with C_{60} in Different Solvents

2.1. Introduction

The various colors produced by C_{60} in different solvents, among other properties, have attracted the attention of many researchers.⁵⁹ The change in the colors of solutions of C_{60} in different solvents when electron-rich receptors such as a calixarene are added, has further stimulated this interest.⁶⁷ The simplicity and efficiency of spectrophotometric measurements has led to their use in studying these changes and determining the stability constants (K_{assoc}) of the complexes formed from C_{60} with such electron-rich receptors. The essential requirement for determining K_{assoc} is that a significant spectral change occurs due to the complexation. This spectral change can be determined by a C_{60} -calixarene titration.

Spectrophotometry can also provide information about the number of species in the tested solution. Consider the case of two species with different absorption spectra. If their spectra pass through a common point, this point of intersection is called an "isobestic point". It is also defined as a wavelength where two species which are in equilibrium with each other show the same absorptivity.⁶⁰ However, it is evident that a system might possess only two states yet fail to exhibit a sharp "isobestic point" if the spectra are solvent-dependent. It is also possible that temperature effects may combine to generate an "isobestic point" even though the system possesses more than two states. Such possibilities have been analyzed in detail, and some authors have concluded that neither the presence nor the absence of an "isobestic point" has any particular value in diagnosing the number of

states in the system.⁶¹

It is important to determine the stoichiometric ratio of the species in a host-guest complex (stoichiometry); such information enables the researcher to use the proper model to study the complexation process and determine the value of K_{assoc} and the thermodynamic data. The stoichiometry of the complexation process is generally determined by the "mole-ratio" method⁶² or the method of "continuous variation"⁶³ In the mole-ratio method, the concentration of C_{60} is fixed while the concentration of the receptor (8 or 9 in this case) is increased. A plot of the absorbance or the absorbance change against the concentration of the receptor will show a break at the concentration where the stoichiometry of the complex is

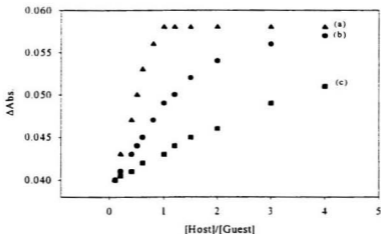


Figure 2.1 Complex formation during spectrophotometric titration:(a) a very stable complex;(b) and (c) complexes of decreasing stability.

established. The shape of the curve depends on the stability of the complex; for a very highly stable complex, a sharp break in the plot will be obtained near the stoichiometry of the complex (Figure 2.1a); the stoichiometry will be represented by the intersection of the tangents corresponding to both branches of the curve. The sharpness of the break and the degree of curvature are related to the stability of the complex formed. Figures 2.1b-c show plots obtained with less stable complexes.⁶²

In the continuous variation method or so-called "Job Method", the total concentration of both C_{60} and the receptor is held constant, while their ratio is changed.⁶³ A plot of the change in the absorbance against the mole fraction of one of the components will show a maximum at the stoichiometric ratio of the complex. In both methods Beer's Law should be obeyed in the concentration range that is used.

The stability constant K_{assoc} of a complex is a measure of the complex stability and of the extent to which the complexation process can proceed. The determination of this constant is one of the objectives in host-guest chemistry. K_{assoc} has also been variously referred to as the binding, formation, or association constant. The reciprocal quantity is a dissociation, or instability constant. The units of K_{assoc} are (concentration)⁻¹, and since the common practice is to use the molar concentration scale, K_{assoc} has units of M⁻¹. K_{assoc} values can be determined by using the Benesi-Hildebrand equation.⁶⁴ This equation is well-applicable in many cases, where straight lines are obtained indicating the formation of 1:1 complexes. When non-linear plots result according to the equation, this indicates that the system is not 1:1. However, in some rare cases, a straight line could be obtained even where

2:1 molar ratio complexes are obtained.⁶⁵ If the complex has a molar ratio which is purely 1:1, the values of K_{assoc} are independent of wavelength and also of the concentration.⁶¹ In order to determine thermodynamic parameters, it is necessary to apply the van't Hoff equation.

2.2. Calix[4]naphthalene complexes with C_{60}

As mentioned previously it has been reported by several authors that calix[*n*]arenes (where *n* = 5, 6, and 8) are able to form complexes with C_{60} in solution as well as in the solid state.²⁸ In all cases, the change in the color of the C_{60} solution is an indication that complexation took place. In toluene, benzene or CS_2 the magenta color of C_{60} solution is changed to brown when mixed with any of the above mentioned calix[*n*]arenes in solution in the same solvents. In the case of compounds **8** or **9**, which possess deeper cavities and are π -electron richer as shown in Chapter One as compared to the corresponding calix[*n*]arene compounds, it was reasoned that these compounds could serve as potentially effective hosts for inclusion of C_{60} and other guests. In principle, therefore, an efficient inclusion of C_{60} could occur, since multi π - π interactions between C_{60} and **8** or **9** are possible. When solutions of **8** or **9** in toluene, benzene, or CS_2 were added to solutions of C_{60} in the same respective solvents, the magenta-colored solutions of the C_{60} changed color to brown. After standing for several days, dark-brown precipitates were formed. In the case of **9**, ruby-red rod-like crystals were formed. However single crystal X-ray diffraction analysis has thus far eluded us since these crystals were found to decompose during the data collection

The +FAB mass spectrum of the precipitate from the toluene solutions of C_{60} :**9** reveals a more complex pattern of peaks than what is observed for the corresponding

spectrum of crystals derived from toluene solutions of **9** alone. No M^+ peak at m/z 1568 for the complex C_{60} -**9** is observed, but additional peaks are evident (among others)^{29a} at 720 (C_{60}); 784 (M^{2+}); 876 ($M+(\text{toluene})_2^{2+}$); and 968 ($M+(\text{toluene})_4^{2+}$). The spectral change induced by the addition of **8** to C_{60} solution in toluene, benzene, and CS_2 are shown in Figures 2.2-2.4, respectively. Similar changes are observed when solutions of **9** are added to C_{60} solutions in the same solvents respectively, as shown in Figures 2.5-2.7. These figures show clearly the formation of new absorption bands in the range 420-540 nm indicating complex formation in all of the solvents which were used. These bands are similar to those obtained by Verhoeven and his group.³⁶ They proposed that the band with a maximum at 420-440 nm is attributed to a charge-transfer transition in which electron-transfer from the electron-rich calixarene to the electron-poor C_{60} takes place. Atwood *et al.*³⁷ obtained a similar band with the CTV complex with C_{60} . They ruled out the existence of a charge-transfer transition, however, and they proposed that this band is characteristic of an interfullerene molecular transition in C_{60} aggregates encapsulated by host calixarene molecules, rather than a charge-transfer transition between the host and guest. However, this explanation does not include the interactions with calixarenes, although formation of aggregates and their stabilization in solution is achieved exclusively due to the cavitands.³⁶ Shinkai *et al.*⁴⁴ studied the complexation of C_{60} with several calixarenes. They concluded that charge-transfer is among other driving forces for the complexation. They subsequently^{22,48} conducted an electrochemical study, in which they confirmed that the charge-transfer is the main reason for the complex formation. Whatever the reason is that accounts for the formation of this

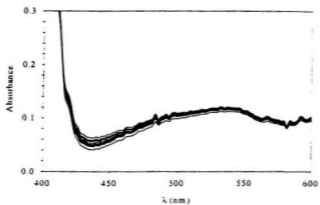


Figure 2.2 Absorption spectra of C₆₀ and 8 in toluene at 25 °C, showing increases in absorption with increasing [8].

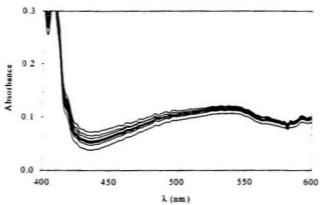


Figure 2.3 Absorption spectra of C₆₀ and 8 in benzene at 25 °C, showing increases in absorption with increasing [8].

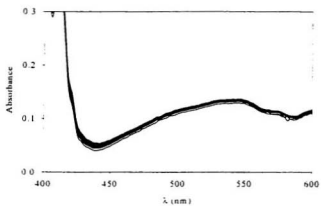


Figure 2.4 Absorption spectra of C_{60} and **8** in CS_2 at 25 °C, showing increases in absorption with increasing [8].

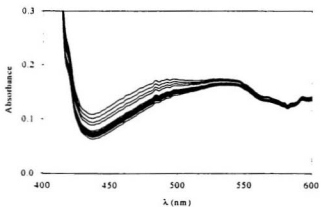


Figure 2.5 Absorption spectra of C_{60} and **9** in toluene at 25 °C, showing increases in absorption with increasing [9].

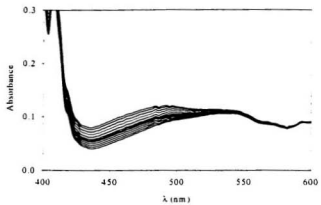


Figure 2.6 Absorption spectra of C_{60} and 9 in benzene at 25 °C, showing increases in absorption with increasing [9].

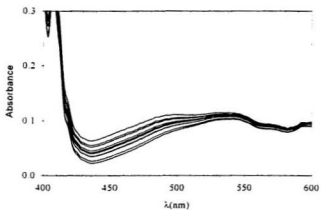


Figure 2.7 Absorption spectra of C_{60} and 9 in CS_2 at 25 °C, showing increases in absorption with increasing [9].

band, it does indicate the formation of a complex, and the spectral changes are used to determine the K_{assoc} values.

The existence of an isosbestic point may be an indication about the number of states in the system. In all our systems an isosbestic point was not observed and neither did most of the reported studies. Fukawaza *et al.*^{45b} observed an isosbestic point at 478 nm for iodocalix[5]arene with C_{60} , and Yamamoto *et al.*⁴⁶ also observed one at 585 nm in their study on the complexation between C_{60} and cyclotrimeratrylenophane which is a bis-cyclotrimeratrylene.

Continuous variation plots for the complexes of **8** and C_{60} at 25 °C are shown in Figures 2.8-2.10 in toluene, benzene or CS_2 , respectively. The maxima at 0.5 mole ratio in each plot indicate the 1:1 stoichiometry of the complex in each case. Figures 2.11-2.13 show the continuous variation plots at 25 °C for **9** C_{60} complexes in toluene, benzene and CS_2 , respectively. The stoichiometries of the **8** C_{60} and **9** C_{60} complexes are also confirmed from the mole ratio plots which are shown in Figures 2.14-2.16 for the **8** C_{60} complexes and Figures 2.17-2.19 for the **9** C_{60} complexes in toluene, benzene and CS_2 , respectively. These figures show changes in the slopes of each plot when the concentrations of **8** or **9** are nearly similar to the concentrations of C_{60} where the stoichiometry is 1:1.

Supramolecular 1:1 complex formation between calix[4]naphthalene **9** for example, with C_{60} in solution, can be represented by equation (2.1):



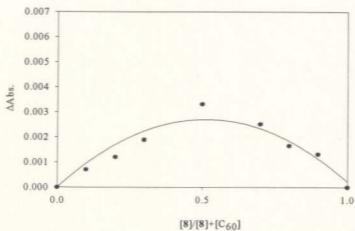


Figure 2.8 Continuous variation plot (Job plot) for the 8:C₆₀ complex in toluene at 25 °C.

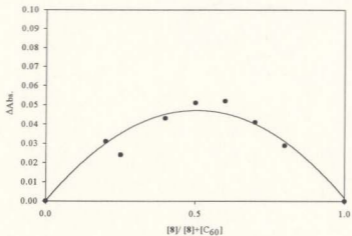


Figure 2.9 Continuous variation plot (Job plot) for the 8:C₆₀ complex in benzene at 25 °C.

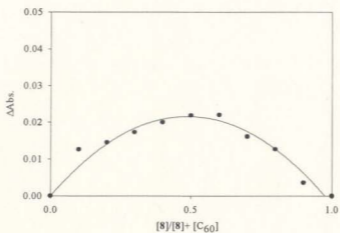


Figure 2.10 Continuous variation plot (Job plot) for the 8:C₆₀ complex in CS₂ at 25°C.

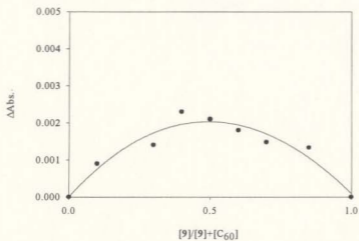


Figure 2.11 Continuous variation plot (Job plot) for the 9:C₆₀ complex in toluene at 25°C.

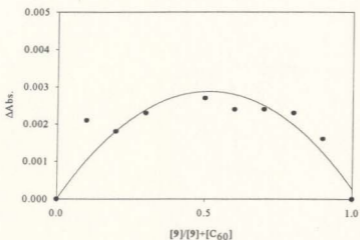


Figure 2.12 Continuous variation plot (Job plot) for the 9:C₆₀ complex in benzene at 25 °C.

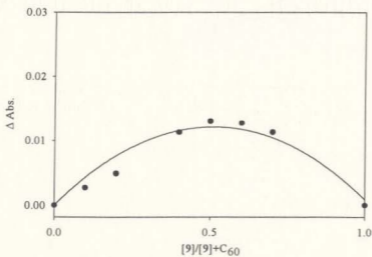


Figure 2.13 Continuous variation plot (Job plot) for the 9:C₆₀ complex in CS₂ at 25 °C.

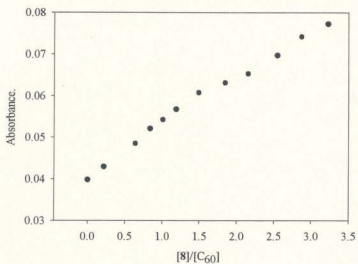


Figure 2.14 Mole ratio plot for the 8:C₆₀ complex in toluene at 25 °C.

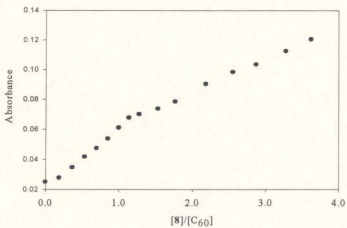


Figure 2.15 Mole ratio plot for the 8:C₆₀ complex in benzene at 25 °C.

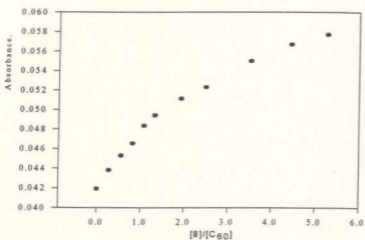


Figure 2.16 Mole ratio plot for the 8:C₆₀ complex in CS₂ at 25 °C.

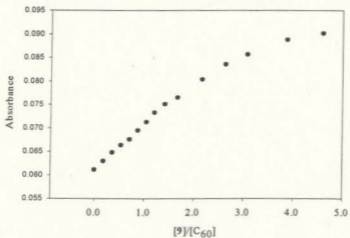


Figure 2.17 Mole ratio plot for the 9:C₆₀ complex in toluene at 25 °C.

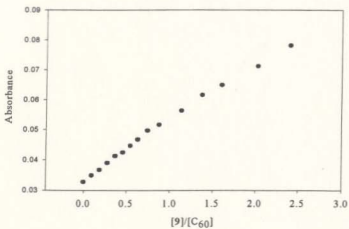


Figure 2.18 Mole ratio plot for the 9:C₆₀ complex in benzene at 25 °C.

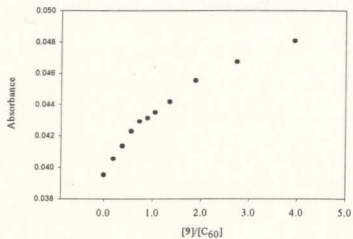


Figure 2.19 Mole ratio plot for the 9:C₆₀ complex in CS₂ at 25 °C.

The corresponding stability constant K_{assoc} for **9** for example, can be defined by equation

(2.2)

$$K_{\text{assoc}} = [C_{90} \cdot \mathbf{9}] / [C_{90}] \cdot [\mathbf{9}] \quad (2.2)$$

and is calculated on the basis of the corresponding Benesi-Hildebrand relationship,³⁴ equation (2.3), where ΔA is the absorbance change at $\lambda = 430$ nm of a solution of C_{90} in the appropriate solvent, upon the successive addition of **9**; $\Delta \epsilon$ represents the difference in the molar extinction coefficient between the $C_{90} \cdot \mathbf{9}$ complex and that of uncomplexed C_{90} .

$$[C_{90}] / \Delta A = 1 / \Delta \epsilon - 1 / (\Delta \epsilon \cdot K_{\text{assoc}} \cdot [\mathbf{9}]) \quad (2.3)$$

Double reciprocal (Benesi-Hildebrand) plots for the **8** C_{90} and **9** C_{90} complexes in toluene, benzene, or CS_2 solutions determined by equation (2.3) are linear, as shown in Figures 2.20 - 2.22 for the complex **8** C_{90} and in Figures 2.23 - 2.25 for the complex **9** C_{90} . K_{assoc} values in each case are calculated by dividing the intercept by the slope (determined by linear regression analysis) of the respective double reciprocal plot. Table 2.1 lists the K_{assoc} values determined at each of five temperatures between 15 and 35 °C for C_{90} and **8** or **9** in each of the three solvents. Equation (2.4), which is obtained from the first derivative of the relationship between K_{assoc} and both the slope and the intercept, is used to calculate the uncertainty ($\sigma_{K_{\text{assoc}}}$) in each value of K_{assoc} :

$$(\sigma_{K_{\text{assoc}}}) = K_{\text{assoc}} \{ (\sigma_{\text{slope}} / \text{slope})^2 + (\sigma_{\text{intercept}} / \text{intercept})^2 \}^{1/2} \quad (2.4)$$

The uncertainties of the individual slopes (σ_{slope}) and intercepts ($\sigma_{\text{intercept}}$) are obtained from the non-linear regression determinations using Sigma-Plot V.3.

As expected, the observed K_{assoc} values at 25 °C are relatively higher than those

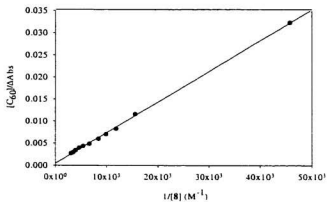


Figure 2.20 Double-reciprocal plot of data for the 8:C₆₀ complex in toluene at 25 °C.

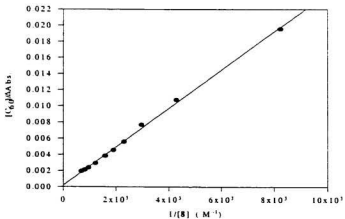


Figure 2.21 Double-reciprocal plot of data for the 8:C₆₀ complex in benzene at 25 °C.

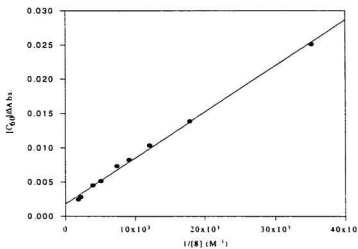


Figure 2.22 Double-reciprocal plot of data for the 8: C_{60} complex in CS_2 at 25 °C.

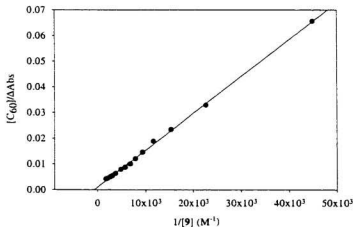


Figure 2.23 Double-reciprocal plot of data for the 9: C_{60} complex in toluene at 25 °C.

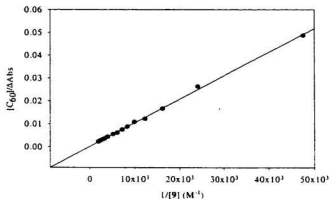


Figure 2.24 Double-reciprocal plot of data for the 9:C₆₀ complex in benzene at 25 °C.

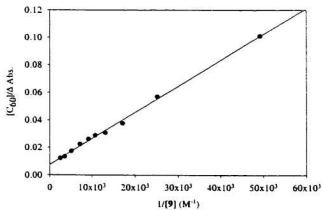


Figure 2.25 Double-reciprocal plot of data for the 9:C₆₀ complex in CS₂ at 25 °C.

observed with the calix[*n*]arenes which have been reported by others.^{43, 44} Shinkai *et al.*^{43, 44} reported that K_{assoc} values for the C_{60} :2 complex in toluene to be $230 \pm 6 \text{ M}^{-1}$, and Averdug *et al.*⁴¹ reported a value of $381 \pm 4 \text{ M}^{-1}$ for the C_{60} : 3 complex in toluene. Thus, it appears as though in addition to the enhanced π - π interactions that may be occurring due to the presence of extra aromatic rings on the naphthalene units, that a solvophobic effect may be present.^{29a} Dormann *et al.*⁵⁸ have shown by thermal gravimetry that CS_2 can form 4:1 complexes with **1** and **2**. On the other hand, toluene can form only 1:1 and 1:1.5 complexes respectively with **1** and **2**. It is therefore conceivable that a similar solvent-complexation could be occurring in our cases and that therefore the displacement of solvent molecules to form 8: C_{60} and 9: C_{60} complexes results in favourable entropic effects, which is typical in solvophobic processes. The trend of K_{assoc} values at 25 °C listed in Tables 2.1 and 2.2 shows that K_{assoc} values increased from benzene to toluene to CS_2 , this trend being opposite to that observed by Haino *et al.*⁶⁷ for calix[5]arene derivatives in toluene solution. To account for their results they argued that the complex formation competes against the solvation of C_{60} in these apolar solvents, since its solubility in CS_2 is highest ($7.98 \text{ mg} \cdot \text{mL}^{-1}$), followed by toluene ($2.1\text{-}3.2 \text{ mg} \cdot \text{mL}^{-1}$) and benzene ($1.4\text{-}1.9 \text{ mg} \cdot \text{mL}^{-1}$).⁶⁹ As shown, the solubility of C_{60} increases in the order, benzene, toluene and CS_2 . The more weakly solvated C_{60} is therefore more strongly attracted to the host. Thus, the complexation process involving the host and C_{60} competes against its solvation.

Other studies^{16, 17} involving complexation between various calix[*n*]arene derivatives and C_{60} in toluene and benzene solutions have reported a similar trend to those shown by

Table 2.1 Log K_{MOC} values for C_{60} with **8** in toluene, benzene and CS_2 , at different temperatures

Temperature	Run	Toluene	Benzene	CS_2
15 °C	1	3.24±0.07	3.07±0.02	3.68±0.06
	2	3.22±0.03	3.13±0.02	3.70±0.02
	Mean values	3.23±0.05	3.10±0.02	3.69±0.04
20 °C	1	3.02±0.05	3.01±0.03	3.56±0.02
	2	2.98±0.02	3.06±0.02	3.57±0.02
	Mean values	3.00±0.04	3.03±0.03	3.57±0.02
25 °C	1	2.82±0.03	2.66±0.06	3.43±0.02
	2	2.83±0.08	2.59±0.08	3.43±0.02
	Mean values	2.82±0.06	2.63±0.07	3.43±0.02
30 °C	1	2.53±0.26	2.52±0.08	3.38±0.02
	2	2.52±0.11	2.59±0.10	3.35±0.02
	Mean values	2.52±0.20	2.56±0.09	3.36±0.02
35 °C	1	2.39±0.11	2.37±0.13	3.24±0.02
	2	2.22±0.26	2.41±0.09	3.25±0.02
	Mean values	2.31±0.18	2.39±0.11	3.24±0.02

Table 2.2 $\text{Log}K_{ow}^*$ values for C_{90} with 9 in toluene, benzene and CS_2 , at different temperatures

Temperature	Run	Toluene	Benzene	CS_2
15 °C	1	3.27±0.04	2.72±0.03	3.83±0.05
	2	3.31±0.08	2.68±0.04	3.81±0.04
	Mean values	3.27±0.06	2.70±0.04	3.82±0.04
20 °C	1	3.12±0.04	2.51±0.05	3.68±0.02
	2	3.15±0.03	2.58±0.03	3.69±0.04
	Mean values	3.14±0.03	2.54±0.04	3.68±0.03
25 °C	1	2.83±0.04	2.49±0.06	3.60±0.02
	2	2.87±0.02	2.47±0.07	3.61±0.04
	Mean values	2.85±0.03	2.48±0.06	3.61±0.03
30 °C	1	2.75±0.08	2.32±0.11	3.53±0.03
	2	2.71±0.08	2.21±0.07	3.52±0.02
	Mean values	2.73±0.08	2.26±0.09	3.52±0.03
35 °C	1	2.58±0.06	2.14±0.11	3.47±0.07
	2	2.60±0.04	2.13±0.08	3.44±0.04
	Mean values	2.59±0.05	2.13±0.10	3.46±0.06

us for the K_{assoc} values. It is our hypothesis that compared to the complexation of C_{60} in toluene or benzene the complexation in CS_2 is accompanied by a larger increase in entropy. This is because relative to toluene and benzene, there is a greater number of CS_2 solvent molecules which are associated with the solutes **8**, **9** or C_{60} . Thus, when desolvation of **8**, **9** or C_{60} occurs in order for a complex to form between **8** and C_{60} , or **9** and C_{60} , a relatively greater number of CS_2 molecules are released into the bulk solution. This will therefore in turn cause more CS_2 molecules compared to toluene or benzene molecules to become free, which will therefore increase the entropy and hence increase the stability of the complexes in CS_2 .

2.3. Thermodynamic Study of the Complexes of Calix[4]naphthalenes with C_{60}

A thermodynamic study has been conducted on the complexation of calix[4]naphthalenes with C_{60} in order to explore our hypothesis involving the solvophobic effect, which is described previously and observed above. The scarcity of thermodynamic data on the complexation of C_{60} with calix[n]arenes or other receptors also motivated us to carry out such a study which provided additional understanding of the complexation process.

Several studies have since been published which have shown that C_{60} also forms supramolecular complexes with various other derivatives of calix[n]arenes, calixresorcenarenes and cyclotrimeratrylene.²⁸ Some of these reports describe formation of solid clathrates with accompanying X-ray structures, while others describe solution studies from which association equilibrium constant values were determined. Most of the data reviewed by Danil de Namor⁷⁰ concern thermodynamic studies of charged ionic guests with

calix[*n*]arene hosts, conducted in polar organic solvents (*e.g.* methanol, acetonitrile, benzonitrile), or in aqueous solution. Furthermore, the thermodynamics of the complexation of fullerenes has not to date been discussed in detail in many papers. With the exception of the data reported by Shinkai *et al.*,⁷¹ there had been no other thermodynamic data reported for complexation of calix[*n*]arenes with C₆₀ in nonpolar organic solvents. After our own thermodynamic results⁷² on the complexation of C₆₀ with calix[4]naphthalenes were published, Shinkai *et al.*^{71b} reported their thermodynamic results on the complexation of *tert*-butylhexahomotrioxacalix[3]arene **19a** with C₆₀ in toluene solution. Fukawaza *et al.*⁷³ also reported their thermodynamic results on the complexation of one of the calix[5]arene derivatives with C₆₀ in toluene and CHCl₃ solutions.

The thermodynamic parameters, ΔH and ΔS were calculated from the corresponding $\log K_{\text{assoc}}$ values at different temperatures using a linear least squares analysis according to equation 2.5:

$$2.303 \log K_{\text{assoc}} = -(\Delta H/R) \cdot (1/T) + (\Delta S/R) \quad (2.5)$$

Plots of $\log_{10} K_{\text{assoc}}$ vs $1/T$ at five different temperatures for C₆₀ and **8** in each of the three solvents tested are shown in Figures 2.26-2.28, and for C₆₀ with **9** in the same tested solvents in Figures 2.29-2.31. All plots are linear and have positive slopes, indicating that the complexation process is exothermic and thus is driven by favourable enthalpy changes. All of the ΔH values determined for C₆₀ and **8** or C₆₀ and **9** in each solvent were exothermic and are listed in Table 2.3. The ΔH values determined for C₆₀ and **8** or C₆₀ and **9** in toluene solution are higher than those noted for the same solvent by Shinkai and Ikeda in their study

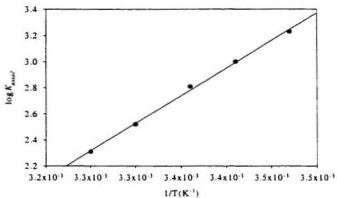


Figure 2.26 van't Hoff plot for the 8:C₆₀ complex in toluene.

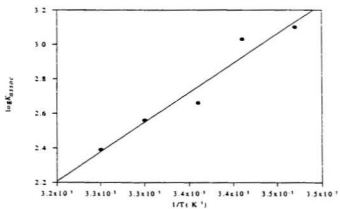


Figure 2.27 van't Hoff plot for the 8:C₆₀ complex in benzene.

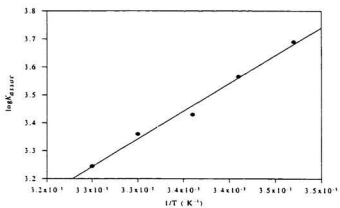


Figure 2.28 van't Hoff plot for the 8: C_{60} complex in CS_2 .

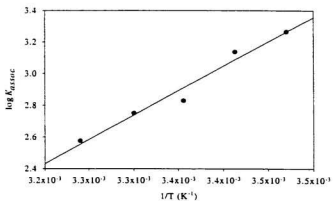


Figure 2.29 van't Hoff plot for the 9: C_{60} complex in toluene.

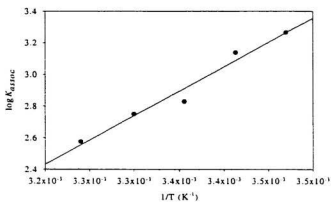


Figure 2.30 van't Hoff plot for the 9: C_{60} complex in benzene.

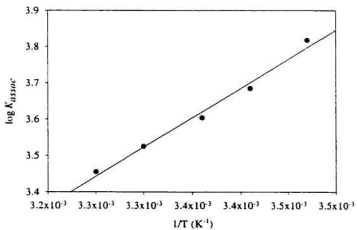


Figure 2.31 van't Hoff plot for the 9: C_{60} complex in CS_2 .

of the complexation of C_{60} and *tert*-butylcalix[5]arene **13**, or *tert*-butylhexahomotrioxacalix[3]arene **19a**^{15b, 24} and also higher than those noted by Fukawaza *et al.*⁷³ in their thermodynamic study on the complexation of calix[5]arene derivative **12** and other derivatives with C_{60} in toluene and $CHCl_3$ solutions. This finding supports the hypothesis that the existence of the extra fused aromatic rings on each naphthalene group in our examples allow for additional attractive π - π interactions. These additional interactions can be either due to the presence of the two extra π -bonds per naphthalene unit as compared with the phenyl groups in calixarenes, or simply due to the fact that the naphthalene rings result in the formation of a deeper and wider cavity, thus potentially allowing for better contact between host and guest.⁷⁴ It is notable that the ΔH values for **9** are lower than those for **8**. This could imply that the *tert*-butyl-methyl- π interactions between the methyl groups of *tert*-butylcalixarene and the π -system of a guest molecule, which were noted by Andreotti *et al.*⁷⁵ to be important considerations, are not factors here. Such interactions accounted for the clathrate formation between toluene and *tert*-butylcalix[4]arene **1** observed by Andreotti *et al.*, and also for an unusual clathrate formed between benzophenone and *tert*-butylcalix[4]arene monotriflate observed by our group.⁷⁶

It is possible however, to rationalize this apparent contradiction by considering that in the present case, the major attractive interactions for complex formation between C_{60} and **8** are the π - π interactions between C_{60} and both of the fused aromatic rings in each naphthalene unit via a deep-cavity inclusion. In the case of complexation between C_{60} and **9** however, a shallower penetration of the guest molecule may be occurring, wherein the *tert*-

butyl-methyl- π interactions may be the dominant ones, thus sterically inhibiting the potentially more effective π - π interactions between the C_{60} guest and the naphthalene rings. Despite the above considerations, however, the K_{assoc} values for the C_{60} -**9** complex are higher than the corresponding values for the C_{60} -**8** complex.

Table 2.3 Thermodynamic values for C_{60} complexes with **8** and **9** in toluene, benzene and CS_2 , at 25 °C

Compound	Solvent	Log K_{assoc}	ΔH	ΔS	$T\Delta S$
			$kJ\ mol^{-1}$	$J\ mol^{-1}\ K^{-1}$	$kJ\ mol^{-1}$
8	Toluene	2.82 \pm 0.06	-77.4 \pm 1.8	-206.8 \pm 4.7	-61.6 \pm 1.4
	Benzene	2.63 \pm 0.07	-65.4 \pm 1.4	-167.1 \pm 3.6	-49.8 \pm 1.1
	CS_2	3.43 \pm 0.02	-38.1 \pm 0.8	-61.7 \pm 1.3	-18.4 \pm 0.4
9	Toluene	2.85 \pm 0.03	-59.7 \pm 1.3	-144.4 \pm 3.1	-43.0 \pm 0.9
	Benzene	2.48 \pm 0.06	-48.2 \pm 1.1	-115.4 \pm 2.5	-34.4 \pm 0.7
	CS_2	3.61 \pm 0.03	-30.9 \pm 0.8	-34.4 \pm 1.4	-10.3 \pm 0.4

The values of both ΔH and ΔS for the complexes in toluene and benzene listed in Table 2.3 become more negative as the K_{assoc} values at 25 °C increase. This may be due to the fact that stronger interactions or non-covalent bonding will increase the enthalpy released from the process and also will lead to a greater reduction in the entropy of the system. The ΔH values are opposite to those that would be predicted simply using the solubility values for C_{60} in benzene (1.4-1.9 mg. ml^{-1}) and toluene (2.1-3.2 mg. ml^{-1}).⁶⁹ However, Haino *et al.*^{45b} have argued that complex formation competes against the solvation of C_{60} in these apolar solvents. The implication therefore would be that in the present study, the ΔH values measured for **8** or **9** in benzene should be higher than the corresponding values in toluene, which is not the case. Nevertheless, if the lower solubility values reported by Letcher *et al.*⁷⁷

for C_{60} in benzene (0.89 mg.ml^{-1}) and toluene (0.54 mg.ml^{-1}) are considered instead, our observed ΔH values are consistent with the trends in the solubilities of C_{60} in toluene, benzene and CS_2 , respectively. Other studies^{45c-47} involving complexation between various calix[n]arene derivatives and C_{60} in toluene and benzene solution have reported similar K_{max} trends to those observed by us.

Table 2.3 also shows that all of the ΔS values are negative, indicating that while complex formation is enthalpy favoured, it is also entropy disfavoured. Formation of the complexes therefore results in a more ordered system, possibly due to the freezing of the motional freedom of both the guest and the host molecules. Tao and Barra have offered a similar rationale for the data that they observed with their particular system.⁷⁸ The magnitudes of the entropy changes observed in CS_2 , benzene and toluene, can be rationalized as follows. During formation of the complex, solvent molecules within the cavity of each calix[4]naphthalene host are displaced by a C_{60} molecule. It is proposed that upon complex formation with C_{60} , more CS_2 solvent molecules than benzene or toluene molecules are displaced. Thus, there is a larger entropy gain achieved from the displacement of CS_2 molecules as compared to the other two solvent molecules.⁷² It is known that more CS_2 molecules are included in calix[n]arene cavities compared to toluene, and presumably to benzene molecules.²¹ It was reported by Olmstead *et al.*⁷⁹ that CS_2 forms a tight complex with C_{60} in which two molecules of C_{60} are non-covalently bonded to three molecules of CS_2 to form an ordered system. Thus, the complexation of C_{60} with calix[n]arenes (and presumably calix[4]naphthalenes) will break this ordered system to form the complex, and

therefore this process will be accompanied by a gain in entropy.

On the other hand, a more ordered state (entropy loss) can result in the case of toluene and benzene due to the solvation of the complex by a "face-to-face" interaction⁶⁰ of these solvent molecules around the complex. This is due to the π - π interactions which are possible between solvent benzene, or toluene with the naphthalene rings of the calix[4]naphthalene molecules, and also with the "aromatic" rings of the C_{60} guest within the complex. The higher ΔH values observed in toluene and benzene solution as compared to CS_2 can also be rationalized in this way. It has been suggested⁷² that a factor which could possibly contribute to the unusual binding trends observed for the different solvents may be desolvation of the fullerene occurring to a lesser degree with the smaller CS_2 molecule as compared with the aromatic solvents.

The entropy changes observed for the complexation of C_{60} and **8** in toluene and benzene solution are larger than those observed for **9**. This reflects the fact that **8** is known to be conformationally more flexible than **9** in solution,¹¹ even though both may become locked in a cone conformation as a result of their complexation with C_{60} , and despite the fact that the rotational freedom inherent in the *tert*-butyl groups on **9** would be expected to add to the entropy of the latter host molecules. It has also been suggested⁷² that a higher degree of residual solvation could also provide some explanation for the smaller entropy loss and hence the stronger binding with the less tightly formed complexes with the *tert*-butyl host.

A linear relationship exists between $T\Delta S$ and ΔH . Such linear relationships are commonly referred to as the enthalpy-entropy compensation or simply, the compensation

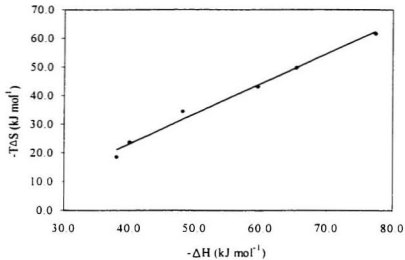


Figure 2.32 The enthalpy-entropy compensation plot for 8 and 9 complexes of with C_{60} .

Table 2.4 The slope (α) and Intercept ($T\Delta S$) of the ΔH - ΔS plot for 1:1 host-guest complexation by various host molecules.

Compound	Slope(α)	$T\Delta S$
		kcal \cdot mol ⁻¹
Glyme/ podand	0.86	2.3
Crown ethers	0.76	2.4
Cryptand	0.51	4.0
Cyclodextrin	0.90	3.1
Calixarenes	1.10	5.0
Calixnaphthalenes.	1.05	4.5

effect.⁸¹ The slope and intercept derived from the linear regression analysis of the plot shown in Figure 2.32 is listed in Table 2.4 along with the data obtained from various host molecules determined by other groups,^{78, 82, 83} although Petersen⁵⁸ pointed out that these relationships can be deceptive. Nevertheless, several authors^{78, 82, 83} have proposed recently that the slopes from $T\Delta S$ vs ΔH plots derived from host-guest complexation studies can be rationalized in terms of the degree of conformational changes of the host during the complexation and that the intercepts can be rationalized in terms of the extent of desolvation upon complexation. Using these arguments, the magnitude of the slope implies that the C_{60} :**8** and C_{60} :**9** complexes are accompanied by large conformational changes and extensive desolvation, as seen from the relatively high intercept values obtained.

In conclusion, association equilibrium constants and thermodynamic parameters have been determined for the complexation of C_{60} and calix[4]naphthalenes **8** and **9** in various commonly employed solvents which have shown that a solvophobic effect and π - π interactions are major driving forces for the complexation process.

2.4 Experimental

Toluene (BDH, Scintillation Grade) was distilled over sodium metal with benzophenone prior to use. Benzene (ACP Chemicals Inc., A.C.S grade, 99%) and CS_2 (Aldrich Chemical Company, Inc., Spectrophotometric Grade, 99+%) were used without further purification. C_{60} (99.5%) was purchased from Aldrich. Calix[4]naphthalenes **8** and **9** were prepared according to methods previously described.¹¹ Uv-vis absorption spectra were recorded on a HP 8452A diode array spectrophotometer with photometric accuracy of

$\pm 0.005\text{AU}$ at 15, 20, 25, 30, 35 °C (the absorption data are shown in the appendix) with thermostated cell compartments. Temperatures were recorded to $\pm 0.1^\circ\text{C}$ with a thermocouple (Kiethley Model 163 digital voltmeter).

To obtain the association equilibrium constants K_{assoc} corresponding to complex formation, changes in absorbance (ΔA) as a function of calix[4]naphthalene concentration were determined. A 2.50 ml aliquot of C_{60} solution (ca. $1.00 \times 10^{-4}\text{M}$ in benzene, toluene or CS_2) was placed in a quartz cell, to which 0.050 or 0.10 mL aliquots from a stock solution (ca. $1.00 \times 10^{-3}\text{M}$) of **8** or **9** (*vide infra*) were added. After each addition and after homogenization of the resulting solutions, the absorption spectra were recorded at $\lambda = 430\text{ nm}$. At least ten data points were measured in each run. Blank solutions consisting of only the solvent were measured before each experiment. A solution of C_{60} in the appropriate solvent was used as the "solvent" with which to prepare the solutions containing **8** or **9**, in order to maintain the concentration of C_{60} constant during the experiment (mole fraction method). Duplicate data sets were obtained for each run. Absorbance was plotted versus concentrations of **8** or **9**.

Linear double reciprocal (Benesi-Hildebrand) plots were used to determine K_{assoc} values from the slope and intercept, obtained from linear regression analyses. Values for K_{assoc} were determined at five different temperatures (288-308 K), from the linear plots of $\log K_{\text{assoc}}$ versus $1/T$. The thermodynamic parameters (*i.e.* enthalpy change ΔH , and entropy change ΔS) for the formation of the complexes were calculated. Each Job plot was constructed from the measurements of the absorbances of series of solutions that were

prepared as follows: A stock solution of ca 1.00×10^{-4} M C_{60} in the solvent under investigation was prepared, then another solution of **8** or **9** with the same concentration in the same solvent was also prepared. A series of solutions with different mole fractions were prepared by mixing the following solutions

- a. 0.200 ± 0.004 mL of C_{60} + 1.80 ± 0.01 mL of **8** or **9** + 0.50 ± 0.01 mL solvent;
- b. 0.40 ± 0.01 mL of C_{60} + 1.60 ± 0.01 mL of **8** or **9** + 0.50 ± 0.01 mL solvent;
- c. 0.60 ± 0.01 mL of C_{60} + 1.40 ± 0.01 mL of **8** or **9** + 0.50 ± 0.01 mL solvent;
- d. 0.80 ± 0.01 mL of C_{60} + 1.20 ± 0.01 mL of **8** or **9** + 0.50 ± 0.01 mL solvent;
- e. 1.00 ± 0.01 mL of C_{60} + 1.00 ± 0.01 mL of **8** or **9** + 0.50 ± 0.01 mL solvent;
- f. 1.20 ± 0.01 mL of C_{60} + 0.80 ± 0.01 mL of **8** or **9** + 0.50 ± 0.01 mL solvent;
- g. 1.40 ± 0.01 mL of C_{60} + 0.60 ± 0.01 mL of **8** or **9** + 0.50 ± 0.01 mL solvent;
- h. 1.60 ± 0.01 mL of C_{60} + 0.40 ± 0.01 mL of **8** or **9** + 0.50 ± 0.01 mL solvent;
- i. 1.80 ± 0.01 mL of C_{60} + 0.200 ± 0.004 mL of **8** or **9** + 0.50 ± 0.01 mL solvent.

The absorbances of these solutions were measured at $\lambda = 430$ nm. The absorbance changes were plotted against the mole fraction of one of the reactants. Duplicate sets of data were collected for each run.

Chapter Three

Synthesis of Hexahomotrioxacalix[3]naphthalenes and Their Binding Properties

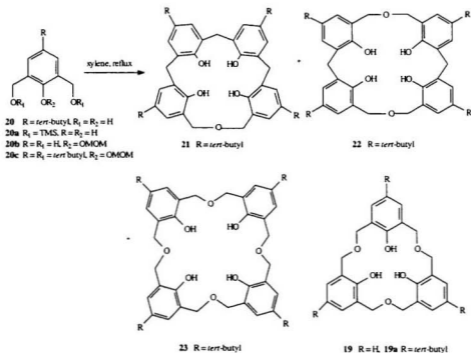
3.1. Introduction

Calixarenes (1-3) and their derivatives continue to be the focus of considerable research activity since they are easily accessible compounds which can show wide-ranging applications as a result of their unique conformational, physicochemical and complexation properties.^{1,84} Most of the chemical modifications of the basic calixarenes have been concerned with modifying either their "upper rims" or their "lower rims" in order to assess and potentially enhance their selectivity towards supramolecular complexation of ionic or neutral species.

Different classes of molecules which are analogues of the calixarenes have been synthesized, such as for example, homocalixarenes, heterocalixarenes and heteracalixarenes. Homocalixarenes such are calixarenes having two or more carbons forming one or more bridges between the aryl moieties,⁸⁵ while heterocalixarenes are calixarenes having their phenolic units substituted by heterocyclic units, such as, calix[4]furan and calix[4]pyrrole. Heteracalixarenes, on the other hand, are calixarenes having the methylene bridges substituted by heteroatoms such as oxacalix[3]arenes.⁸⁵ Homooxacalixarenes have their phenolic units linked by CH_2OCH_2 groups instead of methylene bridges, therefore containing additional methyleneoxy groups in the macrocyclic ring. The best-known example

of these compounds is hexahomotrioxacalix[3]arene **19** whose synthesis involves the cyclotrimerization of 2,6-bis(hydroxymethyl)-4-*tert*-butylphenol **20** as a monomer unit.⁸⁶

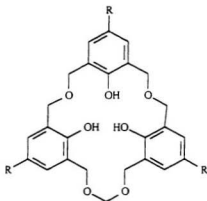
In 1993 Gutsche *et al.*⁸⁶ found that refluxing **20** in xylene affords homooxacalixarenes (**21-23**) in addition to **19** (Scheme 3.1). Vicens *et al.*⁸⁷ reported that compound **19** can be isolated in 6% yield from the mixture of reaction products using column



Scheme 3.1 Synthesis of oxacalixarenes.

chromatography. More recently Hampton *et al.*⁸⁸ reported different and potentially more useful versatile synthetic routes to **19** and other analogues bearing different alkyl

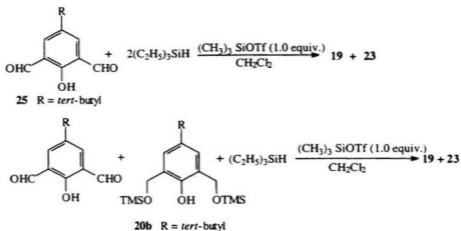
functionalities in their upper-rims and studied the binding of alkali metal cations by these macrocycles. Fuji *et al.*^{89,90} subsequently reported a stepwise synthesis of a variety of hexahomotrioxacalix[3]arenes having different substituents on their upper rims. This



24 R = *tert*-butyl

Figure 3.1 Octahomotetraoxacalix-
[3]arene 24.

synthesis is based on the cyclization of the corresponding linear trimers, or on the condensation reaction between dimers with monomers. They also reported⁸⁵ the synthesis of the tetraoxacalix[3]arene 24, its alkali metal cation binding ability as well as its X-ray crystal structure. The formation of larger homooxacalixarenes from bis(hydroxymethylated) diphenols was reported by Masci.⁹¹ Another synthetic route (Scheme 3.2) was introduced by Komatsu,⁹² in which a reductive homocoupling of 4-substituted-2,6-diformylphenol 25 or heterocoupling with the bis(trimethylsilyl) ether of the 4-substituted-2,6-bis(hydroxymethyl)phenol 20b afforded homooxacalixarenes with different substituents.



Scheme 3.2 Attempted synthesis of oxacalixarenes by reductive homocoupling.

Hexahomotrioxacalix[3]arenes **19** and **19a** have attractive structural properties⁹³ as compared with calix[4]arenes **1** themselves; they have an 18-membered intraannular ring as opposed to the 16-membered intraannular ring of calix[4]arenes. They also have greater conformational mobility compared to calix[4]arenes due to the flexibility of the ether linkages. The existence of a C_3 symmetry element makes these compounds useful receptors for guest species having similar symmetries such as C_{60} and RNi_3 . Nevertheless, despite the fact that these homoxacalixarenes possess the above-mentioned structural features and that some of their derivatives⁹³ show selective ionophoric capabilities, they have received relatively little attention compared to calixarenes. Among recent studies are notable reports from Shinkai's group in which **19a** has been used as a C_3 -symmetrical macromolecular host for chiral recognition of α -amino acid derivatives,⁹⁴ and also as a basic molecular scaffold

on which to generate dimeric capsules, which have served as versatile hosts for C_{60} .⁹⁵ Although compounds **19** and **19a** have received more attention compared to the other oxacalixarenes, all of the oxacalixarenes are potentially interesting candidates for further complexation studies.

As part of our on-going research into developing the chemistry of the calix-naphthalenes⁹⁶ we undertook a program to synthesize hexahomotrioxacalix[3]naphthalene **26**⁹⁷ in order to evaluate its potential as a new inherently chiral supramolecular host or building block. In this Chapter the first synthesis is described of both the C_3 - and C_1 -symmetrical hexahomooxacalix[3]naphthalenes **26** and **27** respectively (Figure 3.2). Also

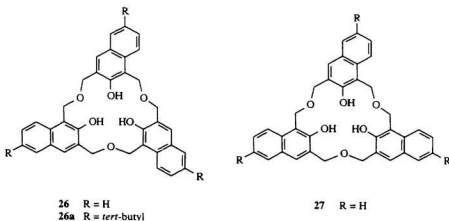


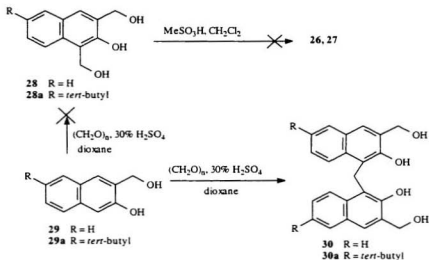
Figure 3.2 C_3 - and C_1 -symmetrical hexahomotrioxacalix[3]naphthalenes.

discussed is a study of the binding properties of alkali-metal cations by **26** using picrate extraction and the binding properties of **26** and **26a** with C_{60} in toluene- d_8 and benzene- d_6 ,

using NMR method. Finally, the X-ray crystal structure for the 2:1 complex of **26a** with C_{60} is described.

3.2. Synthetic Strategy

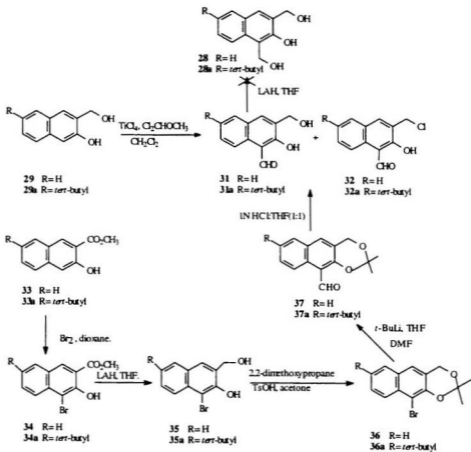
The first synthetic approach towards **26** and/or **27** that was examined employed 1,3-



Scheme 3.3 Attempted synthesis of oxcalixnaphthalenes from **28**.

bis(hydroxymethyl)-2-hydroxynaphthalene (**28**) as the starting compound. This decision was made by analogy to Hampton's⁸⁸ findings that 2,6-bis(hydroxymethyl)-4-substituted phenols self-condensed to form mixtures of oxcalix[3]calixarenes **19** and oxcalix[4]arenes **23**

under high dilution methanesulfonic acid-catalyzed conditions in dimethoxyethane, or CH_2Cl_2 . However in our hands, all attempts at synthesizing **28** directly from 3-hydroxymethyl-2-hydroxynaphthalene (**29**) failed, affording only the dimer **30** in 30% yield



Scheme 3.4 Attempts at the synthesis of **28**.

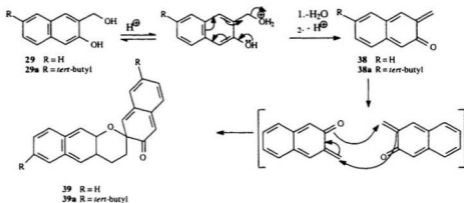
(Scheme 3.3)

An alternative procedure for introducing the hydroxymethyl group at the 1-position of **29** via hydride reduction of the formyl compound **31** is shown in Scheme 3.4. Compound **31** was produced in low yield (18%), upon Rieche formulation of **29**.⁹⁸ This was accompanied by 24% of the chloromethyl product **32**. As a result of this low yield of **31**, this route was not pursued any further.

A different route to **31** was then evaluated (Scheme 3.4), in which bromination of the ester **33** (or **33a**) formed **34** (or **34a**) in 92% (**34a** in 91%) yields. The diol **35** (or **35a**) was obtained in 95% (or **35a** in 54%) yield by the hydride reduction of methyl 4-bromo-3-hydroxy-2-naphthoate **34** (or its 7-*tert*-butyl derivative, **34a**)⁹⁹. The bromoacetone **36** (or **36a**) was prepared in 75% (or **36a** in 74%) yield by reacting of 1-bromo-3-hydroxymethyl-2-hydroxynaphthalene **35** (or **35a**) with 2,2-methoxypropane. Acetone **37** was hydrolyzed in 92% yield by stirring with a 1:1 mixture of aqueous 1M HCl and THF. The precursor acetone **37** itself (or **37a**) was prepared in 87% (or **37a** in 91%) yield by the lithiation of **36** (or **36a**) with *tert*-butyllithium followed by quenching with DMF. Unfortunately, when compound **31** (or **31a**) was finally obtained, its reduction to **28** (or **28a**) was not achieved, instead a mixture of intractable products was obtained.

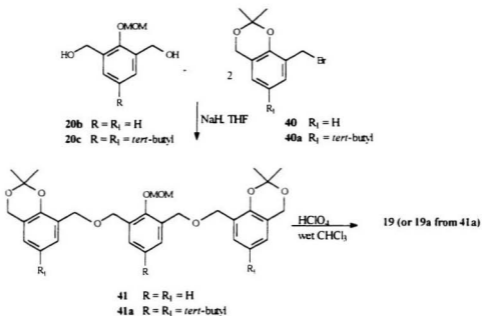
Our experience¹⁰⁰ with **29** under a variety of acidic conditions indicated that hetero-Diels-Alder products **39** (or **39a**) are formed, via *o*-naphthoquinide intermediates (Scheme 3.5). In acidic medium, **29** (or **29a**) loses H₂O to form the *O*-naphthoquinide intermediate

38 (or **38a**) (Scheme 3.5). Hetero [4+2] cycloaddition of **38** (or **38a**) with itself produced the spiro compound **39** (or **39a**). It was concluded therefore, that the direct self-condensation



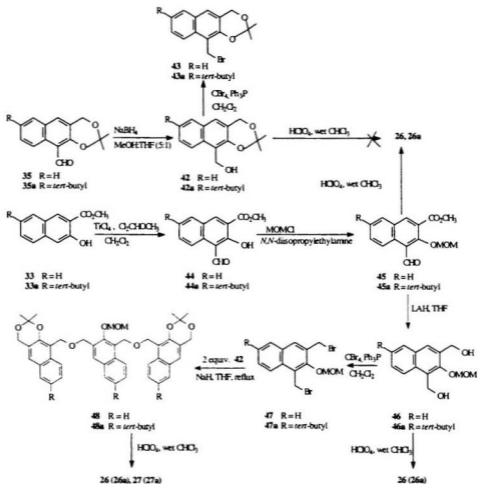
Scheme 3.5 Intermolecular hetero-Diels-Alder reaction of **38**.

approach using **28** (or **28a**) would not likely be successful. During the course of this work, Fuji *et al.*⁸⁹ reported a stepwise convergent synthesis of hexahomotrioxalix[3]arenes **19** and **19a** having different substituents on their upper rims. Their approach involved cyclization of linear “trimers” (N.B.: these are not strictly speaking trimers, but for simplicity they are referred to as such) under high-dilution acidic conditions. These trimers (e.g. **41**) possessed terminal acetonide-bearing aryl rings and were synthesized via alkylation of **20b** with two molar equivalents of the bromomethylacetonides **40** (Scheme 3.6). The corresponding naphthalene ring-based analogues e.g. **48** (or **48a**) were envisioned to be formed by alkylation of **46** (or **46a**) with **43** (or **43a**) (Scheme 3.7). Although the hydroxymethyl acetonide **42** could be obtained in 72% (or **42a** in 51%) yield, its conversion



Scheme 3.6 Synthesis of hexahomotrioxacalix[3]arenes.

to the corresponding bromide **43** was difficult to achieve in good yield (10%). Instead, alkylation of **42** (or **42a**) with the bis(bromomethyl) compound **47** (or **47a**) derived from **46** (or **46a**) was evaluated (Scheme 3.7). Synthesis of the *O*-MOM-protected **46** (or **46a**) was achieved in comparatively good overall yields (40–45%) using a modified route, in which the naphthoate **33** (or **33a**) was formylated using TiCl₄/Cl₂CHOCH₃ conditions to give **44** in 77% (or **44a** in 67%) yield, which in turn was *O*-MOM protected to afford **45** in 85% (or **45a** in 90%) yield. Hydride reduction of **45** (or **45a**) by LAH afforded **46** in 94% (or **46a** in 79%). The desired product(s) could be converted into the corresponding bis(bromomethyl) compounds **47** in 43% yield (or **47a** in 42%) by using CBr₄/Ph₃P conditions. Alkylation of



Scheme 3.7 Synthesis of hexahomotrioxacalix[3]naphthalenes.

47 (or **47a**) with 2 molar equivalents of **42** (or **42a**) in the presence of NaH afforded the linear compound **48** in 98% (or **48a** in 31%) yield.

When **48** was subjected to Fuji's "wet" $\text{CHCl}_3\text{-HClO}_4$ conditions,⁸⁶ two cyclic compounds **26** and **27** were isolated, albeit in low yields (5 and 3 %, respectively). The C_1 symmetrical cyclic compound **27** was anticipated, by analogy with the mechanism proposed by Fuji *et al.*⁸⁶ for their trioxacalix[3]arenes. Formation of the unexpected C_3 -symmetrical **26** however, can be rationalized by presuming that the linear trimer **48** underwent acid-catalyzed ether cleavage as well as the acid-catalyzed acetonide-deprotection, to produce **46** (or possibly the MOM-protected **28**) *in situ*, which could subsequently self-condense to form **26**. Alternatively, the MOM-deprotection step might have occurred after cyclization.

In order to test this hypothesis, **46** was subjected to the same wet $\text{CHCl}_3\text{-HClO}_4$ conditions. Hexahomotrioxacalix[3]naphthalene **26** was produced in this single step and could be isolated in 5-6% yield, which, although relatively low at this stage, indicates an obvious advantage over the convergent route. Its physical and spectral properties were identical with those of the product obtained from the cyclization of the linear trimer **48** (or **48a**). Since this cyclization could be achieved in a single step, a more convenient direct route to **26** was therefore available, one which avoids the prior formation of the linear trimer, and its immediate precursors. Different acid-catalyzed reaction conditions have been investigated in order to improve the yields of **26** from **46**, but thus far have not resulted in any greater improvement in yields. Attempted cyclization of **48** using either Hampton's methanesulfonic acid conditions,⁸⁷ or TFA- CHCl_3 conditions failed to produce any discernable amounts of either **26** or **27**. Using the same conditions that were employed for **46**, cyclization of **46a**

could also be achieved to form the corresponding "upper-rim" *tert*-butyl analogue **26a** in 5-6% yield. All attempts to synthesize **26** or **27** directly from **42** or **42a** respectively, using the same wet $\text{CHCl}_3\text{-HClO}_4$ conditions also failed. Furthermore, the attempts to couple **47** (or **47a**) with **42** (or **42a**) using NaH/ THF under high dilution conditions did not lead to formation of **26** or **27**, respectively.

The ^1H NMR spectrum of **26** in CDCl_3 (Figure 3.3) is very simple, consistent with its predicted C_3 symmetry. Since the two sets of methylene protons appear as singlets at δ

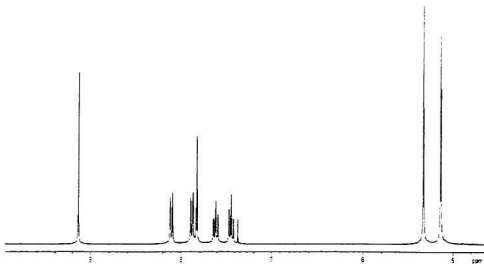


Figure 3.3 ^1H NMR spectrum (CDCl_3) of **26**.

5.02 and 5.20 ppm, the compound is clearly conformationally highly flexible, indicating rapidly interconverting "cone"-like conformers, in which all three hydroxyl groups are on the same face of the 18-membered macrocycle, as opposed to a pair of rapidly interconverting "partial-cone"-like conformers, in which one of the hydroxyl groups is on the opposite face of the macrocycle to the other two. A VT-¹H NMR experiment over the temperature range from 298 K to 203 K showed only a broadening of the hydroxyl proton resonance, and no coalescence temperatures could be observed for the methylene protons. The ¹H NMR spectrum of **26a** is similar to that of **26** apart from the changes due to the presence of the *tert*-butyl groups. Of course, due to the lack of symmetry of the naphthalene rings in either **26** or **26a**, each of the rapidly interconverting cone conformers is chiral.

The lower-rim functionalized bis- and tris((ethoxycarbonyl)methoxy) were also synthesized, and as with the hexahomocalix[3]arenes were found to result in the prevention of interconversion between cone and/or partial cone conformers. The syntheses of these compounds, their conformational and complexation properties with alkali metal cations are discussed in a subsequent chapter.

3.3. Binding of **26** and **26a** with Metal Ions

The ability of **26** or **26a** to bind to silver or alkali metal cations (Rb⁺ not included) was evaluated using a picrate-CHCl₃ extraction procedure.^{101, 102} It was found that both **26** and **26a** showed only weak abilities to bind with the cations investigated (Table 3.1). The absorbances determined spectrophotometrically indicated that with the exception of Na⁺, less than 1 % of **26** binds to the other metals, while **26a** showed a higher binding ability for

K⁺ and Cs⁺, as compared to **26**. Thus the binding of **26** or **26a** with alkali metal cations and silver metal ion is negligible and not significant. These results are consistent with Hampton's reported results with the analogous hexahomotrioxacalix[3]arenes,¹¹ in which he found that less than 0.5% of the ligand bound to the alkali metal ion picrates in CH₂Cl₂. These results are also similar to those observed with compounds **1-3** which also show negligible binding of metal picrates.¹³

Table 3.1 Percentage extractability (%E) of metal picrates into CHCl₃ at 25 °C

	Li ⁺	Na ⁺	K ⁺	Cs ⁺	Ag ⁺
26a Run 1	0.32	0.89	1.12	0.86	0.06
26a Run 2	0.50	1.42	1.98	1.21	0.08
Average	0.40	1.15	1.55	1.04	0.07
26 Run 1	0.61	1.42	0.40	0.46	0.06
26 Run 2	0.47	1.44	0.58	0.35	0.08
Average	0.40	1.43	0.49	0.40	0.07

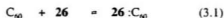
3.4. Complexes of hexahomotrioxacalix[3]naphthalenes with C₆₀

As discussed in a previous chapter the supramolecular complexation of C₆₀ with a variety of macromolecular hosts is a subject of extensive ongoing interest.¹³ In particular, the independent discovery by Atwood,⁶ and later by Shinkai⁷ that *p-tert*-butylcalix[8]arene **3** selectively sequestered C₆₀ from a mixture of higher fullerenes and thus lead to an efficient purification of C₆₀, resulted in many studies involving C₆₀ and other calixarenes. The

complexation of various calixarenes has been discussed in Chapter Two.

Recently, Shinkai *et al.*⁷⁴ showed that *p*-*tert*-butylhexahomooxalix[3]arene **19a** formed inclusion complexes with C₆₀ in solution with 1:1 stoichiometry and K_{assoc} value of $35 \pm 5 \text{ M}^{-1}$ in toluene. In 1998 Fuji and coworkers¹⁰³ reported the first X-ray crystal structure of a 1:1 C₆₀ complex with *p*-bromohexahomooxalix[3]arene and also reported a solution study for the complexes of C₆₀ in toluene with compound **19** and some of its derivatives. They found that K_{assoc} value of $35.6 \pm 0.3 \text{ M}^{-1}$ for the **19**:C₆₀ complex. The synthesis of **26** and **26a** described in the previous sections showed poor alkali-metal cation complexation properties,⁹⁶ but had much stronger complexing abilities with C₆₀. In this Chapter the first X-ray structure of a supramolecular complex formed between C₆₀ and a naphthalene-based calixarene is described.^{296,97} Solution complexation studies using ¹H NMR spectrometry are also described.¹⁰⁴

Supramolecular 1:1 complex formation between **26** (for example) with C₆₀ in solution, can be represented by equation (3.1):



$$K_{\text{assoc}} = [\mathbf{26}:\text{C}_{60}] / [\text{C}_{60}] \bullet [\mathbf{26}] \quad (3.2)$$

The corresponding association constant K_{assoc} can be defined by equation (3.2), and calculated by the Benesi-Hildebrand equation.⁶⁴ This is shown as equation (3.3)¹⁰⁴ where $\delta\Delta$ is the change in chemical shifts upon addition of C₆₀, referenced to uncomplexed **26**, and $\delta\Delta_{\text{nat}}$ is

$$1/\delta\Delta = 1/(\delta\Delta_{m,ar} \cdot K_{assoc} [C_{60}]_0) + 1/\delta\Delta_{m,ar} \quad (3.3)$$

the difference in chemical shifts between those observed in **26** and in the complex, while $[C_{60}]_0$ is the total concentration of C_{60} . Linear plots of $1/\delta\Delta$ against $1/[C_{60}]_0$ for the complexation of C_{60} with **26** and **26a** in toluene- d_6 are shown in Figures 3.4 and 3.5, respectively. Similar plots for the complexation of C_{60} with **26** and **26a** in benzene- d_6 are shown as Figures 3.6 and 3.7, respectively. The values of K_{assoc} are determined from the slope and intercept obtained from a linear regression analysis of these "double reciprocal plots". Table 3.2 lists the values of K_{assoc} at 298 K which were determined for C_{60} with each of **26** and **26a** in toluene- d_6 or benzene- d_6 . The K_{assoc} values listed here are higher than the values reported for the analogous calixarenes: Shinkai *et al.*⁷⁴ reported a value of $35 \pm 5 \text{ M}^{-1}$ for the complex of **19** with C_{60} in toluene using uv-vis measurements, while Fuji *et al.*¹⁰³ reported values of $35.6 \pm 0.3 \text{ M}^{-1}$ for the same complex under the same conditions, and $9.1 \pm 1.0 \text{ M}^{-1}$ for the complex of the unsubstituted **19** with C_{60} in toluene. The latter authors also reported a value of $14.9 \pm 2.0 \text{ M}^{-1}$ for the complex of *p*-bromohexahomooxalix[3]arene with C_{60} in toluene. To our knowledge, there are no other solution studies on these systems that have been reported.

The larger values observed in the present study are consistent with our earlier findings⁷² on the complexation of C_{60} with the closely-related calix[4]naphthalenes. In that study the major attractive interactions for the complex formation between C_{60} and the naphthalene ring-containing ring-containing host molecules was postulated to be due to the

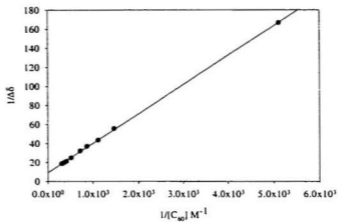


Figure 3.4 Double-reciprocal plot for the complex 26a: C_{60} in toluene- d_6 at 25 °C.

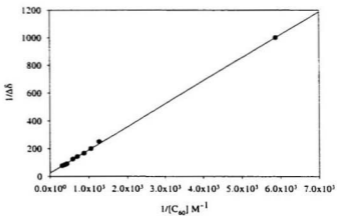


Figure 3.5 Double-reciprocal plot for the complex 26: C_{60} in toluene- d_6 at 25 °C.

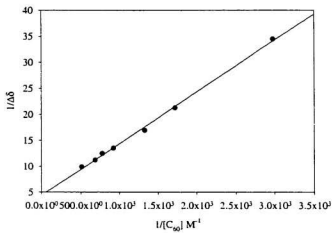


Figure 3.6 Double-reciprocal plot for the complex 26a:C₆₀ in benzene-*d*₆ at 25 °C.

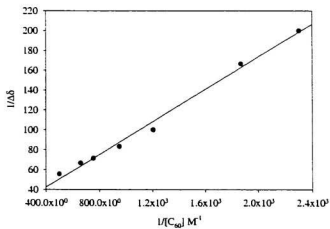


Figure 3.7 Double-reciprocal plot for the complex 26:C₆₀ in benzene-*d*₆ at 25 °C.

Table 3.2 K_{assoc} values for C_{60} complexes with **26** and **26a** in toluene- d_6 and benzene- d_6 at 25 °C.

	Toluene- d_6	Benzene- d_6
26a Run 1	300 ± 9	444 ± 14
26a Run 2	292 ± 9	438 ± 30
Average	296 ± 9	441 ± 23
26 Run 1	146 ± 7	119 ± 7
26 Run 2	154 ± 2	113 ± 5
Average	150 ± 5	116 ± 6

the π - π interactions between C_{60} and both of the fused aromatic rings in each naphthalene unit, via a deep cavity inclusion. The values of K_{assoc} are affected by several factors, among which is the solvent. Haino *et al.*^{45d} showed that the stability of the complex increases as the solubility of C_{60} in the appropriate solvent decreases, since less energy is required for the desolvation of C_{60} which must necessarily precede its complexation with a host molecule. This would explain the higher K_{assoc} value found for the **26a** C_{60} complex in benzene- d_6 , as compared to that in toluene- d_6 , since the solubility of C_{60} is higher in toluene (2.1-3.2 mg mL⁻¹) than in benzene (1.4-1.9 mg mL⁻¹).⁴⁹

In Chapter Two a discussion on the solvophobic effect was presented to explain the values of K_{assoc} .⁷² The solvophobic effect which is mainly entropic was proposed to play a role in our systems and in similar ones, even in non-aqueous solvents.⁷² In Chapter Four are reported the changes in partial molar volumes upon complex formation between C_{60} with **8**, **9**, **26** and **26a**. Those results help to explain the trend in K_{assoc} values. The stoichiometry of

the complex in each solution was determined to be 1:1 from both Job plots⁴³ and the mole ratio method. Job plots for the complexes with **26** and **26a** in toluene-*d*₇ are shown in Figures 3.9-3.10; and for the complexes with **26** and **26a** in benzene-*d*₆ in Figures 3.11-3.12, respectively. All of these figures show maxima in the range of mole ratio = 0.5, which reveal the formation of 1:1 complexes. Figures 3.13-3.14 show the mole ratio plots for the chemical shift changes of all of the protons in **26** and **26a** in toluene-*d*₇, Figures 3.15-3.16 show the chemical shift changes of all of the protons in **26** and **26a** in benzene-*d*₆. It is evident from Figure 3.13 that the hydroxyl proton "H_g" and the aromatic proton labelled "H_h" have the largest changes in their chemical shifts (Figure 3.8). This implies that the C₆₀ guest is included deep into the cavity of **26a** (and **26** shown in Figure 3.13), an interpretation which

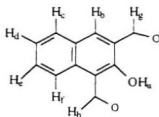


Figure 3.8 Assignment of protons in **26** and (for **26a**, H_d = *tert*-butyl protons for **26a**).

is also supported by the relatively much smaller changes in the chemical shift of the *tert*-butyl protons for **26a**. The +mesomeric effect from the naphthol hydroxy group imparts greater electron density into the naphthalene rings, thereby enhancing the π - π interactions between the electron-rich naphthalene rings and the C₆₀ guest. As a result, a significant shielding effect is experienced by aromatic proton H, and a corresponding deshielding effect.

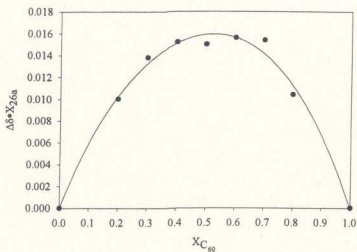


Figure 3.9 Continuous variation plot (Job plot) for the complex 26a: C₆₀ in toluene-*d*₈ at 25 °C.

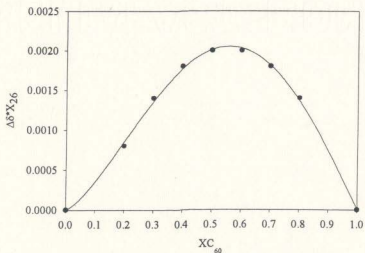


Figure 3.10 Continuous variation plot (Job plot) for the complex 26: C₆₀ in toluene-*d*₈ at 25 °C.

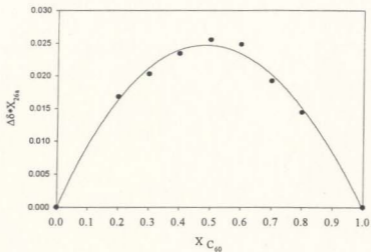


Figure 3.11 Continuous variation plot (Job plot) for the complex 26a: C_{60} in benzene- d_6 at 25 °C.

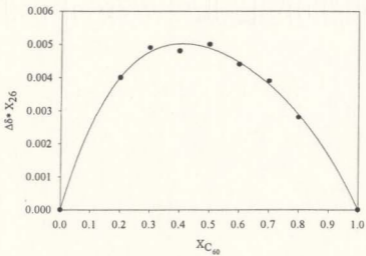


Figure 3.12 Continuous variation plot (Job plot) for the complex 26: C_{60} in benzene- d_6 at 25 °C.

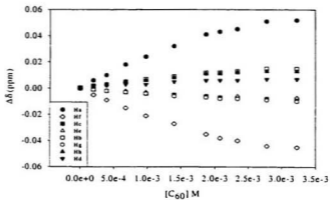


Figure 3.13 Plot of chemical shift changes $\Delta\delta$ vs $[C_{60}]$ for protons H_{a-h} of 26a in toluene- d_6 , $[26a] = 1.279\text{-}3$ M.

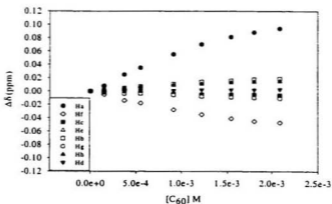


Figure 3.14 Plot of chemical shift changes $\Delta\delta$ vs $[C_{60}]$ for protons H_{a-h} of 26a in benzene- d_6 , $[26a] = 1.122\text{-}3$ M.

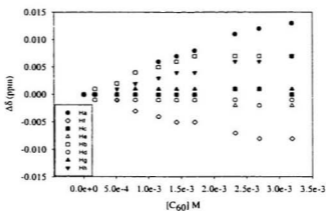


Figure 3.15 Plot of chemical shift changes $\Delta\delta$ vs $[C_{60}]$ for protons H_{a-h} of 26 in toluene- d_8 , $[26] = 1.013e-3$ M.

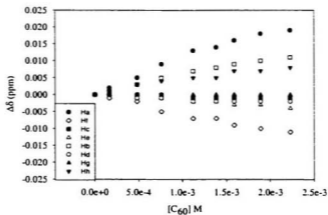


Figure 3.16 Plot of chemical shift changes $\Delta\delta$ vs $[C_{60}]$ for protons H_{a-h} of 26 in benzene- d_6 , $[26] = 1.160e-3$ M.

Shinkai *et al.*⁷⁴ observed larger chemical shift changes for the *tert*-butyl protons than for the hydroxyl and aromatic protons of the shallower cavity-bearing compound, **19**.

The spectral changes induced by the addition of **26a** to a solution of C_{60} in toluene can be seen in Figure 3.17. The most obvious changes are seen at $\lambda = 430$ nm, a finding that is similar to that observed earlier with calix[4]naphthalenes.^{29a}

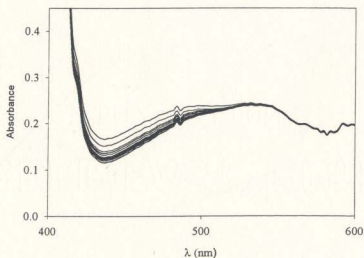


Figure 3.17 Absorption spectra of C_{60} and **26a** in toluene at 25 °C, showing increases in absorption with increasing [**26a**]

Deep red prism crystals having $(26a)_2 : C_{60}$ stoichiometry were obtained from the slow evaporation of a toluene- d_8 solution of C_{60} and **26a**. The single-crystal X-ray structure shown in Figure 3.18 reveals that the complex has C_{3i} symmetry and contains an encapsulated C_{60} molecule within the cavity defined by two molecules of **26a**. The C_{60} molecule adopts a nesting position at the van der Waals contact distance between the two

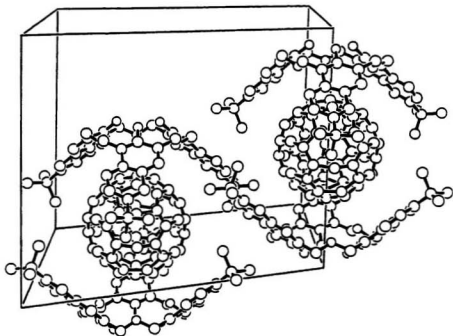


Figure 3.18 X-ray partial packing diagram for $(26a)_2 \cdot C_{60}$ in which the other molecules have been removed for clarity.

concave surfaces of the hexahomotrioxacalix[3]naphthalene. The 18-membered macrocycle of each of the two molecules of **26a** line up with a six-membered ring in the C_{60} , compelling the three adjacent, fused six-membered rings of the C_{60} to reside above the three electron-rich naphthalene units of **26a** to maximize the π - π interactions. Methyl- π interactions similar to those observed in many diverse clathrates of *tert*-butylcalixarenes³⁸ are also evident here as revealed by the methyl groups of each of the *tert*-butyl groups which are directed toward the faces of the remaining six-membered rings in the "equatorial belt" of the C_{60} . Each of the

two molecules of **26a**, which are in *cone* conformations, are staggered with respect to each other, thereby minimizing any potential steric repulsion between them. The C_{60} group in the complex is highly disordered or rotating, and as a result the R values are high; however this phenomenon with other C_{60} examples has been noted by others,^{79, 105} and attempts to refine the R factor by modelling this disorder would not be practical or meaningful.²⁸

There are other instances that have been reported for calixarene: C_{60} complexes, whose solid state compositions have been revealed by their X-ray structures to be different from their solution compositions. For example, Haino *et al.*,^{45a} and Yanase *et al.*¹⁰⁶ reported different solution- and solid-state stoichiometries for C_{60} :calix[5]arene complexes. Atwood *et al.*⁴⁶ reported 2:1 solid-state structures for the complexes of *p*-benzylhexahomotrioxa-calix[3]arene with C_{60} , whereas in solution, 1:1 stoichiometry was determined.

All of the reported X-ray structures show back-to-back stacking of the respective calixarene: C_{60} complexes, in which intermolecular phenolic hydrogen-bonding is present. By comparison, the X-ray structure of the **26a**: C_{60} complex also shows similar back-to-back stacking of the **26a** : C_{60} complexes, but with intermolecular methyl- π interactions being evident.

As noted by other groups^{31,46} symmetry considerations play a significant role in complex formation. Thus, the presence of a common C_3 symmetry element in both **26** and C_{60} facilitates the alignment of both the host and the guest thereby maximizing the number of points of contact within the resulting complex. This, in turn, enhances the overall magnitude of the van der Waals interactions, resulting in the shorter sp^3 - sp^3 distances between C_{60} and

26a as observed from the X-ray data: 3.549(8) Å as compared to 3.615(6) Å reported for the C₆₀ complex with *p*-bromohexahomooxalix[3]arene,¹⁰³ 3.51 Å, and 3.60-3.62 Å for related complexes.

The X-ray structure shown in Figure 3.17 reveals that in each 2:1 complex, a pair of enantiomers of **26a** are present. The complex thus appears to have C_{2h} symmetry.

In conclusion, in this Chapter, it has been demonstrated that supramolecular complexation of C₆₀ with the new class of naphthalene-based homooxalixarenes represented by **26** and **26a**, can exist in both the solid state and in solution. The X-ray structure of the C₆₀ complex with **26a** reveals it to have different stoichiometry from that observed in solution, as determined by ¹H NMR spectrometry.

3.5. Experimental

General Methods. ¹H NMR and ¹³C NMR spectra were recorded at 300 and 75.47 MHz, respectively in CDCl₃ unless otherwise indicated. All reactions were carried out under Ar or N₂ unless otherwise noted. Chromatography was performed with 60 mesh silica gel and preparative layer (1 mm) chromatography (PLC) with standard thin-layer chromatography (tlc) grade silica gel. The complexation study was conducted using BRUKER Avance Instrument at 500 MHz, having a digital resolution of 0.321 Hz. HRMS were conducted at the Department of Chemistry, University of Ottawa, FAB and ESI analysis were conducted by Dr. J. H. Banoub and Mr. G. Sheppard at the North Atlantic Fisheries and Oceans,

Special Project, St. John's, Newfoundland, Canada. Number of ^{13}C NMR peaks in some cases due to coincident may appear less than number of carbon atoms

Dr. M. Ashram is acknowledged for the synthesis of the symmetrical C_{3i} and C_1 hexahomotrioxacalix[3]naphthalene (**26**) and (**27**) from linear trioxatrimmer **48**.

Hexahomotrioxacalix[3]naphthalene (26) and hexahomotrioxacalix[3]naphthalene (27) from linear trioxatrimmer 48. To a solution of **48** (200 mg, 0.31 mmol) in wet⁸⁸ CHCl_3 (40 mL) was added aqueous 60% perchloric acid (0.04 mL). The reaction was stirred at rt for 3 h and was then quenched and washed with water until the aqueous layer was neutral to pH paper. The organic layer was dried with anhydrous MgSO_4 , filtered and the solvent was evaporated on a rotary evaporator to afford a crude product, which was subjected to PLC using CHCl_3 to give the hexahomotrioxacalix[3]naphthalene **26** as a colorless solid. (8 mg, 5 %); m.p. 193-195 °C; ^1H NMR: 5.03 (s, 6H), 5.22 (s, 6H), 7.34 (ddd, $J = 8.7, 7.0, 1.0$ Hz, 3H), 7.52 (ddd, $J = 8.1, 7.0, 1.2$ Hz, 3H), 7.72 (s, 3H), 7.78 (d, $J = 8.1$ Hz, 3H), 8.00 (d, $J = 8.7$ Hz, 3H); ^{13}C NMR : 64.8, 71.8, 115.4, 121.8, 123.3, 125.5, 126.9, 128.2, 128.6, 129.8, 132.8; -EIS MS m/z : 558 (M^+), 557; and **27** as a colorless solid (4 mg, 2 %); m.p. 197-199 °C; ^1H NMR: 4.87 (s, 2H), 4.99 (s, 2H), 5.04 (s, 4H), 5.16 (s, 2H), 5.33 (s, 2H), 7.38-7.50 (m, 3H), 7.58-7.70 (m, 2H), 7.73 (s, 1H), 7.80-7.93 (m, 3H), 8.04 (d, $J = 8.4$ Hz, 1H), 8.21 (d, $J = 8.7$ Hz, 1H), 8.42 (s, 1H), 8.52 (d, $J = 8.7$ Hz, 1H), 8.81 (s, 1H), 8.95 (s, 1H); +FABMS (m/z): 598, 595, 588, 575, 559, 558 (M^+), 528.

Hexahomotrioxacalix[3]naphthalene 26 from 46. Hexahomotrioxacalix[3]naphthalene **26** was also synthesized directly from **46** (1.00 g, 4.03 mmol) as above to give **26** (30 mg, 5%), whose physical and spectral properties were identical with **26** obtained from linear trimer **48**.

tert-Butylhexahomotrioxacalix[3]naphthalene (26a) from 46a. To a stirred solution of **46a** (1.00 g, 3.29 mmol) in wet⁶ CHCl₃ (300 mL) was added aqueous 60% HClO₄ at rt. The reaction mixture was stirred at rt for 2-3 h and monitored by tlc. The reaction was then quenched and washed with water until the aqueous layer was neutral to pH paper. The organic layer was dried with anhydrous MgSO₄, filtered and the solvent was evaporated on a rotary evaporator to afford a crude product which was subjected to flash chromatography using CHCl₃ as solvent, to give **26a** as a pale yellow solid (48 mg, 6 %); m.p. 140-142 °C; ¹H NMR: 1.39 (s, 27H), 5.01 (s, 6H), 5.17 (s, 6H), 7.61 (dd, *J* = 9.0 and 1.8 Hz, 3H), 7.65-7.70 (m, 6H), 7.94 (d, *J* = 9.0 Hz, 3H), 8.82 (s, 3H); ¹³C NMR: 31.2, 34.5, 64.4, 72.0, 115.2, 121.7, 123.5, 125.3, 125.7, 128.1, 129.6, 131.1, 145.9, 153.7; +FABMS (*m/z*): calcd. for C₄₈H₅₄O₈ 726.3920, found 726.4037 (M⁺).

2-Hydroxy-3-hydroxymethyl-1-naphthaldehyde (31). TiCl₄ (1.50 mL, 14.4 mmol) was added to a stirred solution of 3-hydroxymethyl-2-hydroxynaphthalene (**29**) (1.50 g, 8.62 mmol) in anhydrous CH₂Cl₂ (80 mL) at 0 °C, followed by the addition of Cl₂CHOCH₃ (0.70mL, 8.62 mmol). The mixture was stirred for 5 min at 0 °C then allowed to warm to room temperature and stirred for a further 45 min. The reaction was quenched by adding cold water (20 mL). The organic layer was separated and the aqueous layer was extracted with

CH_2Cl_2 (3x20 mL). The combined organic layers were dried over anhydrous MgSO_4 , filtered and the solvent evaporated on a rotary evaporator. The crude product was separated by PLC using ethyl acetate:hexane (3:7) as the solvent system to afford **31** as a yellow solid, (320 mg, 18%); m.p. 91-92 °C; $^1\text{H NMR}$: 2.84 (br s, 1H), 4.83 (s, 2H), 7.39 (t, $J = 7.2$ Hz, 1H), 7.55 (t, $J = 7.2$ Hz, 1H), 7.70 (d, $J = 7.8$ Hz, 1H), 7.94 (s, 1H), 8.20 (d, $J = 8.4$ Hz, 1H), 10.67 (s, 1H); $^{13}\text{C NMR}$: 60.9, 111.0, 118.4, 124.7, 127.3, 128.8, 129.4, 130.0, 132.2, 136.6, 163.2, 193.9; MS m/z (%): 202 (M^+ , 45), 185 (13), 184 (73), 157 (8), 156 (63), 129 (12), 128 (100), 127 (42), 115 (22); HRMS calc'd for $\text{C}_{12}\text{H}_{10}\text{O}_3$ (M^+) 202.0630, found 202.0639. A second major product isolated was **32** as a yellow solid, (450 mg, 24%); m.p. 87-88 °C; $^1\text{H NMR}$: 4.83 (s, 2H), 7.47 (dd, $J = 7.5$ and 7.1 Hz, 1H), 7.65 (dd, $J = 8.5$, 7.1 Hz, 1H), 7.85 (d, $J = 7.5$ Hz, 1H), 8.13 (s, 1H), 8.35 (d, $J = 8.5$ Hz, 1H), 10.83 (s, 1H); $^{13}\text{C NMR}$: 37.7, 108.5, 115.6, 122.1, 124.2, 124.6, 126.8, 126.9, 130.3, 136.2, 160.2, 190.9; MS m/z (%) 223 (4), 222 (26), 221 (11), 220 (M^+ , 82), 186 (14), 185 (100), 157 (15), 156 (33), 129 (34), 128 (91), 102 (12); HRMS calc'd for $\text{C}_{12}\text{H}_8\text{ClO}_2$ (M^+) 220.0291, found 220.0278.

Compound **31** can also be prepared from the acetonide **37** in 92% yield: A solution of **37** (300 mg, 1.24 mmol) in a 1:1 mixture of THF: aqueous 1.0 M HCl (5.0 mL) was stirred at rt for 24 h. The yellow solution was extracted with CHCl_3 (50 mL). The combined organic layers were dried over anhydrous MgSO_4 , filtered and the solvent evaporated on a rotary evaporator to afford **31** (230 mg, 92%) which was pure enough (by tlc) to be used in subsequent reactions.

Methyl 4-bromo-3-hydroxy-2-naphthoate (34). To a solution of methyl 3-hydroxy-2-naphthoate **33** (1.09 g, 5.5 mmol) in dioxane (10 mL) was added a dioxane solution (10 mL) of dioxanedibromide (1.51 g, 5.94 mmol) at rt. The reaction was stirred at rt for 30 min. Cold water was gradually added until a precipitate formed. The precipitate was separated by filtration and washed with water. The product was air dried to afford **34** as a yellow solid (1.39g, 92%)¹¹; m.p. 108-109 °C; ¹H NMR: 4.07 (s, 3H), 7.41 (t, *J* = 8.4 Hz, 1H), 7.66 (t, *J* = 8.4 Hz, 1H), 7.82 (d, *J* = 8.4 Hz, 1H), 8.19 (d, *J* = 8.4 Hz, 1H), 8.50 (s, 1H). ¹³C NMR: 53.0, 106.8, 113.8, 124.5, 125.6, 127.3, 129.6, 130.4, 131.8, 136.0, 152.9, 169.9. MS *m/z* (%) 282 (32), 280 (34), 251 (16), 250 (100), 249 (16), 248 (96), 222 (19), 220 (20), 195 (6), 194 (14); HRMS calc'd for C₁₂H₉BrO₂, 279.9735 found 279.9774

Methyl 4-bromo-7-tert-butyl-3-hydroxy-2-naphthoate (34a). Methyl naphthoate **33a** (300 mg, 1.16 mmol) was subjected to the same reaction conditions as **33** to afford **34a** as a yellow solid (355 mg, 91%), m.p. 111-112 °C. ¹H NMR: 1.42 (s, 9H), 4.06 (s, 3H), 7.75 (s, 1H), 7.78 (dd, *J* = 8.7 and 1.8 Hz, 1H), 8.13 (dd, *J* = 8.7 and 1.0 Hz, 1H), 8.50 (s, 1H); ¹³C NMR: 30.9, 34.6, 52.9, 106.6, 114.1, 124.5, 125.7, 127.5, 129.7, 131.9, 134.5, 147.3, 152.8, 170.2. MS *m/z* (%): 338 (38), 336 (M⁺, 39), 323 (16), 321 (17), 307 (19), 306 (99), 305 (21), 304 (100), 292 (10), 291 (65), 290 (12), 289 (66); HRMS calc'd for C₁₈H₁₇BrO₂, 336.0361 found 336.0348.

1-Bromo-3-hydroxymethyl-2-hydroxynaphthalene (35). To a suspension of LAH (140 mg, 3.58 mmol) in anhydrous THF (10 mL) was added a solution of **34** (500 mg, 1.78 mmol)

in anhydrous THF (10mL) at rt. The reaction was quenched after 5 min by adding into wet diethyl ether (30 mL) at 0 °C. The solution was then acidified with aqueous 10% HCl. The organic layer was separated and the aqueous layer was extracted with diethyl ether (2×10 mL). The combined organic layers were dried over anhydrous MgSO₄, filtered and evaporated on a rotary evaporator to afford **35** as a pale yellow solid (0.45 g, 95%). After washing with CH₂Cl₂, the sample was pure enough for use in subsequent reactions. An analytical sample was purified by PLC using ethyl acetate:hexane (3:7) as solvent system to afford **35** as pale yellow crystals, m.p. 92-93 °C; ¹H NMR: 2.50 (br t, 1H), 4.92 (br d, *J* = 4.8 Hz, 2H), 6.73 (s, 1H), 7.39 (ddd, *J* = 8.7, 7.5, 1.2 Hz, 1H), 7.55 (ddd, *J* = 8.1, 7.5, 1.2 Hz, 1H), 7.66 (s, 1H), 7.74 (d, *J* = 8.1 Hz, 1H), 8.03 (d, *J* = 8.7 Hz, 1H); ¹³C NMR: 62.9, 106.7, 124.5, 125.3, 127.2, 127.7, 128.1, 128.4, 129.2, 132.0, 149.2; MS *m/z* (%): 254 (24), 252 (M⁺, 25), 237 (10), 236 (66), 234 (67), 208 (26), 206 (27), 156 (14), 155 (100); HRMS calc'd for C₁₁H₉BrO₂; 251.9786 found 251.9798.

1-Bromo-6-*tert*-butyl-3-hydroxymethyl-2-hydroxynaphthalene (35a). The naphthoate **34a** (3.42 g, 10.2 mmol) was subjected to the same reaction conditions as **34** to afford **35a** as a colorless solid (1.70 g, 54%); m.p. 106-107 °C; ¹H NMR: 1.41 (s, 9H), 2.52 (br t, *J* = 4.8, 1H), 4.92 (br d, *J* = 4.8, 2H), 6.67 (s, 1H), 7.63-7.69 (m, 3H), 7.97 (d, *J* = 9.0 Hz, 1H); ¹³C NMR: 31.1, 34.4, 63.2, 106.5, 123.3, 125.4, 126.6, 127.1, 128.3, 129.1, 130.3, 147.2, 148.8; MS *m/z* (%): 310 (4), 308 (M⁺, 4), 304 (10), 292 (18), 290 (18), 277 (16), 275 (21),

242 (25), 241 (8), 228 (12), 227 (67), 225 (10), 213 (52), 199 (39); HRMS calc'd for $C_{15}H_{17}BrO_2$ 308.0412 found 308.0405.

1-Bromonaphthalene acetonide 36. To a solution of **35** (400 mg, 1.59 mmol) and 2,2-dimethoxypropane (0.68 mL, 5.57 mmol) in acetone (20 mL) was added a catalytic amount of *p*-toluenesulfonic acid. The reaction was stirred at rt for 24 h. An excess amount of solid $NaHCO_3$ was added to the reaction mixture, which was then filtered and the solvent evaporated on a rotary evaporator. The crude product was dissolved in $CHCl_3$ (20 mL) and the organic layer was washed with water (2x10 mL), dried over anhydrous $MgSO_4$, filtered and evaporated on a rotary evaporator to afford **36** as a pale yellow solid (300 mg, 75%); which was sufficiently pure enough to use in the subsequent reaction; it can also be purified by flash chromatography using $CHCl_3$:hexane (1:1) as solvent system: m.p. 86–87°C, 1H NMR: 1.67 (s, 6H), 5.08 (s, 2H), 7.40 (ddd, $J = 8.4, 6.0$ Hz, 1H), 7.47 (s, 1H), 7.54 (ddd, $J = 8.1, 6.0$ Hz, 1H), 7.72 (d, $J = 8.1$ Hz, 1H), 8.20 (d, $J = 8.4$ Hz, 1H); ^{13}C NMR: 25.0, 61.0, 101.1, 107.6, 121.6, 122.9, 124.5, 125.9, 127.1, 127.6, 129.1, 132.5, 147.0; MS m/z (%): 294 (17), 292 (M^+ , 18), 237 (14), 236 (98), 235 (15), 234 (97), 208 (24), 206 (25), 156 (12), 155 (100), 127 (74); HRMS calc'd for $C_{14}H_{13}BrO_2$ 292.0099 found 292.0120.

7-tert-Butyl-1-bromonaphthalene acetonide 36a. *tert*-butyl naphthoate **35a** was subjected (1.70 g, 5.52 mmol) to the same reaction conditions as **35** to afford a crude product which was purified by flash chromatography using ethyl acetate:hexane (1:9) as solvent system to give **36a** as an oily product (1.42 g, 74%); 1H NMR : 1.40 (s, 9H), 1.64 (s, 6H),

5.05 (s, 2H), 7.43 (br s, 1H), 7.58-7.64 (m, 2H), 8.12 (dd, $J = 10.0$ and 1.0 Hz, 1H); ^{13}C NMR: 24.9, 31.1, 34.8, 61.0, 101.0, 107.2, 121.4, 122.6, 122.8, 125.6, 126.1, 128.9, 130.5, 146.4, 147.4; MS m/z (%): 504 (M-1+ *tosyl*, 6), 351 (26), 350 (5), 348 (M⁺, 24), 293 (18), 292 (100), 291 (22), 290 (91), 277 (12), 275 (10); HRMS calc'd for $\text{C}_{14}\text{H}_{21}\text{BrO}_2$: 348.0725 found 348.0727.

Naphthalenecarboxaldehyde acetonide (37). *tert*-butyllithium (8.52 mL, 14.5 mmol) was added dropwise to a solution of bromo compound **36** (3.86 g, 13.2 mmol) in anhydrous THF (150 mL) at -78 °C. The reaction mixture was stirred at -78 °C for a further 1 h after which time, anhydrous DMF (2.1 mL, 26.4 mmol) was added. The reaction was allowed to warm to rt and was stirred for 16 h after which time it was quenched by adding cold water (20 mL). The reaction mixture was extracted with CH_2Cl_2 (2 \times 30 mL). The combined organic layers were dried over anhydrous MgSO_4 , filtered and the solvent was evaporated on a rotary evaporator to afford crude **37** as a yellow solid (2.81 g, 87%) which can be further purified by washing with methanol. m.p. 126-127 °C; ^1H NMR: 1.69 (s, 6H), 5.10 (s, 2H), 7.42 (ddd, $J = 8.7, 7.8$ Hz, 1H), 7.61 (ddd, $J = 9.9, 7.8$ Hz, 1H), 7.70-7.74 (m, 2H), 9.27 (d, $J = 8.7$ Hz, 1H) 10.85 (s, 1H); ^{13}C NMR: 25.1, 60.6, 101.3, 115.8, 119.9, 122.8, 124.4, 124.8, 124.9, 127.6, 127.8, 129.4, 131.3, 157.4, 191.2; MS m/z (%): 242 (M⁺, 25), 214 (3), 185 (19), 184 (100), 171 (13), 156 (80), 155 (24), 129 (11), 128 (95), 127 (32), 102 (11); HRMS calc'd for $\text{C}_{15}\text{H}_{14}\text{O}_3$: 242.0943 found 242.0942.

6-*tert*-Butyl-naphthalenecarboxaldehyde acetonide (37a). *tert*-butyl bromoacetone **36a**

(1.42 g, 4.08 mmol) was subjected to the same reaction conditions as **36** to afford a viscous oily product (1.10 g, 90%) which was sufficiently pure for the next step. An analytical sample was purified by PLC using ethyl acetate hexane (1.5:8.5) as solvent system. ¹H NMR: 1.40 (s, 9H), 1.64 (s, 6H), 5.05 (s, 2H), 7.62-7.75 (m, 3H), 9.21 (d, *J* = 9.3 Hz, 1H), 10.84 (s, 1H), ¹³C NMR: 24.9, 30.9, 34.3, 60.8, 101.2, 115.7, 122.9, 124.6, 127.7, 128.3, 128.9, 131.4, 147.6, 156.8, 191.3; MS *m/z* (%): 298 (M⁺, 8), 241 (10), 240 (43), 226 (17), 225 (100), 197 (12), HRMS calc'd for C₁₉H₂₂O₃ 298.1569 found 298.1567.

Linear trimer 48. To a suspension of NaH (180 mg, 4.84 mmol) in anhydrous THF (35 mL) was added a THF solution consisting both the dibromo **47** (450 mg, 1.21 mmol) and **42** (595 mg, 2.42 mmol) at reflux temperature over 2 h. The reaction was stirred at reflux temperature for 10 h. The reaction mixture was worked-up by adding cold water gradually and the mixture was extracted with CH₂Cl₂ (2 × 25 mL). The combined organic extracts were dried over anhydrous MgSO₄, filtered and the solvent evaporated on a rotary evaporator to afford **48** as a colorless solid (767 mg, 98%), m.p. 88-90°C; ¹H NMR: 1.56 (s, 6H), 1.60 (s, 6H), 3.40 (s, 3H), 4.80 (s, 2H), 4.90 (s, 2H), 4.98 (s, 2H), 5.06 (d, *J* = 1.0 Hz, 2H), 5.08 (br s, 2H), 5.11 (s, 2H), 5.20 (s, 2H), 7.29-7.49 (m, 7H), 7.70-7.75 (m, 3H), 7.89 (s, 1H), 7.92-7.95 (m, 1H), 8.10 (d, *J* = 8.1 Hz, 1H), 8.17 (d, *J* = 8.7 Hz, 1H); ¹³C NMR: 25.0, 29.7, 57.4, 61.2, 62.0, 62.9, 63.2, 67.7, 101.5, 102.9, 117.4, 117.7, 120.5, 120.6, 123.8, 124.2, 124.3,

124.7, 124.8, 126.2, 126.3, 127.8, 128.1, 128.4, 129.2, 129.3, 130.9, 131.6, 133.0, 133.1, 133.3, 148.3, 148.5, 153.1; +FABMS (NOBA) m/z : 748, 723, 701 ($M^+ + 1$), 685, 657

tert-Butyl linear trimer 48a. The *tert*-butyl precursor compounds dibromo compound **47a** (250 mg, 0.584 mmol) and **42a** (345 mg, 1.15 mmol) were subjected to the same reaction conditions as **48a** to afford after PLC using ethyl acetate: hexane (1:4) as solvent system, a colorless solid (151 mg, 31%), m.p. 90-95°C. $^1\text{H NMR}$ 1.36 (s, 9H), 1.40 (s, 9H), 1.41 (s, 9H), 1.56 (s, 6H), 1.59 (s, 6H), 3.40 (s, 3H), 4.80 (s, 2H), 4.87 (s, 2H), 4.94 (s, 2H), 5.07-5.09 (m, 6H), 5.19 (s, 2H), 7.37-7.68 (m, 9H), 7.85 (d, $J = 8.7$ Hz, 1H), 7.89 (s, 1H), 8.06 (d, $J = 9.3$ Hz, 1H), 8.12 (d, $J = 9.0$ Hz, 1H). $^{13}\text{C NMR}$ 25.0, 31.3, 34.5, 57.4, 61.3, 61.9, 63.0, 67.8, 100.1, 101.7, 117.3, 117.5, 117.6, 120.5, 122.6, 123.1, 123.6, 123.7, 123.8, 124.2, 124.3, 124.4, 125.1, 125.2, 125.3, 128.4, 129.3, 129.3, 129.4, 130.1, 130.9, 131.2, 131.3, 131.5, 146.4, 146.6, 147.3, 147.8, 148.1, 152.8; +FABMS (NOBA) (m/z): 999, 975, 957, 915, 867, 868 (M^+).

1,3-Bis(hydroxymethyl)-2-O-methoxymethylnaphthalene (46). To a suspension of LAH (792 mg, 20.8 mmol) in anhydrous THF (100 mL) was added a THF solution of **45** (1.89 g, 6.90 mmol) at rt. After 5 min the reaction was quenched by pouring into wet diethyl ether (100 mL) at 0 °C. The reaction mixture was then slowly acidified with aqueous 5% HCl until the aqueous layer become slightly acidic. The organic layer was separated and the aqueous layer was extracted with diethyl ether. The combined organic layers were dried over anhydrous MgSO_4 , filtered and evaporated on a rotary evaporator to give **46** as a colorless

solid (1.60 g, 94%); m.p 87-88 °C; ¹H NMR: 2.98 (d, 2H), 3.63 (s, 3H), 4.73 (s, 2H), 5.02 (s, 4H), 7.45 (ddd, *J* = 8.1, 7.5, 1.2 Hz, 1H), 7.54 (ddd, *J* = 8.4, 7.5, 1.2 Hz, 1H), 7.79 (s, 1H), 7.78 (d, *J* = 8.4 Hz, 1H), 8.16 (d, *J* = 8.1 Hz, 1H); ¹³C NMR: 55.9, 56.0, 57.6, 61.8, 100.7, 123.4, 124.0, 125.5, 127.0, 128.4, 129.5, 131.3, 132.8, 133.4; MS *m/z* (%): 248 (M⁺, 2), 216 (7), 187 (5), 186 (35), 185 (16), 158 (27), 157 (27), 141 (10), 130 (6), 129 (21), 128 (26), 127 (17); HRMS calc'd for C₁₄H₁₆O₄ 248.1049 found 248.1041.

6-*tert*-Butyl-1,3-bis(hydroxymethyl)-2-*O*-methoxymethylnaphthalene (46a).

Carboxaldehyde **45a** (1.68 g, 5.10 mmol) was subjected to the same reaction conditions as **46** to afford **46a** after PLC purification, **46a** as a viscous yellow oil (1.22 mg, 79%); ¹H NMR: 1.41 (s, 9H), 2.92 (br, 2H), 3.64 (s, 3H), 4.75 (s, 2H), 5.04 (s, 4H), 7.65 (dd, *J* = 9.0, 2.1 Hz, 1H), 7.75 (d, *J* = 2.1 Hz, 1H), 7.81 (s, 1H), 8.13 (d, *J* = 9.0 Hz, 1H); ¹³C NMR: 31.1, 34.6, 56.0, 57.4, 61.8, 100.7, 123.4, 123.7, 125.9, 127.8, 129.5, 130.7, 131.3, 133.2, 148.2, 152.7; MS *m/z* (%): 304 (M⁺, 4), 272 (4), 242 (16), 228 (7), 227 (39), 213 (17), 199 (11). HRMS calc'd for C₁₈H₂₄O₄ 304.1674 found 304.1670.

1-Bromomethylnaphthalene acetone 43. To a solution of alcohol **42** (180 mg, 0.74 mmol) and CBr₄ (370 mg, 1.11 mmol) in anhydrous THF (40 mL) at 0 °C was added a THF solution (10 mL) of Ph₃P (390 mg, 1.48 mmol). The reaction was stirred and allowed to gradually warm to rt. After 6 h, the reaction was worked up by filtering off the colorless precipitate and evaporating the solvent. The residue was purified by PLC using CHCl₃ petroleum ether (1:1) to afford **43** as a colorless solid (35 mg, 15%); m.p. 86-87 °C

(decomposes upon standing), $^1\text{H NMR}$: 1.64 (s, 6H), 4.66 (s, 2H), 5.20 (s, 2H), 7.30-7.76 (m, 5H), $^{13}\text{C NMR}$: 24.4, 28.5, 59.6, 61.1, 120.66, 124.0, 127.2, 128.7, 129.2; MS m/z (%): 308 (3), 306 (M $^+$, 3), 250 (5), 248 (5), 170 (13), 169 (100), 142 (4), 141 (28), 140 (4), 139 (11).

1-Hydroxymethylnaphthalene acetone 42. NaBH_4 (35 mg, 0.91 mmol) was added to a solution of aldehyde **35** (220 mg, 0.91 mmol) in a mixture of MeOH:THF (5 mL:1 mL) at 0°C. The reaction was stirred for a further 1 h at 0°C. The reaction mixture was quenched by adding cold water (5 mL) and was then extracted with CHCl_3 (2 \times 10 mL). The combined organic extracts were dried over anhydrous MgSO_4 , filtered and the solvent evaporated on a rotary evaporator to afford **42** as a colorless solid (160 mg, 72%), m.p. 153-154 °C. For a larger scale sample, the product can be purified by washing with diethylether. $^1\text{H NMR}$: 1.63 (s, 6H), 1.92 (t, $J = 6.3$ Hz, 1H), 5.07 (s, 2H), 5.15 (d, $J = 6.3$ Hz, 2H), 7.35 (ddd, $J = 8.1, 6.9, 1.2$ Hz, 1H), 7.47 (br s, 1H), 7.49 (ddd, $J = 8.4, 6.9, 1.5$ Hz, 1H), 7.73 (d, $J = 8.1$ Hz, 1H), 8.09 (d, $J = 8.4$ Hz, 1H), $^{13}\text{C NMR}$ (acetone- d_6): 25.4, 54.5, 61.8, 101.0, 122.3, 124.5, 124.7, 124.9, 126.8, 128.9, 129.7, 133.9, 148.6; MS m/z (%): 244 (M $^+$, 15), 187 (6), 186 (52), 185 (15), 159 (11), 158 (100), 157 (79), 141 (10), 130 (16), 129 (34), 128 (27), 115 (21). HRMS calc'd for $\text{C}_{15}\text{H}_{16}\text{O}_3$: 244.1099 found 244.1098.

6-tert-Butylhydroxymethylnaphthalene acetone 42a. The *tert*-butyl aldehyde **35a** (970 mg, 3.24 mmol) was subjected to the same reaction conditions as **35**. The crude product was purified by flash chromatography using ethyl acetate:hexane (3:7) as solvent system to afford **42a** as a colorless semi-solid (496 mg, 51%): $^1\text{H NMR}$: 1.41 (s, 9H), 1.62 (s, 6H), 2.02 (br

t, $J = 6.3$ Hz), 5.06 (s, 2H), 5.15 (br d, $J = 6.3$, 2H), 7.45 (br s, 1H), 7.60 (dd, $J = 9.0$, 2.1 Hz, 1H), 7.66 (d, $J = 2.1$ Hz, 1H), 8.05 (d, $J = 9.0$ Hz, 1H); ^{13}C NMR: 25.0, 31.1, 34.6, 55.4, 61.2, 100.1, 120.3, 120.6, 122.7, 122.9, 123.9, 125.5, 128.4, 130.1, 146.5, 147.4; MS m/z (%): 300 (M⁺, 17), 243 (16), 242 (88), 227 (36), 214 (48), 213 (100), 200 (11), 199 (73); HRMS calc'd for $\text{C}_{19}\text{H}_{22}\text{O}$, 300.1725 found 300.1700.

1,3-Bis(bromomethyl)-2-*O*-methoxymethylnaphthalene (47). To a mixture of **46** (1.55 g, 6.27 mmol) and Ph₃P (6.59 g, 25.0 mmol) in anhydrous CH_2Cl_2 (100 mL) was added CBr_4 (8.24 g, 25.0 mmol) in small portions over 10 min. The reaction was stirred for an additional 10 min and then quenched by adding cold aqueous 10% NaHCO_3 until the aqueous layer became basic. The organic layer was separated and then washed with several portions of cold water until the aqueous layer was neutral. After drying over anhydrous MgSO_4 , filtering and then evaporating the solvent a viscous product was obtained which was purified by flash chromatography using ethyl acetate/hexane (1/9) as the solvent to give **45** as a colorless solid (1.01 g, 43%), m.p. 114–115 °C and which decomposes on standing at rt for any length of time; ^1H NMR: 3.76 (s, 3H), 4.80 (s, 2H), 5.10 (s, 2H), 5.38 (s, 2H), 7.52 (ddd, $J = 8.1$, 6.9, 1.2 Hz, 1H), 7.66 (ddd, $J = 8.4$, 6.9, 1.2 Hz, 1H), 7.85 (d, $J = 8.1$ Hz, 1H), 7.96 (s, 1H), 8.12 (d, $J = 8.4$ Hz, 1H); ^{13}C NMR: 25.1, 29.2, 30.4, 57.8, 100.4, 122.5, 123.7, 124.7, 125.9, 127.6, 128.0, 128.7, 131.2, 132.4, 153.0; MS m/z (%): 376 (0.1), 374 (0.5), 280 (1), 278 (1), 250 (6), 248 (6), 182 (2), 172 (2), 171 (13), 170 (19), 169 (100), 142 (11), 141 (41), 115 (25); HRMS calc'd for $\text{C}_{11}\text{H}_{14}\text{Br}_2\text{O}_2$, 371.9361 found 371.9350.

1,3-Bis(bromomethyl)-6-*tert*-butyl-2-*O*-methoxymethylnaphthalene (47a). The *tert*-butyl diol **46a** (1.14 g, 3.74 mmol) was subjected to the same reaction conditions as **46** to afford after flash chromatography using ethyl acetate:hexane (1:9) as the solvent, **47a** as a pale yellow oil (669 mg, 42%); ¹H NMR: 1.44 (s, 9H), 3.75 (s, 3H), 4.80 (s, 2H), 5.10 (s, 2H), 5.37 (s, 2H), 7.74-7.80 (m, 2H), 7.94 (s, 1H), 8.06 (d, *J* = 9.0 Hz, 1H); ¹³C NMR: 24.8, 25.5, 29.6, 31.1, 34.7, 57.8, 100.3, 122.3, 123.4, 123.7, 123.8, 125.2, 126.6, 126.9, 130.5, 131.0, 131.2, 132.4, 132.5, 148.7, 152.3; MS *m/z* (%): 350 (3), 348 (4), 306 (4), 304 (3), 293 (18), 292 (100), 291 (20), 290 (98), 277 (22), 275 (22), 249 (6), 225 (52), 211 (52), 196 (13); HRMS calc'd for C₁₈H₂₂Br₂O₂ 427.9986 found 427.9996.

Methyl 4-formyl-3-hydroxy-2-naphthoate (44). To a solution of the methyl ester **33** (9.2 g, 45.5 mmol) in anhydrous CH₂Cl₂ (185 mL) was added TiCl₄ (8.28 mL, 76.2 mmol) at rt, followed by Cl₂CHOCH₃ (12.9 mL, 138 mmol) The reaction mixture was refluxed for 2 h, then quenched by slowly adding cold water while cooling the reaction mixture at 0 °C. The mixture was diluted with 50 mL of CH₂Cl₂. The organic layer was separated, dried in the usual manner, and concentrated on a rotary evaporator. The crude product was dissolved in 20 mL of CHCl₃, the solution was boiled with 0.40 g charcoal and the hot solution was filtered. The filtrate was evaporated to give **44** as a yellow solid (8.10 g, 77%); m.p. 140-141 °C; ¹H NMR: 4.06 (s, 3H), 7.43 (ddd, *J* = 8.1, 6.9 and 1.2 Hz, 1H), 7.70 (ddd, *J* = 8.6, 6.9, 1.5 Hz, 1H), 7.83 (d, *J* = 8.1 Hz, 1H), 8.69 (s, 1H), 9.11 (d, *J* = 8.7, 1H), 10.94 (s, 1H), 12.03 (br s, 1H); ¹³C NMR: 52.9, 123.9, 125.1, 126.4, 130.3, 132.5, 134.5, 140.5, 163.8,

191.9; MS m/z (%): 230 (M^+ , 37), 202 (27), 197 (11), 171 (13), 170 (100), 142 (43), 114 (30), 113 (25); HRMS calc'd for $C_{13}H_{10}O_4$ 230.0579 found 230.0576. **Methyl 6-*tert*-butyl-4-formyl-3-hydroxy-2-naphthoate (44a)**. *tert*-Butyl methyl ester **33a** (1.00g, 3.88 mmol)¹⁴ was subjected to the same reaction conditions as **15** to afford after PLC purification, **44a** as a dark yellow solid (747 mg, 67%); m.p. 220-221 °C; 1H NMR: 1.40 (s, 9H), 4.05 (s, 3H), 7.75 (d, $J = 1.8$ Hz, 1H), 7.80 (dd, $J = 9.3$ and 2.1 Hz, 1H), 8.68 (s, 1H), 9.04 (d, $J = 9.0$ Hz, 1H), 10.91 (s, 1H), 11.92 (br s, 1H); ^{13}C NMR: 30.9, 34.4, 52.7, 114.6, 123.4, 125.1, 126.4, 131.5, 132.8, 140.6, 147.9, 163.3, 169.1, 191.7; MS m/z (%): 286 (M^+ , 52), 272 (9), 271 (51), 258 (12), 239 (55), 226 (100), 211 (16); HRMS calc'd for $C_{17}H_{18}O_4$ 286.1205 found 286.1199.

Methyl 4-formyl-3-*O*-methoxymethyl-2-naphthoate (45). To a solution of ester **44** (100 mg, 0.435 mmol) in anhydrous CH_2Cl_2 (10 mL) at rt was added MOMCl (0.10 mL, 1.305 mmol) followed with 0.33 mL (1.74 mmol) of diisopropylethyl amine. The mixture was refluxed for 30 min, cooled to rt and then the organic layer was washed gradually with portions of aqueous 1% HCl until the aq. layers became acidic. Drying and evaporating the solvent afforded **45** as a yellow solid (110 mg, 85%); m.p. 63-64 °C; 1H NMR: 3.61 (s, 3H), 3.98 (s, 3H), 5.23 (s, 2H), 7.57 (ddd, $J = 8.1, 6.9, 1.5$ Hz, 1H), 7.75 (ddd, $J = 8.7, 6.9, 1.5$ Hz, 1H), 7.90 (d, $J = 8.1$ Hz, 1H), 8.67 (s, 1H), 9.23 (d, $J = 8.7$ Hz, 1H), 10.84 (s, 1H); ^{13}C NMR: 52.6, 58.2, 102.6, 123.44, 125.22, 126.7, 129.3, 131.5, 132.6, 139.8, 160.9, 165.5, 193.3; MS

m/z (%): 274 (M^+ , 2), 243 (5), 242 (7), 229 (8), 198 (2), 197 (12), 170 (14), 45 (100); HRMS calc'd for $C_{13}H_{14}O_3$, 274.0841 found 274.0832.

Methyl 7-*tert*-butyl-4-formyl-3-*O*-methoxymethyl-2-naphthoate (45a). *tert*-Butyl methyl ester **44a** was subjected to the same reaction conditions as **46** to afford after PLC purification, **45a** as an oily yellow product (297 mg, 90%), 1H NMR: 1.39 (s, 9H), 3.60 (s, 3H), 3.98 (s, 3H), 5.21 (s, 2H), 7.81 (s, 1H), 7.83 (dd, $J = 9.0$ and 1.2 Hz, 1H), 8.66 (s, 1H), 9.15 (d, $J = 9.0$ Hz, 1H), 10.83 (s, 1H); ^{13}C NMR: 30.8, 34.6, 52.5, 58.0, 102.6, 123.2, 124.3, 124.8, 129.8, 130.7, 140.1, 149.4, 165.5, 193.2; MS *m/z* (%): 330 (M^+ , 10), 299 (8), 285 (25), 284 (23), 269 (20), 255 (8), 253 (21), 226 (44); HRMS calc'd for $C_{19}H_{22}O_3$, 330.1467 found 330.1486.

Metal picrate binding studies. Extractions of metal picrates from deionized water into chloroform (spectrograde) were performed according to the following typical procedure: 5.00 mL of an aqueous 1.00×10^{-4} M solution of the metal picrate and 5.00 mL of a chloroform 1.00×10^{-4} M solution of **26** or **26a** in $CHCl_3$ were mechanically shaken in a teflon[®]-lined stoppered glass tube for 24 h. The mixture was then equilibrated in a thermostated water bath at 25.0 ± 0.1 °C for 2 h in order to achieve good phase separation. The absorbance of the metal picrate remaining in the aqueous phase was then determined spectrophotometrically at 358 nm on a HP 8452A diode array UV-vis spectrophotometer. Percentage extraction (%E) is calculated from the expression $\%E = 100(A_0 - A)/A_0$. Where A_0 is the absorbance of the aqueous solution of the metal picrate without **26** or **26a**.

The alkali metal picrates were prepared⁴² by adding stepwise a 0.02 M aqueous solution of picric acid to a 0.2 M aqueous solution of metal hydroxide, until neutralization. The picrate is then filtered off and recrystallized from water.

The alkali metal picrates were prepared⁴² by adding stepwise a 0.02 M aqueous solution of picric acid to a 0.2 M aqueous solution of metal hydroxide, until neutralization. The picrate is then filtered off and recrystallized from water.

Complexation studies. Compounds **26** and **26a** were prepared according to the methods described above. All ¹H NMR spectra were recorded at 500 MHz at 25 °C in toluene-*d*₆ (99.6%) and benzene-*d*₆ (99.6%). Mass determinations were done on a CAHN-27 electromicro-balance which is capable of mass determinations to 5 × 10⁻⁷ g. To obtain the association constants K_{assoc} corresponding to complex formation, changes in the chemical shifts ($\Delta\delta$) as a function of $[C_{60}]$ were determined. Approximately 1.0 mg of the compound was dissolved in 1.0 mL of the desired solvent in an NMR tube, to which were added portions of C_{60} (approximately 0.100 mg amounts). After sonication for 15 min to dissolve all of the C_{60} the NMR data was collected. At least 8-10 data points were collected for each run and a duplicate data set was obtained for each run. The changes in ($\Delta\delta$) were plotted against $[C_{60}]$ for each run, and the resulting plots show the formation of plateaus around a 1:1 ratio of C_{60} and **26** or **26a**, indicating the formation of a 1:1 complex in each case. These molar ratios were confirmed from Job plots in which the mole fraction of C_{60} was plotted against the mole fraction of **26** or **26a** multiplied by ($\Delta\delta$) for which the maxima are around

Chapter Four

Volumetric Study of the Complexation of Calixnaphthalenes with C_{60}

4.1. Introduction

Volumetric studies have been shown to provide useful information concerning the role of a solvent in biochemical and physicochemical processes, for example, protein folding,¹⁰⁶ DNA-ligand interactions,¹⁰⁷ micelle formation,¹⁰⁸ complex formation between crown ethers with alkali and alkaline earth cations in aqueous solution,^{109, 110} and complex formation between cyclodextrins with anions,¹¹¹ sucrose¹¹² and surfactants.¹¹³⁻¹¹⁵

Hoiland *et al.*¹⁰⁹⁻¹¹¹ reported volumetric studies on the complexation of crown ethers with cations and cyclodextrins with anions in aqueous solutions. They found that in the case of cation-crown ether complex formation the volume changes are positive and that the cations become dehydrated as they entered the crown ether cavity.¹¹⁰ In the case of anion-cyclodextrin complexes they found that the volume changes are negative, indicating that dehydration of the anions does not occur.¹¹¹ Bakshi¹¹² reported a host-guest interaction, volumetric study of the complexation of sucrose with β -cyclodextrin in water. His results show that formation of inclusion complexes between sucrose and cyclodextrin molecules occurred with 1:2 and 1:1 mole ratios. Other volumetric studies¹¹²⁻¹¹⁵ in which the complexation of β -cyclodextrin (or modified cyclodextrin) with hydrocarbon or fluorocarbon surfactants in aqueous solutions have been reported. Another group reported¹¹⁶ a volumetric study on the complexation between a calix[4]resorcinarene derivative, or a 18-crown-6 derivative, D- α -manno-naphtho-18-crown-6 (Figure 4.1), with

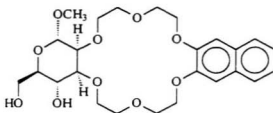


Figure 4.1 D- α -manno-naphtho-18-crown-6.

dipeptides in aqueous solution. They stated that the complexation of dipeptides is different depending on the nature of the host macrocyclic receptor, with the magnitude of the interactions being much larger with the crown ether. They also reported a 5.5 mL mol^{-1} volume change upon the complexation of alanine-serine dipeptide with the calix[4]resorcinarene derivative.

Earlier, in 1992, Letcher *et al.*¹¹⁷ reported a volumetric study on 18-crown-6 in organic solvents with different polarities and molar volumes. They concluded that the partial molar volume of 18-crown-6 itself at infinite dilution showed a remarkable dependency on the molar volume of the solvent. The partial molar volume of the crown ether was found to increase as the solvent molar volume increased. In 1996 Ruelle *et al.*¹¹⁸ determined the partial molar volume of solid C_{60} at infinite dilution in each of 12 different organic solvents. They found, among other things, that the limiting partial molar volume increases roughly proportionally with decreasing solubility of C_{60} in the particular solvent.

Isaacs *et al.*¹¹⁹ reported a volumetric study on molecular inclusion of 3-nitrophenol or methylorange by α -cyclodextrin. They found that the reaction volume ($\Delta V_{c \rightarrow 0}$) associated

orange encapsulation by two molecules of α -cyclodextrin was $27 \text{ mL}\cdot\text{mol}^{-1}$. These volume changes were interpreted in terms of displacement of solvent molecules from the cavity of α -cyclodextrin and/or solvation of the guest molecule.

As described above, several studies have been reported dealing with "host-guest" interactions using different hosts and guests, but in none of these studies was C_{60} used as a guest. In 1997 however, Isaacs *et al.*⁴⁹ reported a volumetric study of the inclusion complex of C_{60} with *p*-benzylcalix[5]arene **11**, in toluene. They found that the change in the partial molar volume due to the complexation is $195 \text{ mL}\cdot\text{mol}^{-1}$ which was proposed to be associated with the displacement of two molecules of toluene from the cavity of the calixarene. These authors measured the change in partial molar volume using a high-precision densitometer. This technique was used earlier by Ruelle *et al.*¹¹⁸ to measure the partial molar volume of C_{60} itself in different solvents. Their densitometric analysis were based on Liron and Cohen's method^{120,121} for determining limiting partial molar volumes of various solutes at infinite dilution.

The inclusion properties of container molecules or cavitands with guest molecules in general is a subject of considerable current interest¹⁵ and there are many recent studies which have been reported that are concerned with the inclusion complexes of C_{60} with various host molecules such as calixarenes, resorcinarenes and cyclotrimeratrylene.¹²² Volumetric studies using high-precision densitometry is a potentially general and simple experimental method to probe the nature of these "host-guest" interactions in solution.^{49,119} However, at the outset of this work there had not been any other studies reported beside

those described above.

We have shown previously in Chapter Two that the *endo*-calix[4]naphthalene **8** and its *tert*-butylated derivative **9**, form stable inclusion complexes with C_{60} . These results have been published.^{26a,72} The respective association equilibrium constants K_{assoc} determined for the 1:1 supramolecular complexes in benzene, toluene or CS_2 solution were found to increase from benzene to toluene to CS_2 and the hypothesis was presented that this trend could be due to a solvophobic effect.¹⁵ The results obtained from the thermodynamic study on the above systems also discussed in Chapter Two were consistent with this hypothesis. In order to ascertain whether partial molar volume changes could provide further insights into the nature of the inclusion complexation observed, high-precision densitometry was employed. The results and their interpretation are presented in this Chapter

4.2. Volumetric Study of **8** and **9** with C_{60}

The partial molar volume of a solute, v_x is the change in volume of its solution V , as a function of the change in the number of moles of the solute, n_x as shown in equation (4.1):

$$v_x = \delta V / \delta n_x \quad (4.1)$$

The partial molar volume v_x can be obtained by an extrapolation to infinite dilution, of the plot of V_σ against the molality of the solution. V_σ , the apparent molar volume¹²³ is given by equation (4.2) where m is the molality of the solution and ρ_1 is the density of the solvent, ρ is the density of the solution, and M_x is the molar mass of solute x :

$$V_\sigma = 1 / m_x [(1000 + m_x M_x) / \rho - (1000 / \rho_1)] \quad (4.2)$$

Since the concentrations of the solutions which were employed were very dilute ($\sim 10^{-4}m$), extrapolations were not conducted to infinite dilutions as Isaacs and Young¹¹⁹ did in their study. Nevertheless, the average of the V_{ϕ} values which were obtained could be shown to represent very closely the calculated values which could be expected at infinite dilutions. The partial molar volumes were calculated using equation (4.2) with the average V'_{ϕ} values are shown in Tables 4.1 and 4.2 as Method *a*.

Figures 4.2-4.4 show the plots of V'_{ϕ} versus molality for the solutions in toluene, benzene, and CS₂ of C₆₀, **8** and the presumed 1:1 complex, respectively. Figures 4.5-4.7 show the plots of V'_{ϕ} versus molality for the solutions in toluene, benzene, and CS₂ of C₆₀, **9** and the presumed 1:1 complex respectively. Young's equation¹²⁴ (equation 4.3) was applied to the calculations for the partial molar volumes of the 1:1 complexes of C₆₀ with **8**, and **9**. In equation (4.3), χ_n is the mole fraction and $V'_{\phi n}$ is the apparent molar volume of

$$V'_{\phi} = \sum \chi_n \cdot V'_{\phi n} \quad (4.3)$$

each solute in a multicomponent system of *n* solutes. Table 4.2 contains the corresponding data for the volumetric studies on the complex formation between C₆₀ and **8**.

The partial specific volume V'_{sx} of the solute *x* can also be calculated (Method *b*) from the sum of the slope of a plot of the reciprocal of the density of the solution, ρ (the specific volume, V_s) versus the mass fraction (c_x) of *x*, and the (extrapolated) intercept at the ordinate where $c_x = 0$. V'_{sx} is related to v_x by equation (4.4).^{120,121}

$$v_x = M_x \cdot V'_{sx} \quad (4.4)$$

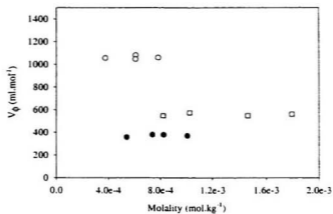


Figure 4.2 Apparent molar volumes (V_{ϕ}) of solutes 8 (○), C_{80} (●) vs. their molalities in toluene.

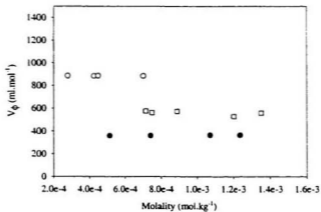


Figure 4.3 Apparent molar volumes (V_{ϕ}) of solutes 8 (○), C_{80} (●) vs. their molalities in benzene.

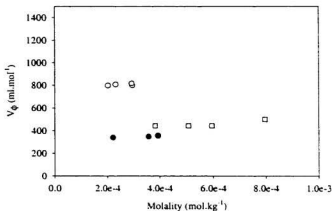


Figure 4.4 Apparent molar volumes (V_ϕ) of solutes 8 (□), C₆₀ (●) 8:C₆₀ (○) vs. their molalities in CS₂.

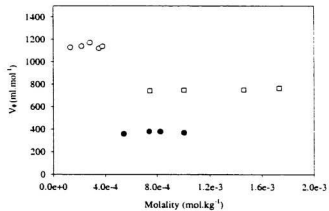


Figure 4.5 Apparent molar volumes (V_ϕ) of solutes 9 (□), C₆₀ (●) 9:C₆₀ (○) vs. their molalities in toluene.

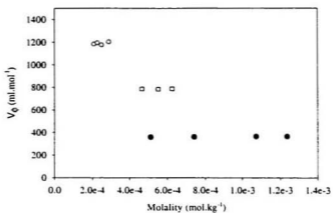


Figure 4.6 Apparent molar volumes (V_ϕ) of solutes 9 (\square), C₆₀ (\bullet) 9:C₆₀ (\circ) vs. their molalities in benzene.

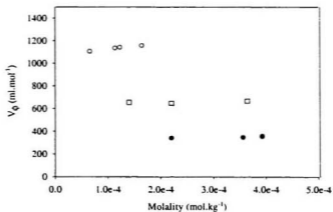


Figure 4.7 Apparent molar volumes (V_ϕ) of solutes 9 (\square), C₆₀ (\bullet) 9:C₆₀ (\circ) vs. their molalities in CS₂.

The same data points used previously were employed to calculate the partial molar volumes using equation (4.2) above and to calculate v_s using equation (4.4). The partial molar volumes calculated by both methods show good agreement, within experimental error. The experimental curves shown in Figures (4.8–4.10) which are typical, were obtained directly from the density measurements of toluene, benzene, and CS₂ solutions having known mass fractions of each of the solutes C₆₀, **8**, and the presumed 1:1 complex **8** C₆₀, respectively. Figures (4.11–4.13) which are typical, were obtained directly from the density measurements of toluene, benzene, and CS₂ solutions having known mass fractions of each of the solutes C₆₀, **9**, and the presumed 1:1 complex **9** C₆₀, respectively.

The following discussion of the results obtained is based upon the results calculated using Method *a* since they contain corrections for the excess, presumably uncomplexed, solutes in the respective solutions, although in general the results obtained using either method are in close agreement. When the error limits for the mean values obtained from our assays are taken into account, our data for the partial molar volumes of C₆₀ itself in each of the three solvents are basically in agreement with those reported by Ruelle *et al.*¹²⁰ and with the values obtained in toluene by Isaacs *et al.*⁴⁹

Using the mean values obtained from Method *a*, a trend can be seen in the partial molar volumes of *tert*-butylcalix[4]naphthalene **9** (Table 4.2), being largest in benzene (782±31 mL·mol⁻¹), followed by toluene (749±36 mL·mol⁻¹) and CS₂ (642±16 mL·mol⁻¹). A similar trend can be seen in the partial molar volumes of calix[4]naphthalene **8** (Table 4.1)

Table 4.1. Partial molar volumes of C_{60} , **8** and of the C_{60} ...**8** complex in different solvents

Solvent	Run #	Method	Solute partial molar volumes (v _i) mL·mol ⁻¹						ΔV, mL·mol ⁻¹
			C ₆₀	$c \times 10^4$ (b)	8	$c \times 10^4$ (b)	C ₆₀ ... 8	$c \times 10^4$ (b)	
toluene	1	a	370±14	4 0-7.3 (4)	548±21	4 6-11.2 (5)	1064±59	5 0-10.5 (4)	
	2	a	366±10	4 7-7.3 (5)	521±19	2 3-6.7 (4)	1083 ± 23	1 2-8.5 (3)	
		Mean values	368±12		535±20		1074 ± 45		171 ± 51
	1	b	361±23	4 0-7.3 (5)	580±15	4 6-11.2 (5)	1110±38	5 0-10.5 (4)	
benzene	2	b	367±13	4 7-7.3 (4)	528±35	2 3-5.5 (4)	1075±22	1 2-8.5 (4)	
		Mean values	364±19		554±27		1092±31		174 ± 45
	1	a	363±3	4 0-9.0 (4)	560±30	2 7-4.7 (5)	837±40	3 0-5.7 (5)	
	2	a	355±18	1 7-3.0 (5)	545±25	3 0-8.0 (4)	857±26	3 0-9.4 (5)	
CS ₂		Mean values	359±13		552±28		847±34		-64±46
	1	b	371±2	4 0-9.0 (4)	542±39	2 7-4.7 (5)	841±54	3 0-5.7 (5)	
	2	b	349±48	1 7-3.0 (5)	559±9	3 0-8.0 (4)	879±40	3 0-9.4 (5)	
		Mean values	360±34		551±28		860±48		-62±56
CS ₂	1	a	345±12	2 0-2.8 (3)	458±28	1 4-4.0 (4)	784±15	0 80-1.6 (4)	
	2	a	348±8	1 6-3.0 (3)	480±20	1 0-2.0 (6)	813±12	2 7-4.0 (4)	
	3	a	342±8	7 0-16.0 (5)	491±5	6 0-12.0 (6)	812±10	6 0-16.0 (4)	

Table 4.1. continued

	<i>Mean values</i>	345±10		476±20		803±13		-18±21
1	<i>b</i>	348±11	2.0-2.8 (3)	446±26	1.4-4.0 (4)	800±36	0.80-1.6 (4)	
2	<i>b</i>	370±9	1.6-3.0 (3)	458±18	1.0-2.0 (6)	851±22	2.7-4.0 (4)	
3	<i>b</i>	341±18	7.0-16.0(5)	489±11	6.0-12.0(7)	817±14	6.0-16.0(4)	
	<i>Mean values</i>	353±13		464±19		823±26		-10±34

n = no. of data points; *c* = mass fraction; ± values are standard deviations ; σ [for Method *a*: from the statistical treatment (SigmaPlot v 3.0) and for Method *b*: from a non-linear least-squares analysis (SigmaPlot v 3.0)]

Table 4.2. Partial molar volumes of C_{60} , 9 and of the C_{60} , 9 complex in different solvents.

Solvent	Run #	Method	Solute partial molar volumes (v_j) mL \cdot mol $^{-1}$					ΔV , mL \cdot mol $^{-1}$	
			C_{60}	9	$c \times 10^3$ (g)	$C_{60} \cdot 9$	$c \times 10^3$ (g)		
toluene	1	<i>a</i>	370 \pm 14	4 0-7 3 (4)	746 \pm 15	4 2-15(5)	1178 \pm 40	6.0-13 (3)	
	2	<i>a</i>	366 \pm 10	4 7-7 3 (4)	753 \pm 48	4 0-12 (4)	1139 \pm 19	2.0-6.0 (5)	
		Mean values	368 \pm 12		749 \pm 36		1158 \pm 31		41 \pm 49
	1	<i>b</i>	361 \pm 23	4 0-7 3 (5)	748 \pm 12	4 2-15 (5)	1187 \pm 36	6.0-13 (5)	
	2	<i>b</i>	367 \pm 13	4 7-7 3 (4)	729 \pm 40	4 0-12 (4)	1194 \pm 26	2.0-6.0 (4)	
		Mean values	364 \pm 19		739 \pm 29		1190 \pm 31		87 \pm 46
benzene	1	<i>a</i>	363 \pm 3	4 0-9 0 (5)	777 \pm 44	4 0-5 5 (4)	1196 \pm 19	3 2-4 6 (4)	
	2	<i>a</i>	355 \pm 18	1 6-3 0 (4)	786 \pm 2	3 5-5 5 (3)	1190 \pm 30	2 5-4 3 (4)	
		Mean values	359 \pm 13		782 \pm 31		1193 \pm 25		52 \pm 42
	1	<i>b</i>	371 \pm 2	4 0-9 0 (4)	798 \pm 47	4 0-5 5 (3)	1229 \pm 28	3 2-4 6 (4)	
	2	<i>b</i>	349 \pm 48	1 6-3 0 (5)	812 \pm 7	3 5-5 5 (4)	1168 \pm 44	2 5-4 3 (4)	
		Mean values	360 \pm 34		805 \pm 34		1198 \pm 37		22 \pm 50
CS $_2$	1	<i>a</i>	345 \pm 12	2 0-2 8 (3)	630 \pm 20	1 0-1 5 (4)	1115 \pm 38	1 0-3 0 (4)	
	2	<i>a</i>	348 \pm 8	1 6-3 0 (3)	655 \pm 18	1 6-3 3 (4)	1104 \pm 28	1 0-2 0 (4)	
	3	<i>a</i>	342 \pm 8	7 0-1 6 (0.5)	640 \pm 9	6 5-1 6 (0.6)	1073 \pm 33	6 0-1 6 (4)	
	Mean values	345 \pm 10		642 \pm 16		1097 \pm 33		110 \pm 39	

Table 4.2. continued

1	<i>b</i>	370±9	1.6-3.0 (3)	654±38	1.6-3.3 (4)	1101±70	1.0-2.0 (4)	
2	<i>b</i>	341±18	7.0-16.0(5)	617±6	6.5-16.0(6)	1035±8	6.0-16(4)	
3	<i>b</i>	348±11	2.0-2.8(3)	630±36	1.0-1.5(4)	1095±44	1.0-3.0(4)	
	<i>Mean values</i>	353±13		634±30		1077±48		98±69

n = no. of data points; *c* = mass fraction; ± values are standard deviations : σ [for Method *a*: from the statistical treatment (Sigmaplot v 3.0) and for Method *b*: from a non-linear least-squares analysis (Sigmaplot v 3.0)].

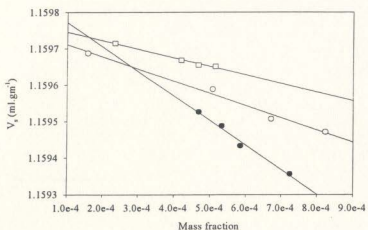


Figure 4.8 Specific volumes (V_s) of solutions in toluene of solutes 8 (□), C₆₀ (●) 8:C₆₀ (○) vs. mass fractions.

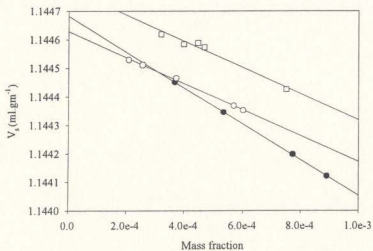


Figure 4.9 Specific volumes (V_s) of solutions in benzene of solutes 8 (□), C₆₀ (●) 8:C₆₀ (○) vs. mass fractions.

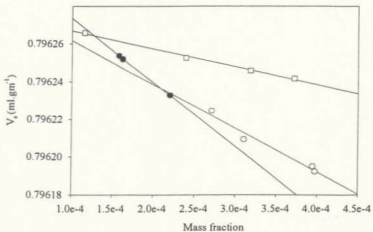


Figure 4.10 Specific volumes (V_s) of solutions in CS_2 of solutes 8 (□), C_{60} (●) 8: C_{60} (○) vs. mass fractions.

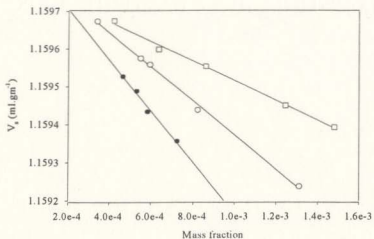


Figure 4.11 Specific volumes (V_s) of solutions in toluene of solutes 9 (□), C_{60} (●) 9: C_{60} (○) vs. mass fractions.

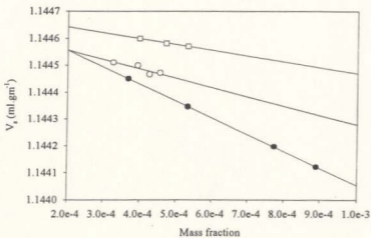


Figure 4.12 Specific volumes (V_s) of solutions in benzene of solutes 9 (□), C₆₀ (●) 9:C₆₀ (○) vs. mass fractions.

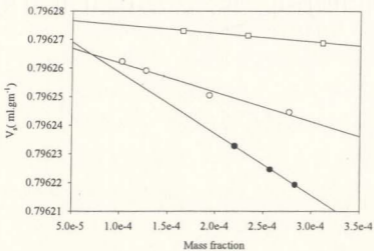


Figure 4.13 Specific volumes (V_s) of solutions in CS₂ of solutes 9 (□), C₆₀ (●) 9:C₆₀ (○) vs. mass fractions.

measured in the same respective solvents, being $552 \pm 28 \text{ mL} \cdot \text{mol}^{-1}$ in benzene, $535 \pm 20 \text{ mL} \cdot \text{mol}^{-1}$ in toluene and $476 \pm 20 \text{ mL} \cdot \text{mol}^{-1}$ in CS_2 .

Handa and Benson¹²⁵ have noted that the volume changes observed on mixing two liquids can be a result of any one of several factors such as (i) differences in sizes and shapes of the component molecules, (ii) structural changes, (iii) differences in the intermolecular interaction energy between like and unlike molecules, and/or (iv) formation of new chemical species. Using these considerations as well as observations noted by Ruelle *et al.*¹¹⁸ and others,¹²⁶⁻¹²⁸ it is possible to rationalize the changes that were observed for **8** or **9** with the different solvents, as follows.

Firstly, the trend in solubilities of **8** and **9** in each of the three solvents decreases in the following order: CS_2 ($>10 \text{ mg} \cdot \text{mL}^{-1}$) $>$ toluene ($1.8 \text{ mg} \cdot \text{mL}^{-1}$) $>$ benzene ($1.7 \text{ mg} \cdot \text{mL}^{-1}$) for **8** and CS_2 ($>10 \text{ mg} \cdot \text{mL}^{-1}$) $>$ toluene ($3.5 \text{ mg} \cdot \text{mL}^{-1}$) $>$ benzene ($2.6 \text{ mg} \cdot \text{mL}^{-1}$) for **9**. Increases in the limiting partial molar volume changes of solutes in various solvents are known to be roughly almost inversely proportional to their solubilities in the respective solvents.¹²⁶⁻¹²⁸ This is indeed the trend that was noted above, with the smallest partial molar volumes of either **8** or **9** being in CS_2 , the solvent in which both calixnaphthalenes have the highest solubilities.

A second factor to consider is the difference in size and shape of the component molecules in each case, outlined as factor (i) above, and which Ruelle *et al.* considered in their intensive study of C_{60} itself in different solvents. The latter determined a good correlation between the solvent molar volume and the variation in the molar volume of C_{60}

in solution. For our calixnaphthalene compounds however this does not appear to be the case: CS₂ has the smallest reported molar volume followed by benzene then toluene, whereas the trend in partial molar volumes in these solvents follows a different order: benzene > toluene > CS₂. An additional factor, outlined as factor (iv) above could account for the apparent anomaly between benzene and toluene as solvents of either **8** or **9**. This factor could be the enhanced intermolecular π -methyl interaction energy that is possible between the naphthalene rings and the methyl group of toluene, interactions that are not present when benzene is the solvent. This supposition is supported by the well-known fact that a stable toluene:tert-butylcalixarene clathrate forms, as first reported by Andreotti *et al.*⁷⁵

The partial molar volumes of the 1:1 complexes of **8** and of **9** with C₆₀ in the respective solvents were also determined in the same way, and were calculated using Method α . However, it should be noted that the low solubilities of the calixnaphthalenes in benzene or toluene limited the concentration ranges that could be employed and resulted in uncertainties of the order of 3-6%, which nevertheless are comparable to the findings reported by Isaacs *et al.*⁴⁹

The calculated reaction volumes ($\Delta V_{r,0}^{\ddagger}$)¹¹⁹ for the **9**:C₆₀ complex formation are +110 mL.mol⁻¹ in CS₂, +52 mL.mol⁻¹ in benzene and +41 mL.mol⁻¹ in toluene. Based on the molar volumes of each of the solvents, these reaction volumes are roughly equivalent to the partial molar volumes of 2.0, 0.6 and 0.4 molecules of the respective solvents which, as pointed out by Isaacs *et al.*,⁴⁹ can be interpreted to be displaced upon complex formation. The trend is consistent with our hypothesis that the solvophobic effect⁷² (*i.e.* that a larger number of

molecules of CS₂ are displaced from the cavitand cavity upon complex formation) is a driving force in the complex formation processes studied.

For **8**.C₆₀ complex formation, the calculated reaction volumes (ΔV_{c-o}) are -18 mL.mol⁻¹ in CS₂, -64 mL.mol⁻¹ in benzene and +171 mL.mol⁻¹ in toluene. These values do not support the solvophobic effect hypothesis since in CS₂ and in benzene they are lower than expected when compared with the corresponding values obtained for the **9**.C₆₀ complex. Thus, for the **8**.C₆₀ complex in which a deeper penetration of C₆₀ into the cavity is possible than in the **9**.C₆₀ complex, solvation of the complex by CS₂ and benzene could therefore be stronger, thus negating a possible solvophobic effect. For toluene as the solvent, approximately two molecules of toluene are displaced upon complex formation, similar to the finding observed by Isaacs *et al.*⁴⁹ in their system.

When the toluene data for the two complexation processes are compared, more solvent molecules are displaced upon formation of the **8**.C₆₀ complex than with the formation of the **9**.C₆₀ complex. This is also consistent with our earlier rationalization⁷² that there is deep-cavity inclusion in the case of **8**.C₆₀ complex. By contrast, a shallower penetration of the C₆₀ guest molecule may be occurring in the case of the **9**.C₆₀ complex, since the *tert*-butyl-methyl ... C₆₀ π interactions might sterically inhibit the potentially more effective π-π interactions between C₆₀ and the naphthalene rings.

There appears to be no direct simple correlation between the stability constants which we determined earlier⁷² and the reaction volume changes. On the other hand, a positive correlation is found for the volume changes and ΔS values determined earlier for the

formation of $8:C_{60}$, and a negative correlation for the formation of complex $9:C_{60}$.

Connors published an extensive review in 1997 on cyclodextrin complexes in solution.¹²⁹ In this review he correctly points out that interpretations based upon small calculated molar volume changes which have relatively large uncertainties should be considered with care and that only after the collection of very many experimental results for a wide range of substrate types, will accurate patterns emerge. The same holds true for calixarene-based host-guest complexation processes, and we are continuing to design and study other calixnaphthalenes towards this purpose.

In conclusion, the results presented herein show that partial molar volumes measurements can be employed to study host-guest complexation processes and can provide some information as to how deep inclusion of a guest into the substrate can occur. However, it is important to also take into account additional information such as the solvation of all of the individual species concerned, solvent molar volumes and other factors identified by Handa and Benson,¹²⁵ which may require additional physical methodologies to be employed.

4.3 Volumetric Study of Hexahomotrioxacalix[3]naphthalenes 26 and 26a with C_{60}

The partial molar volume of a solute, v_x , as shown above and represented by equation (4.1) can be obtained by an extrapolation to infinite dilution, of the plot of V_g against the molality of the solution. Since the concentration ranges that we are working with are similar to that in compounds **8** and **9**, the partial molar volumes are calculated from the average of the V_g values. The partial molar volumes which were obtained are shown in Tables 4.3 and 4.4 under those values calculated by Method *a*.

Figures 4.14–4.16 show the plots of V_p versus molality for the solutions in toluene, benzene, and CS_2 of C_{60} , **26** and the presumed 1:1 complex, respectively. Figures 4.17–4.19 show the plots of V_p versus molality for the solutions in toluene, benzene, and CS_2 of C_{60} , **26a** and the presumed 1:1 complex respectively. Young's equation¹²⁴ (equation 4.3) was applied to the calculations for the partial molar volumes of the 1:1 complexes of C_{60} with **26**, and **26a**.

The partial specific volume V_{sx} of the solute x can also be calculated (Method *b*) as shown above from the slope of a plot of the reciprocal of the density of the solution, ρ versus the mass fraction (c_x) of x , and the (extrapolated) intercept at the ordinate where $c_x = 0$. V_{sx} is related to v_x by equation (4.4).^{120,121}

The same data points used previously to calculate the partial molar volumes using (Method *a*) above were employed to calculate v_x using (Method *b*). The partial molar volumes calculated by both methods show good agreement within experimental error as shown in Tables 4.3 and 4.4. The experimental curves shown in Figures (4.20–4.22) which are typical, were obtained directly from the density measurements of toluene, benzene, and CS_2 solutions having known mass fractions of each of the solutes C_{60} , **26**, and the presumed 1:1 complex of **26**: C_{60} , respectively. Figures (4.23–4.25) which are typical, were obtained directly from the density measurements of toluene, benzene, and CS_2 solutions having known mass fractions of each of the solutes C_{60} , **26a**, and the presumed 1:1 complex of **26a**: C_{60} , respectively.

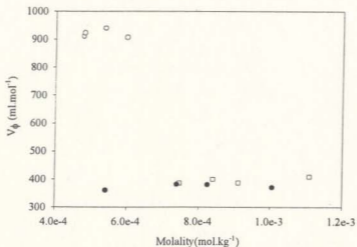


Figure 4.14 Apparent molar volumes (V_{ϕ}) of solutes 26(□), C₆₀(●) 26:C₆₀(○) vs. molalities in toluene.

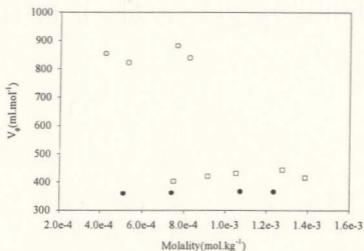


Figure 4.15 Apparent molar volumes (V_{ϕ}) of solutes 26(□), C₆₀(●) 26:C₆₀(○) vs. molalities in benzene.

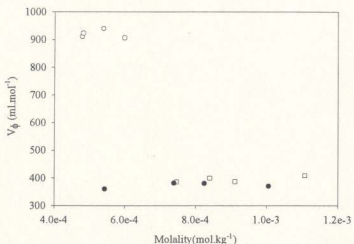


Figure 4.14 Apparent molar volumes (V_{ϕ}) of solutes 26(□),C₆₀(●) 26:C₆₀(○) vs. molalities in toluene.

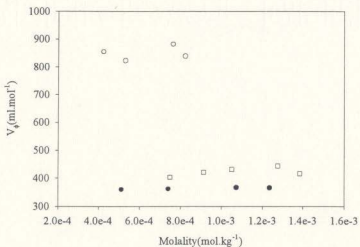


Figure 4.15 Apparent molar volumes (V_{ϕ}) of solutes 26(□),C₆₀(●) 26:C₆₀(○) vs. molalities in benzene.

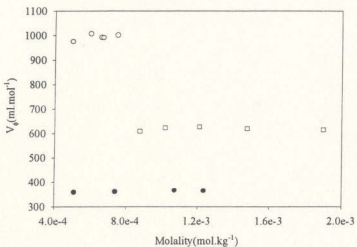


Figure 4.18 Apparent molar volumes (V_{ϕ}) of solutes 26a(□), C_{60} (●) 26a: C_{60} (○) vs. molalities in benzene.

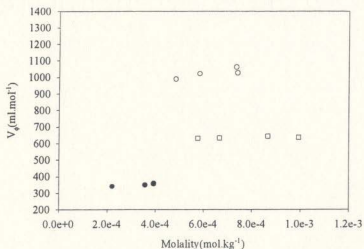


Figure 4.19 Apparent molar volumes (V_{ϕ}) of solutes 26a(□), C_{60} (●) 26a: C_{60} (○) vs. molalities in CS_2 .

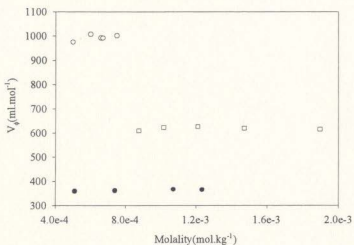


Figure 4.18 Apparent molar volumes (V_{ϕ}) of solutes 26a(\square), C_{60} (\bullet) 26a: C_{60} (\circ) vs. molalities in benzene.

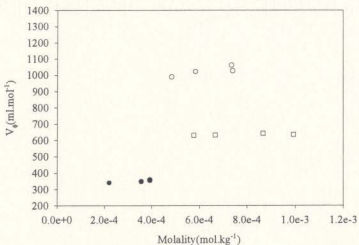


Figure 4.19 Apparent molar volumes (V_{ϕ}) of solutes 26a(\square), C_{60} (\bullet) 26a: C_{60} (\circ) vs. molalities in CS_2 .

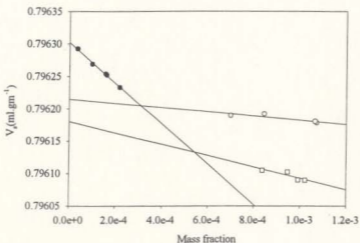


Figure 4.22 Specific volumes (V_s) of solutions in CS_2 of solutes 26 (□), C_{60} (●), 26: C_{60} (○) vs. mass fractions.

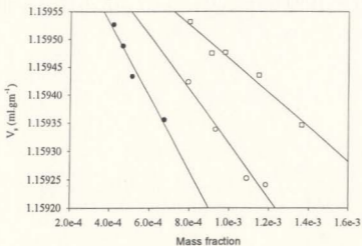


Figure 4.23 Specific volumes (V_s) of solutions in toluene of solutes 26a(□), C_{60} (●), 26a: C_{60} (○) vs. mass fractions.

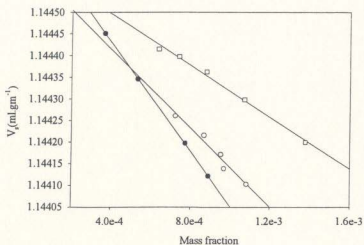


Figure 4.24 Specific volumes (V_s) of solutions in benzene of solutes 26a(□), C₆₀(●), 26a:C₆₀(○) vs. mass fractions.

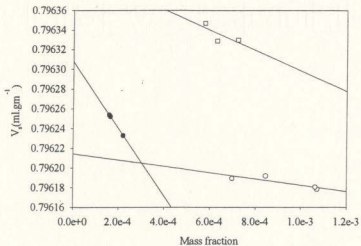


Figure 4.25 Specific volumes (V_s) of solutions in CS₂ of solutes 26a(□), C₆₀(●), 26a:C₆₀(○) vs. mass fractions.

Table 4.3 Partial molar volumes of C_{60} , 26a and of the 26a C_{60} complex in different solvents

Solvent	Run #	Method	Solute partial molar volumes (v_j) ml. \cdot mol $^{-1}$						ΔV_s , ml. \cdot mol $^{-1}$
			C_{60}	$c \times 10^3$ (m)	26a	$c \times 10^3$ (m)	26a C_{60} complex	$c \times 10^3$ (m)	
toluene	1	<i>a</i>	370 \pm 14	4.0-7.3 (5)	600 \pm 15	5.0-10(4)	972 \pm 40	7.0-12.0(4)	
	2	<i>a</i>	366 \pm 10	4.7-7.3 (4)	601 \pm 11	8.0-14 (5)	971 \pm 48	5.0-12.0 (4)	
		<i>Mean values</i>	368 \pm 12		601 \pm 13		972 \pm 44		34.50
	1	<i>b</i>	361 \pm 23	4.0-7.3 (5)	583 \pm 25	4.0-10(5)	982 \pm 96	7.0-12.0(4)	
	2	<i>b</i>	367 \pm 13	4.7-7.3 (4)	622 \pm 6	8.0-14 (5)	941 \pm 101	5.0-12.0 (4)	
		<i>Mean values</i>	364 \pm 19		603 \pm 18		962 \pm 98		-5 \pm 101
benzene	1	<i>a</i>	363 \pm 3	4.0-9.0 (4)	619 \pm 7	6.0-14 (5)	993 \pm 12	7.0-11.0 (5)	
		<i>a</i>	355 \pm 18	1.6-3.0 (5)	617 \pm 9	8.5-18 (4)	999 \pm 52	6.0-11.0 (5)	
		<i>Mean values</i>	359 \pm 13		618 \pm 8		996 \pm 38		19 \pm 41
	1	<i>b</i>	371 \pm 2	4.0-9.0 (4)	615 \pm 11	6.0-14 (5)	999 \pm 76	7.0-11.0 (5)	
	2	<i>b</i>	349 \pm 48	1.6-3.0 (5)	636 \pm 17	8.5-18 (4)	1069 \pm 44	6.0-11.0 (5)	
		<i>Mean values</i>	360 \pm 34		625 \pm 14		1034 \pm 62		49 \pm 72
CS $_2$	1	<i>a</i>	345 \pm 12	2.0-2.8 (3)	662 \pm 22	5.5-8.0 (5)	1013 \pm 28	6.0-11.0 (5)	
	2	<i>a</i>	348 \pm 8	1.6-3.0 (4)	635 \pm 5	4.0-7.5 (4)	1022 \pm 29	6.0-11.0 (5)	
			342 \pm 8	7.0-16.0 (5)	<i>no data</i>		<i>no data</i>		
		<i>Mean values</i>	345 \pm 10		647 \pm 13		1018 \pm 28		26 \pm 32
	1	<i>b</i>	348 \pm 11	2.0-2.8 (3)	616 \pm 41	5.5-8.0 (3)	995 \pm 48	6.0-11.0 (5)	

Table 4.3. continued

2	<i>b</i>	370±9	1.6-3.0 (4)	650±12	4.0-7.5 (4)	1106±70	6.0-11.0 (4)
		341±18	7.0-16.0 (5)	no data		no data	
	<i>Mean values</i>	353±13		633±30		1050±60	64±68

n = no. of data points; *c* = mass fraction, ± values are standard deviations; σ for Method *a*, from the statistical treatment (Sigmaplot v 3.0) and for Method *b* from a non-linear least-squares analysis (Sigmaplot v 3.0)

Table 4.4. Partial molar volumes of C_{60} , 26 and of the 26 C_{60} complex in different solvents.

Solvent	Run #	Method	Solute partial molar volumes (v_p) mL \cdot mol $^{-1}$					
			C_{60}	$c \times 10^4$ (m)	26	$c \times 10^4$ (m)	26 C_{60} complex	$c \times 10^4$ (m)
toluene	1	a	370 \pm 14	4 0-7.3 (5)	396 \pm 11	4 0-7.0 (4)	919 \pm 15	5 0-8.0 (4)
	2	a	366 \pm 10	4 7-7.3 (5)	424 \pm 6	5 0-9.5 (5)	897 \pm 8	6 0-12.0 (3)
		Mean values	368 \pm 12		410 \pm 9		908 \pm 12	130 \pm 19
		b	361 \pm 23	4 0-7.3 (5)	420 \pm 28	4 0-7.0 (4)	936 \pm 80	5 0-8.0 (4)
benzene	2	b	367 \pm 13	4 7-7.3 (4)	399 \pm 9	5 0-9.5 (5)	914 \pm 41	6 0-12.0 (5)
		Mean values	364 \pm 19		410 \pm 21		925 \pm 63	151 \pm 46
	1	a	363 \pm 3	4 0-9.0 (4)	429 \pm 18	5 0-10.0 (6)	849 \pm 25	5 0-11.0 (4)
	2	a	355 \pm 18	1 7-3.0 (5)	423 \pm 15	4 0-9.0 (5)	824 \pm 9	7 0-10.5 (5)
CS_2		Mean values	359 \pm 13		427 \pm 17		837 \pm 19	51 \pm 29
	1	b	371 \pm 2	4 0-9.0 (4)	435 \pm 41	5 0-10.0 (6)	838 \pm 101	5 0-11.0 (4)
	2	b	349 \pm 48	1 7-3.0 (5)	450 \pm 32	4 0-9.0 (5)	851 \pm 30	7 0-10.5 (5)
		Mean values	360 \pm 34		442 \pm 37		845 \pm 75	43 \pm 90
	1	a	345 \pm 12	2 0-2.8 (3)	438 \pm 3	4 0-7.0 (4)	779 \pm 12	8 0-10.6 (4)
	2	a	348 \pm 8	1 6-3.0 (3)	no data	no data	no data	no data
	3	a	342 \pm 8	7 0-16.0 (5)	442 \pm 7	6 0-12.0 (6)	782 \pm 15	4 0-11.0 (4)
		Mean values	345 \pm 10		440 \pm 5		781 \pm 13	-4 \pm 17
	1	b	348 \pm 11	2 0-2.8 (3)	425 \pm 5.0	4 0-7.0 (4)	790 \pm 93	8 0-10.6 (4)

Table 4.4. continued

2	b	370±9	1 6-3 0 (3)	467±6 0	6 0-12 0(3)	802±33	4 0-11 0(4)	
3	b	341±18	7 0-16 0(6)	no data	no data	no data	no data	
	Mean values	353±13		446±5		796±70		-3 ±71

n = no. of data points, c = mass fraction, \pm values are standard deviations : σ [for Method a from the statistical treatment (Signaplot v 3 0)] and for Method b from a non-linear least-squares analysis (Signaplot v 3 0).

The discussion of the results obtained which follows, is based upon the results calculated using Method *a* since they contain corrections for the excess, presumably uncomplexed, solutes in the respective solutions, although in general the results obtained using either method are in close agreement. Using the mean values obtained from Method *a*, a trend can be seen in the partial molar volumes of **26a** (Table 4.3), being largest in CS₂ (647±13 mL.mol⁻¹), followed by benzene (618±8 mL.mol⁻¹) and toluene (601±13 mL.mol⁻¹). A similar trend can be seen in the partial molar volumes of **26** (Table 4.4) measured in the same respective solvents, being (446±5 mL.mol⁻¹) in CS₂, (427±17 mL.mol⁻¹) in benzene and (410±9 mL.mol⁻¹) in toluene.

In contrast to what was observed in the case of compounds **8** and **9** and to what may be expected based on the molar volume of the solvent molecules, the partial molar volumes of both **26** and **26a** have higher values in CS₂ compared to what they have in toluene or benzene. Based on Handa and Benson's considerations mentioned earlier, factor (*iii*) seems to be a major factor in this case, while the other factors have less effect. Both toluene and benzene are able to have stronger π - π interactions with the naphthyl groups of **26** or **26a**, compared to that with CS₂. This causes the partial molar volumes of **26** and **26a** determined in CS₂ to be the larger than those determined in toluene or benzene. Obviously, this conclusion does not preclude CS₂ itself interacting with **26** or **26a**. The small difference between the partial molar volumes of benzene and toluene might be due the difference in the solubilities of **26** and **26a** in toluene and benzene. The solubilities of **26** and **26a** in both toluene and benzene are in the following order: toluene (9.2 mg.mL⁻¹) > benzene (6.0 mg.

mL⁻¹) for **26** and toluene (19.8 mg.mL⁻¹) > benzene (11.0 mg.mL⁻¹) for **26a**. As discussed earlier, the higher the solubility, the lower the partial molar volume will be. An additional factor, outlined as factor (iv) in Handa and Benson's considerations could account for the apparent anomaly between benzene and toluene as solvents of either **26** or **26a**. This factor could be the enhanced intermolecular π - π -methyl interaction energy that is possible between the naphthalene rings and the methyl group of toluene, interactions that are not present when benzene is the solvent. As discussed previously this supposition is supported by the stable toluene *tert*-butylcalixarene clathrate forms reported by Andreotti *et al.*¹⁵

The partial molar volumes of the 1:1 complexes of **26** and of **26a** with C₆₀ in the respective solvents were also determined in the same way used to determine the partial molar volumes of **8** and **9** earlier and were calculated using Method *a*. Examining Tables (4.3) and (4.4) shows that the trend in partial molar volumes of the complexes **26**.C₆₀ and **26a**.C₆₀ in these solvents follow different orders; for the **26a**.C₆₀ complexes, the trend is CS₂ > benzene > toluene, while the trend for the **26**.C₆₀ complexes is toluene > benzene > CS₂. The trend of the **26**.C₆₀ complexes could be related to factor (i) of Handa and Benson¹²⁵ in which the size of the solvent molecules is a major factor. Increases in the limiting partial molar volumes changes of solvents are known to be roughly proportional to the size of solvent molecules. This is indeed the trend that we noted above for the **26**.C₆₀ complexes, with the smallest partial molar volume in CS₂ which has the smallest size, then benzene and finally toluene, which has the largest volume. The trend for the **26a**.C₆₀ complexes is opposite to that of the **26**.C₆₀ complexes. This trend reveals that the π - π interaction factor, which was

discussed for **26** and **26a**, is the major factor and applies to these complexes.

The calculated reaction volumes ($\Delta V_{r-d}^{\ddagger}$)¹¹⁹ for the **26**:C₆₀ complex formation are +130 mL.mol⁻¹ in toluene, +52 mL.mol⁻¹ in benzene and -4 mL.mol⁻¹ in CS₂. Based on the molar volumes of each of the solvents, these reaction volumes are roughly equivalent to the partial molar volumes of 1.0, 0.6 and 0.0 molecules of the respective solvents which, as pointed out by Isaacs *et al.*⁴⁹ can be interpreted to be displaced upon complex formation. The trend again is consistent with our earlier hypothesis⁷² that a solvophobic effect (*i.e.* that a larger number of molecules of toluene are displaced from the cavitand cavity upon complex formation) is a driving force in the complex formation processes studied, which may result in a higher K_{assoc} value in toluene being observed as compared to that in benzene.

For **26a**:C₆₀ complex formation, the calculated reaction volumes ($\Delta V_{r-d}^{\ddagger}$) are 26 mL.mol⁻¹ in CS₂, 19 mL.mol⁻¹ in benzene and 3 mL.mol⁻¹ in toluene. these volume changes are roughly equivalent to 0.3, 0.2, and 0.0 molecules of the above solvents respectively. In spite of their small values, these volume changes support the solvophobic effect hypothesis since a larger partial molar volume change is observed in benzene compared with the corresponding value obtained in toluene, which also accounts for the higher K_{assoc} value in benzene. Factor (iv) of Handa and Benson's considerations mentioned earlier may account for the smaller value of partial molar volume of **26a**:C₆₀ complex in toluene compared to that in benzene factor could be the enhanced intermolecular π •••methyl interaction energy that is possible between the naphthalene rings and the methyl group of toluene, interactions that are not present when benzene is the solvent.

4.4. Experimental

Toluene (BDH, Scintillation Grade) was distilled over sodium metal with benzophenone prior to use. Benzene (ACP Chemicals Inc., A.C.S grade, 99%) and CS₂ (Aldrich Chemical Company, Inc., Spectrophotometric Grade, 99+%) and anhydrous ethanol (Commercial Alcohols Inc.) were used without further purification. C₆₀ (99.5%) was purchased from Aldrich. Hexahomotrioxacalix[3]naphthalenes **26** and **26a** were prepared according to methods described in Chapter Three and previously described.⁹⁶ For all the solvents tested 4-6 solution samples with decreasing mass fraction were prepared by using the specific amount of a pre-prepared stock solution of a known mass fraction then diluted with known mass of solvent. In the case of the complex mixtures an exact masses of **8** or **9** stock solution were mixed with an exact mass of C₆₀ stock solution that will give a 1:1 mole ratio, then this mixture is diluted with known mass of solvent. All solutions were weighed with a precision of $\pm 10^{-4}$ g. The high-precision density measurements were carried out at 25.0 ± 0.1 °C using a Picker-type densitometer (Sodev Model D03). Before each series of measurements, the apparatus is calibrated with absolute ethanol and the solvent system used in the experiment whose densities were taken from the published data.¹³⁰ In a typical experiment, approximately 2.0 ml of the tested solution was injected in the densitometer using a glass syringe. For each data point V'_p the apparent molar volume, is calculated using equation (4.2). The partial molar volume, v_p is calculated from the average of all the data points in that experiment (Method *a*). The same data points were analyzed by plotting the specific volume ($1/\rho$) of a series of solutions against the mass fractions. From these plots,

the partial molar volumes could also be calculated using equation (4.4) (Method *b*). Measurements in each solvent were conducted in duplicate or triplicate. Statistical analyses were conducted using *Sigmaplot v 3.0* and curve fittings were conducted using *Excel 97*.

4.5. Vibrating Tube Densitometer

This tube is used to measure very precise liquid densities by measuring the natural vibrational frequency of tubes containing the liquid under investigation. The essential features of the instrument are shown in Figure 4.26.¹³¹ It consists of a U-shaped vibrating tube, two permanent magnets, two driving bars and two pick-up bars. The liquid to be studied is injected into the vibrating tube via a glass syringe. The tube is driven to vibrate by the force generated by the interaction between the permanent magnetic field and an alternating current through the "driving bar". The "pick-up bar" serves to sense the vibration. Then the tube starts to vibrate, starting from the static equilibrium position by an initial displacement, and if the elastic force is proportional to the displacement x , with a stiffness coefficient k , and the vibration is not damped, then the equation of motion that governs the free vibration of the system is given by equations (4.5) or (4.6):

$$m (d^2 x / dt^2) + kx = 0 \quad (4.5)$$

$$d^2 x / dt^2 - \omega^2 x = 0 \quad (4.6)$$

where m is the mass of the tube and $\omega = (k/m)^{1/2}$ is the natural frequency of vibration. For a real system where damping is considered, and if it is proportional to the velocity with a positive proportionality coefficient c , the system will be represented by equation 4.7:

$$m (d^2 x / dt^2) + c (dx / dt) + kx = 0 \quad (4.7)$$

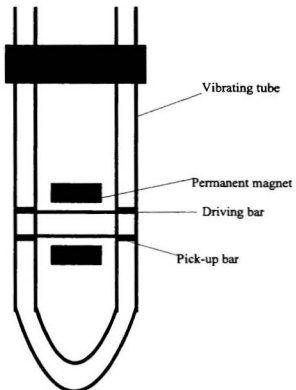


Figure 4.26 Schematic representation for the Picker-type densitometer (Sodev Model D03).

The natural frequency ω is the only quantity needed to calculate the density of the liquidfills the tube in both cases, whether the motion is damped or not. The density of the liquid ρ is given in equation 4.8 where V_i is the volume of the vibrating tube.

$$\rho = ((k/\omega^2) - m)/V_i \quad (4.8)$$

If ω_o is the natural frequency for a reference liquid is measured, then the relative density ρ/ρ_o is given by equation 4.9:

$$\rho/\rho_o = K (1/\omega^2 - 1/\omega_o^2) \quad (4.9)$$

where ρ_o is the density of the reference liquid and $K = k/V_i$ is the characteristic constant which is determined during the calibration process with two liquids with known densities.

Chapter Five

Ester Derivatives of Hexahomotrioxacalix[3]naphthalenes and Their Binding Properties

5.1. Introduction

The previous chapters have demonstrated that calix[*n*]arenes have the ability to accommodate small molecules in their cavities to form inclusion compounds.¹ On the other hand, they show very little ionophoric activity for alkali metal cations, as shown by their inability to transport such ions from neutral aqueous solution through a chloroform membrane.¹³² Several attempts have been undertaken to enhance their ability to form complexes with alkali metal cations, among them being the modification of the lower rim by forming ester derivatives. By analogy with the fact that biological receptors are rich in ester-type carbonyl groups and selectively bind metal cations, ester derivatives of calixarenes and presumably calixnaphthalenes could increase their ability to form complexes with alkali metal cations.¹³³

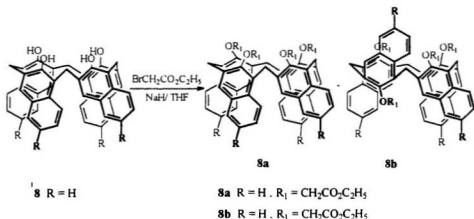
Esters were the earliest of lower rim-modified calixarenes to be prepared and have their complexing abilities studied.¹³³ It was found that they can selectively form complexes with alkali metal cations. This observation was ascribed to the interactions which are possible between hard oxygen bases and hard alkali metal cations, as is seen with crown ethers. The tetraester of calix[4]arene **4** forms complexes with Na⁺ and K⁺, while the hexaester of calix[6]arene forms complexes with Rb⁺ or Cs⁺, but poorly with Na⁺. An X-ray

crystal structure for the complex of 4K^+ shows that **4** has a cone conformation.¹³³ In principle, functionalization of the lower rim hydroxy groups by esterification may serve to restrict any of the four main possible conformations of calixarenes or calix[4]naphthalenes, provided the residues are bulky enough to inhibit the oxygen-through-the annulus rotation. McKervey *et al.*¹³³ found that the alkylation of **1** using ethyl bromoacetate in the presence of sodium or potassium ions leads to tetraester, **4**, in the cone conformation, while the partial-cone conformation is found predominantly in the presence of the cesium cation.⁸⁴

In this chapter the synthesis of hexahomotrioxacalix[3]naphthalene ester derivatives in both the cone and the partial-cone conformations will be discussed, as will their abilities to form complexes with alkali-metal cations and silver cation.

5.2. Ester Derivatives of Calixnaphthalenes

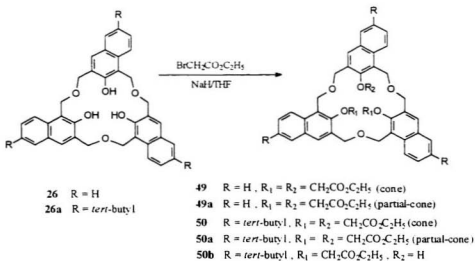
Modification of the calix[4]naphthalene lower rims is expected to enhance their



Scheme 5.1 Alkylation of calix[4]naphthalenes.

ability to form complexes with alkali metal cations and also enhance their solubilities in different solvents. Tetraesters of **8** were prepared by the treatment of **8** with ethyl bromoacetate in THF using NaH as base to give compounds **8a** (9% yield) and **8b** (21%) as shown in Scheme 5.1.¹¹ Both compounds **8a** and **8b** were found to be more soluble in chloroform than the parent compounds.¹¹ Ashram previously found that alkylation of **9** under the same conditions as were used for alkylation of **8** unexpectedly did not produce the tetraesters of **9**, but only afforded the monoester as a minor product, and the 1,3-diester as the major product.¹¹

Hexahomotrioxacalix[3]naphthalenes **26** or **26a**, which were synthesized⁹⁷ as described in Chapter Three, only weakly bind alkali metal cations and silver cation during



Scheme 5.2 Alkylation of hexahomotrioxacalix[3]naphthalenes.

the picrate-extraction process. By analogy with the calixarenes, it was anticipated that ethoxycarbonylmethyl groups attached to the phenolic groups in **26** or **26a** would result in molecules having a high degree of phase-transfer affinity for alkali metal cations. The alkylation of **26** or **26a** was carried out by using NaH/THF or K₂CO₃/acetone conditions (Scheme 5.2). The products from the reaction of **26** or **26a** with ethylbromoacetate are summarized in Table 5.1. Table 5.1 reveals that alkylation of **26** or **26a** using NaH/THF gives both cone and partial-cone conformers with preference for the cone conformation. Using K₂CO₃/acetone affords only the partial-cone conformer in a 47% and 24% yield for

Table 5.1 Distribution of the products of alkylation of **26** and **26a** between cone and partial-cone

Base	Substrate	Solvent	Product	Yield
K ₂ CO ₃	26	acetone	49a	47%
NaH	26	THF	49a	10%
			49	25%
K ₂ CO ₃	26a	acetone	50a	24%
NaH	26a	THF	50a	17%
			50	25%

49a and **50a** respectively. Similar results were obtained in the synthesis of calixarene esters³³. Shinkai *et al*^{101a} suggested that the partial-cone conformer of **4** is sterically less crowded than the cone conformer and therefore forms predominantly. Examination of Table 5.1 reveals that a significant amount of cone conformer results when the base contains Na⁺ and is strong like NaH. These findings are consistent with what was found by Shinkai *et al*^{101a} and support the view that when substituents are introduced into

hexahomotrioxacalix[3]naphthalenes or hexahomotrioxacalix[3]arenes they preferably form the partial-cone conformer to minimize steric crowding. Only when the template metal can hold the ester group(s) and the oxide group(s) on the same side of the hexahomotrioxacalix[3]naphthalene can the cone conformation result. When a weak base is used, the undissociated OH group forms intramolecular hydrogen bonds with the dissociated OH group, which will weaken the metal template effect arising from the $M^+ \cdots O^-$ interaction. This change leads to the increase in the formation of the partial-cone conformer.

The conformational characteristics of calix[4]arenes (or calix[4]naphthalenes) and their *O*-ester derivatives can be conveniently estimated by the splitting patterns in their 1H NMR spectra. The methyl protons of the ethyl ester groups in compound **4** (or **8a**) in the cone conformation appear as one triplet, while in the partial-cone conformation they appear as three sets of triplets in the ratio 1:2:1. In the pinched-cone conformation they appear as two sets of triplets in a 1:1 ratio.⁹ The methyl protons of the ethyl ester groups for the triesters **49** or **50** in the cone conformation appear as one triplet, while in the partial-cone conformation they appear as three sets of triplets in a 1:1:1 ratio. These characteristics could be used for establishing the conformations of the triester derivatives of **26** or **26a**. Since compound **49** (or **50**) adopts a cone conformation, the bridge methylene groups are divided into two sets, the protons of each set reveal an AB system in the 1H NMR spectrum. The three OCH_2-CO methylene groups are equivalent but due to the inherent chirality of the molecule, each of the protons is diastereotopic and should appear as an AB system. All of

the methyl protons in the ethyl moiety (CH_2CH_3) of the ethyl ester groups are equivalent and appear as one triplet only. The methylene protons however are diastereotopic and showed two overlapping quartets.

Figure 5.1 shows the ^1H NMR spectrum (CDCl_3) of **49** in the cone conformation. It reveals one triplet centered at δ 1.38 ppm ($J = 6.9$ Hz), coupled to the quartet centered at δ 4.31 and 4.36 ppm ($J = 6.9$ Hz). It also reveals three AB systems, one centered at δ 4.38 and 4.55 ppm ($J = 15.3$ Hz), the other at δ 4.79 and 4.92 ppm ($J = 16.5$ Hz) and the third at δ

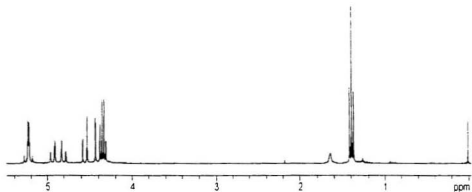


Figure 5.1 ^1H NMR Spectrum of **49** in CDCl_3 .

5.19 and 5.25 ppm ($J = 12.6$ Hz). It is most likely that the first two AB systems are due to the two sets of the bridge methylene protons, which is similar to what was reported for the spectra of the tetraesters **4**^{5d} and **8a**¹¹ where the chemical shift differences between the pairs of doublets of the methylene bridges are larger than those reported for the $\text{OCH}_2\text{-CO}$ methylene protons. The AB system centered at δ 5.19 and 5.25 ppm is due to the diastereotopic $\text{OCH}_2\text{-CO}$ methylene protons. Similar splitting patterns are also observed for

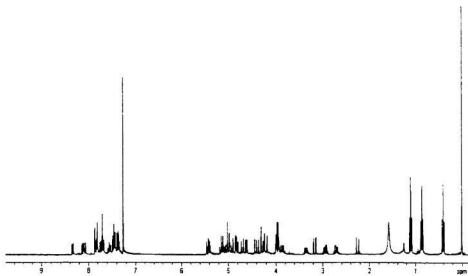


Figure 5.2 ^1H NMR Spectrum of **49a** in CDCl_3 .

50, in addition to the singlet at δ 1.26 ppm corresponding to the *tert*-butyl methyl protons. In the ^1H NMR spectrum in CDCl_3 of the partial-cone triester **49a**, the methyl groups appear as three sets of triplets in a 1:1:1 ratio. Figure 5.2 also reveals very complex splitting patterns in both the methylene and aromatic regions. Similar splitting patterns were also observed for the partial-cone triester of **50a** which contains additionally three singlets at δ 1.33 ppm, 1.37 ppm, and 1.42 ppm due to each of the *tert*-butyl groups.

The X-ray structure of **49a** shows that the compound adopts a partial-cone conformation in the solid state (Figure 5.3).

5.3. Binding of **49** and **50** with metal ions

Izatt *et al.*¹³² were the first to report the solvent extraction of alkali metal cations by calix[*n*]arenes. They showed that all the calixarenes tested, such as **1**, **2** and **3** had selectivity towards Cs^+ ions. Later, Ungaro *et al.*,^{8a} Mckerverey *et al.*,¹³³ and Cheng *et al.*¹³⁴ demonstrated that calixarenes could be converted to neutral ligands capable of binding alkali metal cations by modifying the hydroxyl groups to form ester or amide derivatives. They also showed that the metal ion selectivity is dependent on the ring size of the calixarene, by analogy with the crown ethers.^{93,101a,133}

Solvent extraction experiments with alkali metal cations and silver ion with the triesters **49** (or **49a**) or **50** (or **50a**) in CHCl_3 were performed at 25 °C. The results are shown in Table 5.2. As can be seen in Table 5.2., the extractability percentage (%E) is greatly affected by the conformation of the receptor. The cone conformer in general has higher %E values than the partial-cone conformer. This implies that the lower-rim ionophoric cavity

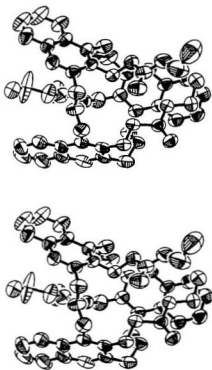


Figure 5.3. Stereoviews of the X-ray crystal structure for 49a.

formed by the three ester groups is more efficient for metal binding than if it was composed of only two ester groups and the naphthyl group. In addition to that, the cone conformer in both **49** and **50** shows selectivity toward K^+ , but the peak selectivity is clearly shown in **50** more than in **49**, as revealed in Figure 5.4

Table 5.2 $\log E$ values for alkali metal picrates and silver picrate with **49** and **50** triesters in to $CHCl_3$

	Li^+	Na^+	K^+	Rb^+	Cs^+	Ag^+
49a Run 1	1.6	1.1	1.9	4.1	0.7	0.1
49a Run 2	2.8	1.9	1.3	4.5	1.1	0.3
<i>Average</i>	2.2	1.5	1.6	4.4	0.9	0.2
49 Run 1	5.0	4.5	5.0	4.8	3.2	4.2
49 Run 2	4.2	6.0	7.0	5.4	3.7	5.4
<i>Average</i>	4.6	5.3	6.0	5.2	3.5	4.8
50a Run 1	5.1	3.9	3.8	5.9	3.6	1.6
50a Run 2	5.1	4.0	3.9	5.8	3.8	2.1
<i>Average</i>	5.1	4.0	3.9	5.9	3.7	1.8
50 Run 1	6.0	4.7	9.7	4.4	5.2	2.0
50 Run 2	5.3	5.6	9.6	5.0	5.1	3.2
<i>Average</i>	5.6	5.2	9.7	4.7	5.2	2.6

The size of the metal ion has no effect in the case of cone conformers while it has a great effect in the case of partial-cone conformers, where the percentage extractabilities decrease as the ionic radius increases, i.e. the partial-cone triesters **49a** and **50a** are more

selective towards the smaller cations. For triester **50a** this trend reveals that the existence of a *tert*-butyl group on the same side as the two ester groups favors binding with the smaller, rather than the larger, cations. The cone conformers **49** and **50** have higher % E values than the partial-cone, conformers **49a** and **50a** and show peak selectivity towards K^+ (Figure 5.4),

Comparison of the results obtained with triesters **49** (or **49a**) and **50** (or **50a**) shows that the latter compounds have higher %E values in either conformation. This might be

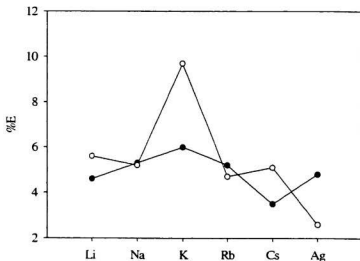


Figure 5.4 %E of ● **49** and ○ **50** for Metal picrates in $CHCl_3$.

explained by considering the flexibility of each conformer: **49** (or **49a**) is relatively more flexible than **50** (or **50a**), which does not restrict the mobility of the ester moiety and its ability to receive the small cation (Li^+) nearly as much the large cation (Cs^+), while **26a**

triester which has lower flexibility that resulted the ester moiety to have deficient cavity and able to receive only the metal that fits the size of this moiety, which is K^+ in this case.

The extraction of alkali metal cations with the triester of **19**, which is analogous to triesters **49** and **50** was reported by Shinkai *et al.*,^{101a} but with basic metal picrates. Therefore, it is not appropriate to compare our results with those of Shinkai's group.

5.4. Experimental

5.4.1 Alkylation of **26** with ethyl bromoacetate

a. K_2CO_3 /acetone conditions:

Ethyl bromoacetate (0.03 mL, 0.27 mmol) was added to a mixture of **26** (19 mg, 0.034 mmol) and K_2CO_3 (28 mg, 0.20 mmol) in anhydrous acetone (10 mL) at room temperature. The mixture was refluxed for 48 h, and worked up by first evaporating the solvent, then dissolving the crude product in $CHCl_3$ (20 mL) and then washing with aqueous 1% HCl. The organic layer was separated and washed with H_2O (10 mL). Drying over $MgSO_4$, filtered and evaporating the solvent afforded a residue, from which excess ethyl bromoacetate was evaporated under high vacuum. The crude product was purified by PLC using ethyl acetate:hexane (3:7) to afford **49a** (13 mg, 47%), m.p. 113-115 °C, 1H NMR ($CDCl_3$): 0.40 (t, $J = 7.2$, 3H), 0.86 (t, $J = 7.2$, 3H), 1.10 (t, $J = 7.2$, 3H), 2.26 (d, $J = 15.9$, 1H), 2.65-2.75 (m, 1H), 2.85-3.00 (m, 1H), 3.15 (d, $J = 15.3$, 1H), 3.28-3.40 (m, 1H), 3.80-3.90 (m, 1H), 3.92-4.02 (dt, $J = 9.5$, 3.0, 2H), 4.30 (s, 1H), 4.17-4.42 (m, 4H), 4.59 (d, $J = 9.3$, 1H), 4.71(d, $J = 12.9$, 1H), 4.84 (d, $J = 5.1$, 1H), 4.90 (d, $J = 10.5$, 1H), 4.98 (d, $J = 2.7$, 1H), 5.01 (s, 2H), 5.22 (d, $J = 9.6$, 2H), 5.25 (d, $J = 9.6$, 2H), 5.41 (t, $J = 12$, 2H), 7.37 (t,

7.46 (t, $J = 8.1$, 3H), 7.56 (t, $J = 5.4$, 1H), 7.71 (m, 3H), 7.83 (m, 3H), 8.09 (d, $J = 8.1$, 1H), 8.12 (d, $J = 7.8$, 1H), 8.33 (d, $J = 8.4$, 1H); ^{13}C NMR (CDCl_3): 13.2, 13.7, 14.0, 59.4, 60.3, 60.4, 60.8, 63.3, 67.3, 69.3, 69.9, 70.3, 72.4, 72.7, 123.3, 124.4, 125.0, 125.1, 125.7, 126.2, 126.4, 127.6, 127.9, 128.2, 130.2, 130.3, 130.4, 130.6, 130.7, 130.9, 131.6, 131.7, 133.5, 133.9, 153.3, 154.6, 155.9, 168.5, 169.5, 169.6; ES^- calcd for $\text{C}_{18}\text{H}_{18}\text{O}_{12}$, 816.3. found 816.2

b. NaH/THF conditions:

To a solution of **26** (50 mg, 0.09 mmol) in anhydrous THF (20 mL) at rt was added NaH (15 mg, 0.62 mmol). The mixture was stirred for 5 min at rt and then ethyl bromoacetate (0.08 mL, 0.7 mmol) was added. The reaction mixture was refluxed for 8 h, cooled to rt and then the solvent was evaporated using a rotary evaporator. The crude product was dissolved in CHCl_3 (20 mL) and the mixture was washed carefully with aqueous 5% HCl. The organic layer was separated and washed with H_2O (10 mL). Drying over MgSO_4 , filtration and evaporation of the solvent afforded a residue from which excess ethyl bromoacetate was evaporated under high vacuum. The crude product and was then purified by tlc using ethylacetate/pet. ether (3:7) to give (i) 7 mg (10%) of **49a** and (ii) 18 mg (25%) of **49**, m.p. 60–62 °C. ^1H NMR (CDCl_3): 1.38 (t, $J = 6.9$ Hz, 9H), 4.31 (d, $J = 6.9$ Hz, 3H), 4.36 (d, $J = 7.3$ Hz, 3H), 4.38 (d, $J = 15.9$ Hz, 3H), 4.55 (d, $J = 15.3$ Hz, 3H), 4.79 (d, $J = 16.5$ Hz, 3H), 4.92 (d, $J = 15.9$ Hz, 3H), 5.19 (d, $J = 12.6$, 3H), 5.25 (d, $J = 12.6$ Hz, 3H), 6.76 (d, $J = 8.1$ Hz, 3H), 7.00 (s, 3H), 7.16 (ddd, $J = 7.6, 7.2, 1.0$, 3H), 7.46 (ddd, 7.6, 6.9, 1.0, 3H), 8.20 (d, $J = 8.1$ Hz, 3H); ^{13}C NMR (CDCl_3): 14.2, 61.2, 64.9, 68.3, 71.5, 123.5, 124.4, 124.5, 125.5, 127.4, 127.9, 130.5, 130.9, 132.2, 151.9, 168.7; ES^- calcd for $\text{C}_{18}\text{H}_{18}\text{O}_{12}$

816.3, found 816.2

5.4.2 Alkylation of 26a with ethyl bromoacetate

a. K_2CO_3 /acetone conditions

Ethyl bromoacetate (0.03 mL, 0.3 mmol) was added to a mixture of **26a** (25 mg, 0.034 mmol) and K_2CO_3 (29 mg, 0.21 mmol) in 10 mL anhydrous acetone at rt. The mixture was refluxed for 48 h, and worked up by first evaporating the solvent, and then dissolving the crude product in $CHCl_3$ (20 mL) and washed carefully with aqueous 1% HCl. The organic layer was separated and washed with H_2O (10 mL). Drying over $MgSO_4$, filtration and evaporation of the solvent afforded a residue from which excess ethyl bromoacetate was evaporated under high vacuum. The crude product was purified by tlc using ethyl acetate/hexane (3/7) to afford (*ii*) **diester 50b**, as a colorless solid (8 mg, 26%), m.p. 120-122 °C; 1H NMR ($CDCl_3$): 0.62 (t, $J = 6.9$ Hz, 3H), 0.82 (t, $J = 7.2$ Hz, 3H), 1.38 (s, 9H), 1.42 (s, 9H), 1.44 (s, 9H), 3.12-3.42 (m, 1H), 3.40-3.62 (m, 4H), 3.91 (d, $J = 16.2$ Hz, 1H), 4.21 (t, $J = 15.9$ Hz, 2H), 4.45 (d, $J = 11.7$ Hz, 1H), 4.55 (d, $J = 13.8$ Hz, 1H), 4.77 (d, $J = 4.8$ Hz, 1H), 4.84 (d, $J = 4.8$ Hz, 1H), 4.90 (t, $J = 12.3$ Hz, 2H), 5.00-5.13 (m, 4H), 5.31 (t, $J = 11.7$ Hz, 1H), 7.54-7.98 (m, 10H), 8.17 (d, $J = 9.0$ Hz, 1H), 8.34 (d, $J = 9.0$ Hz, 1H). ^{13}C NMR ($CDCl_3$): 13.5, 13.7, 14.1, 29.7, 34.7, 59.9, 60.1, 61.2, 62.0, 63.1, 66.2, 68.6, 70.0, 71.2, 115.4, 120.2, 122.0, 123.3, 123.4, 123.5, 124.4, 124.7, 125.5, 125.6, 126.1, 128.0, 129.3, 130.2, 130.3, 130.5, 130.6, 130.7, 131.2, 131.4, 131.7, 145.5, 147.1, 147.8, 153.1, 154.5, 168.9, 169.2, ES⁺ calcd for $C_{60}H_{12}O_{12}$, 985.2, found 985.3, and (*ii*) **triester 50a**, as a colorless solid (8 mg, 24%), m.p. 114-116 °C; 1H NMR ($CDCl_3$): 0.36 (t, $J = 7.2$

Hz, 3H), 0.77 (t, $J = 7.2$ Hz, 3H), 1.13 (t, $J = 7.2$ Hz, 3H), 1.33 (s, 9H), 1.37 (s, 9H), 1.42 (s, 9H), 1.14 (t, 9H), 2.12 (d, $J = 15.6$ Hz, 1H), 2.56 (m, 1H), 2.86 (m, 1H), 3.05 (m, 1H), 3.22 (d, $J = 15.6$ Hz, 1H), 3.97 (m, 2H), 3.95 (m, 2H), 4.13-4.40 (m, 4H), 4.53 (d, $J = 8.4$ Hz, 1H), 4.72 (m, 2H), 4.89-5.11 (m, 8H), 5.45 (m, 2H), 7.49 (d, 1H), 7.54 (m, 2H), 7.57 (d, 1H), 7.65 (m, 3H), 7.70 (s, 1H), 7.75 (d, 2H), 7.76 (s, 1H), 7.82 (s, 1H), 7.96 (d, $J = 9.0$ Hz, 1H), 8.06 (d, $J = 9.0$ Hz, 1H), 8.29 (d, $J = 9.0$ Hz, 1H), ^{13}C NMR (CDCl_3): 13.2, 13.8, 14.0, 31.1, 31.2, 34.6, 34.7, 59.2, 59.9, 60.2, 60.4, 60.8, 63.2, 67.5, 69.6, 69.8, 70.7, 72.5, 73.1, 122.9, 123.1, 124.1, 124.3, 125.3, 125.4, 125.7, 126.1, 127.5, 130.1, 130.3, 130.6, 130.7, 130.8, 131.6, 131.7, 132.0, 148.2, 148.3, 152.2, 152.7, 153.3, 154.2, 155.7, 168.7, 169.3, 169.8, 171.2; ES $^-$ calcd for $\text{C}_{40}\text{H}_{42}\text{O}_{12} = 985.2$, found = 985.3

b. NaH/THF conditions:

To a solution of **26a** (27 mg, 0.037 mmol) in anhydrous THF (20 mL) at rt was added NaH (15 mg, 0.62 mmol). The mixture was stirred for 5 min at rt and then ethyl bromoacetate (0.03 mL, 0.3 mmol) was added. The reaction mixture was refluxed for 8 h, cooled to rt and then the solvent was evaporated using a rotary evaporator. The crude product was dissolved in CHCl_3 (20 mL) and the mixture was washed with aqueous 5% HCl. The organic layer was separated and washed with H_2O (10 mL). Drying over MgSO_4 , filtration and evaporation of the solvent afforded a residue from which excess ethyl bromoacetate was evaporated under high vacuum. The crude product was then purified by TLC using ethylacetate:pet ether (3:7) to afford (*i*) **50a** as a colorless solid (6 mg) whose spectral properties were identical to that of the product obtained from K_2CO_3 /acetone

conditions, and (ii) **50** as a colorless solid (9 mg, 25%) in the cone conformation, m p. 75-77 °C, ¹H NMR (CDCl₃): 1.26 (s, 27H), 1.36 (t, *J* = 6.9 Hz, 6H), 4.28 (d, *J* = 7.2 Hz, 4H), 4.33 (d, *J* = 6.9 Hz, 4H), 4.50 (d, *J* = 16.2 Hz, 4H), 4.74 (d, *J* = 14.1 Hz, 4H), 4.85 (d, *J* = 15.9 Hz, 4H), 5.01 (d, *J* = 12.3 Hz, 4H), 5.17 (d, *J* = 12.3 Hz, 4H), 7.08 (d, *J* = 2.1 Hz, 3H), 7.10 (s, 3H), 7.20 (dd, *J* = 1.8 Hz, 7.5, 3H), 7.76 (d, *J* = 9.0 Hz, 3H); ¹³C NMR (CDCl₃): 14.1, 31.1, 34.4, 60.9, 64.2, 69.8, 71.6, 122.8, 123.4, 124.3, 124.6, 128.6, 130.4, 131.1, 146.8, 153.4, 169.6; ES⁻ calcd for C₃₀H₄₂O₁₂: 985.2, found 985.3

5.4.3. Metal picrate binding studies.

Extractions of metal picrates from deionized-water into chloroform (spectrograde) were performed according to the following typical procedure: 5 ml of an aqueous 1.7×10^{-4} M solution of the metal picrate and 5 ml of a chloroform 1.7×10^{-4} M solution of triester **49** (or **49a**), or triester **50** (or **50a**) in CHCl₃ were mechanically shaken in a Teflon[®]-lined stoppered glass tube for 24 h. The mixture was then equilibrated in a thermostated water bath at 25.0 ± 0.1 °C for 2 h in order to achieve a good phase separation. The absorbance of the metal picrate remaining in the aqueous phase was then determined spectrophotometrically at 358 nm on a HP 8452A diode array uv-vis spectrophotometer. The percentage extraction (%E) for each solution was calculated from the expression $\%E = 100(A_0 - A)/A_0$. Where A_0 is the absorbance of the aqueous solution of the metal picrate without the triesters. The results are listed in Table 5.1.

References

1. C. D. Gutsche, *Calixarenes Revisited*, pp 1-17, Monographs in Supramolecular Chemistry, J. F. Stoddard (Ed.), Royal Society of Chemistry, Cambridge, 1998.
2. J. W. Cornforth, P. D'Arcy Hart, G. A. Nicholls, R. J. W. Rees and J. A. Stock, *Br. J. Pharmacol.* 1955, **10**, 73.
3. C. D. Gutsche, B. Dhawan, J. A. Levine, K. H. No and L. J. Bauer, *Tetrahedron* 1983, **39**, 409.
4. (a) C. D. Gutsche, *Aldrichim. Acta* 1995, **28**, 3. (b) G. D. Andreetti and F. Uguzzoli.: in *Calixarenes: A Versatile Class of Macrocyclic Compounds* pp 87-123. Topics In Inclusion Science, J. Vicens and V. Bohmer (Ed.), Kluwer Academic Publishers, Dordrecht, 1991.
5. S. R. Izatt, R. T. Hawkins, J. J. Christensen and R. M. Izatt, *J. Am. Chem. Soc.* 1985, **107**, 63.
6. J. L. Atwood, G. A. Koutsantonis and C. L. Raston, *Nature* 1994, 368, 229.
7. T. Suzuki, K. Nakashima and S. Shinkai, *Chem. Lett.* 1994, 699.
8. (a) A. Arduini, A. Pochini, S. Reverberi, R. Ungaro and G. D. Andreetti, *Tetrahedron*, 1986, **42**, 2089. (b) S. K. Chang and I. Cho, *J. Chem. Soc., Perkin Trans. 2* 1986, 211 (c) A. Barrett, M. A. McKervey, J. F. Malone, A. Walker, C. D. Gutsche and D. R. Stewart, *J. Chem. Soc., Perkin Trans. 2* 1993, 1475. (e) K. Iwamoto and S. Shinkai, *J. Org. Chem.* 1992, **57**, 7066. (f) E. M. Collins, M. A. McKervey and S. J. Harris, *J. Chem. Soc., Perkin Trans. 1* 1989, 372.

- 9 S. Shinkai, S. Mori, H. Koreishi, T. Tsubaki and O. Manabe, *J. Am. Chem. Soc.* 1986, **108**, 2409.
10. (a) P. E. Georghiou and Z.-P. Li, *Tetrahedron Lett.* 1993, **34**, 2887. (b) P. E. Georghiou, M. Ashram, Z. Li and S. G. Chaulk, *J. Org. Chem.* 1995, **60**, 7284.
- 11 M. Ashram, *Synthesis of calix[4]naphthalenes and their properties*, Ph.D Dissertation, Memorial University of Newfoundland, St. John's, Newfoundland, Canada, 1997.
- 12 These calculations were performed using the programs implemented in PC SPARTAN Pro 5.0 from Wavefunction Inc., Irvine, CA 92612.
13. (a) H.-J. Schneider and A. K. Yatsimirsky, *Principles and Methods in Supramolecular Chemistry*, Wiley, Chichester, 2000. (b) F. Vogtle, *Supramolecular Chemistry*, Wiley, NY, 1991. (c) J.-M. Lehn, *Supramolecular Chemistry*, VCH, Weinheim, 1995. (d) P. D. Beer, P. A. Gale and D. K. Smith, *Supramolecular Chemistry*, Oxford, 1999.
14. B. Dietrich, P. Viout and J.-M. Lehn, *Macrocyclic Chemistry*, VCH, Weinheim, 1993, and references therein.
- 15 D. J. Cram and J. M. Cram, *Container Molecules and Their Guests*, The Royal Society of Chemistry, Cambridge, 1994.
- 16 H. S. Frank and M. W. Evans, *J. Phys. Chem.* 1945, **13**, 507.
17. (a) A. Ben-Naim, *J. Chem. Phys.* 1971, **54**, 1387. (b) E. Frieden, *J. Chem. Ed.* 1975, **52**, 754. (c) B. R. Baker, *J. Chem. Ed.* 1967, **44**, 610. (d) S. N. Timasheff, *Acc.*

- Chem. Res.* 1970, **3**, 1970.
18. R. Foster, *Organic Charge-Transfer Complexes*, Academic Press, Elsevier, New York, 1950.
 19. R. Taylor (Ed.), *The Chemistry of Fullerenes*, Advanced Series in Fullerenes, Vol. 4, World Scientific Publishing Co. Pte. Ltd., Singapore, 1995, and references therein.
 20. K. Kampe, N. Egger and M. Vogel, *Angew. Chem., Int. Ed. Engl.* 1993, **32**, 1174.
 21. F. D. Weiss, J. L. Elkind, S. C. O'Brien, R. F. Curl and R. E. Smalley, *J. Am. Chem. Soc.* 1988, **110**, 4464.
 22. D. E. Clifffel, A. J. Bard and S. Shinkai, *Anal. Chem.* 1998, **70**, 4146.
 23. A. L. Balch, J. W. Lee, B. C. Noll and M. M. Olmstead, *J. Chem. Soc., Chem. Commun.* 1993, 56.
 24. J. D. Crane, P. B. Hitchcock, H. W. Kroto, R. Taylor and D. M. R. Walton, *J. Chem. Soc., Chem. Commun.* 1992, 1764.
 25. R. E. Douthwaite, M. I. H. Green, S. J. Hayes, M. J. Rosseinsky and J. F. C. Turner, *J. Chem. Soc., Chem. Commun.* 1994, 1367.
 26. F. Diederich and M. G. Lopez, *Chem. Soc. Rev.* 1999, **28**, 263.
 27. O. Ermer, *Helv. Chim. Acta* 1991, **74**, 1339.
 28. J. Wang, S. G. Bodige, W. H. Watson and C. D. Gutsche, *J. Org. Chem.* 2000, **65**, 8260, and references therein.
 29. (a) P. E. Georghiou, S. Mizyed and S. Chowdhury, *Tetrahedron Lett.* 1999, **40**, 611.

- (b) S. Mizyed, M. Ashram, D. O. Miller and P. E. Georghiou, *J. Chem. Soc., Perkin Trans. 2*. 2001, 1916. (c) S. Mizyed, P. E. Georghiou, M. Bancu, B. Cuadra, A. K. Rai, P. Cheng and L. T. Scott, *J. Am. Chem. Soc.* 2001, **123**, 12770.
30. T. Anderson, K. Nilsson, M. Sundahl, W. Westman and Q. Wennerstrom, *J. Chem. Soc., Chem. Commun.* 1992, 604.
31. J. W. Steed, P. C. Junk, J. L. Atwood, M. J. Barnes, C. L. Raston and R. S. Burkhalter, *J. Am. Chem. Soc.* 1994, **116**, 10346.
32. A. Izuoka, T. Tachikawa, T. Sugawara, Y. Suzuki, M. Konno, Y. Saito and H. Shinohara, *J. Chem. Soc., Chem. Commun.* 1992, 1472.
33. A. Ikeda, T. Hatano, M. Kawagushi, H. Suenaga and S. Shinkai, *J. Chem. Soc., Chem. Commun.* 1999, 1403.
34. N. Martin, L. Sanchez, B. Illescas and I. Perez, *Chem. Rev.* 1998, **98**, 2527.
35. S. H. Friedman, D. L. Decamp, R. P. Sijbesma, G. Srdanov, F. Wudl and G. L. Kenyon, *J. Am. Chem. Soc.* 1993, **115**, 6506.
36. R. M. Williams and J. W. Verhoeven, *Recl. Trav. Chim. Pays-Bas*. 1992, **111**, 531.
37. J. L. Atwood, S. G. Bott, C. Jones and C. L. Raston, *J. Chem. Soc., Chem. Commun.* 1992, 1349.
38. C. L. Raston, J. L. Atwood, P. J. Nichols and I. B. N. Sudria, *J. Chem. Soc., Chem. Commun.* 1996, 2615.
39. B. Paci, G. Amoretti, G. Arduini, G. Ruani, S. Shinkai, T. Suzuki, F. Vgozzoli and

- R. Caciuffo, *Phys. Rev. B* 1997, **55**, 5566.
40. R. M. Williams, J. M. Zwier and J. W. Verhoeven, *J. Am. Chem. Soc.* 1994, **116**, 6965.
41. J. Averdung, T. Budwach, W. Iwanek, I. Schlachter, G. T. Gracia and J. Mattay, in *Physics and Chemistry of Fullerenes and Derivatives*, pp 137-141, H. Kuzmany, J. Fink, M. Mehring and S. Roth (Ed.), World Scientific Publishing Co. Pte. Ltd., Singapore, 1995.
42. J. L. Atwood, L. J. Barbour, C. L. Raston and I. B. N. Sudria, *Angew. Chem., Int. Ed. Engl.* 1998, **37**, 981.
43. K. Araki, K. Akao, A. Ikeda, T. Suzuki and S. Shinkai, *Tetrahedron Lett.* 1995, **36**, 73.
44. A. Ikeda, M. Yoshimura and S. Shinkai, *Tetrahedron Lett.* 1997, **38**, 2107.
45. (a) T. Haino, M. Yanase and Y. Fukazawa. *Angew. Chem., Int. Ed. Engl.* 1997, **36**, 259. (b) T. Haino, M. Yanase and Y. Fukazawa, *Tetrahedron Lett.* 1997, **38**, 3739. (c) T. Haino, M. Yanase and Y. Fukazawa. *Angew. Chem., Int. Ed. Engl.* 1998, **37**, 997.
46. J. L. Atwood, L. J. Barbour, P. J. Nichols, C. L. Raston and C. A. Sandoval, *Chem. Eur. J.* 1999, **5** (3),990.
47. J. Wang and C. D. Gutsche, *J. Am. Chem. Soc.* 1998, **120**, 12226.
48. M. Kawaguchi, A. Ikeda, S. Shinkai and I. Neda *J. Incl. Phenom.* 2000, **37**, 253.
49. N. S. Isaacs, P. J. Nichols, C. L. Raston, C. A. Sandoval and D. J. Young, *J. Chem.*

- Soc., Chem. Commun.* 1997, 1839.
50. M. J. Hardie and C. L. Raston, *J. Chem. Soc., Chem. Commun.* 1999, 1153.
51. L. J. Barbour, G. W. Orr and J. L. Atwood, *J. Chem. Soc., Chem. Commun.* 1998, 1901.
52. L. J. Barbour, G. W. Orr and J. L. Atwood, *J. Chem. Soc., Chem. Commun.* 1997, 1439.
53. A. G. S. Hogberg, *J. Org. Chem.* 1980, **45**, 4498.
54. L. M. Tunstad, J. A. Tucker, E. Dalcanale, J. Weiser, J. A. Bryant, J. C. Sherman, R. C. Helgeson, C. B. Knobler and D. J. Cram, *J. Org. Chem.* 1989, **54**, 1305.
55. (a) M. M. Garcia, R. T. Cabanas, A. T. Ochoa, A. Toscano and R. C. Almanza, *Fullerene Science and Technology* 2000, **8**, 475. (b) M. M. Garcia, M. I. Chavez Urbi, E. Bautishi Palacios, F. Lara Ochoa, T. Toscano, J. A. Cogordan, S. Rios and R. C. Almanza, *Tetrahedron* 1999, **55**, 6019.
56. K. N. Rose, L. J. Barbour, G. W. Orr and J. L. Atwood, *J. Chem. Soc., Chem. Commun.* 1998, 407.
57. R. M. Izatt, and J. J. Christensen, *Progress in Macrocyclic Chemistry*, Vol. 3. John Wiley and Sons, Toronto, 1987.
58. C. J. Pedersen, *J. Am. Chem. Soc.* 1967, **89**, 7017.
59. J. Catalan, J. L. Saiz, J. L. Laynez, N. Jagerovic and J. Elguero, *Angew. Chem., Int. Ed. Engl.* 1995, **34**, 105.
60. E. D. Olsen, *Modern Optical Methods of Analysis*. McGraw-Hill, New York, 1974.

61. K. A. Connors, *Binding Constants, The Measurements of Molecular Complex Stability*. Wiley-Interscience, New York, 1987.
62. L. Sommer, *Studies in Analytical Chemistry 8, Analytical Absorption Spectrophotometry in the Visible and Ultraviolet*. E.Pungor, W. Simon, H. Malissa and J. Inczedy (Eds.) Elsevier, Amsterdam, 1989J. Brynestad, G. P. Smith, *J. Phy. Chem.*, 1968, **72**, 296.
63. P. Job, *Ann. Chim Phys.* 1928, **9**, 113.
64. A. Benesi and J. H. Hildebrand, *J. Am. Chem. Soc.* 1949, **71**, 2703.
65. J. Szejtli, *Cyclodextrins and Their Inclusion Complexes*. Akademia Kiado, Budapest, 1982.
66. O. P. Dimitriev, Z. I. Kazantseva and N. V. Lavrik, *J. Inclusion Phenom.* 1999, **35**, 85.
67. (a) H. Matsubara, T. Shimora, A. Hasegawa, M. Semba, K. Asano and K. Yamamoto, *Chem. Lett.* 1998, 1099. (b) H. Matsubara, A. Hasegawa, K. Shiwaku, K. Asano, M. Uno, S. Takahashi and K. Yamamoto, *Chem. Lett.* 1998, 923
68. J. Dormann, A. Lentz, S. Rastatter, F. Schildlach and J. Schatz, *Presented as a poster at the 4th International Conference on Calixarenes*, Parma, Italy, 1997.
69. N. Sivaraman, R. Dhamodaran, I. Kaliappen, T. G. Srinivassan, P. R. Vasudeva Rao and C. K. Matthews, *J. Org. Chem.* 1992, **57**, 6077.
70. A. F. Danil de Namor, R. M. Cleverly and M. L. Zapata-Ormachea, *Chem. Rev.* 1998, **98**, 2495.

71. (a) S. Shinkai and A. Ikeda, *Gazz. Chim. It.* 1997, **127**, 657. (b) A. Ikeda, M. Kawaguchi, Y. Suzuki, T. Hanato, M. Numata, S. Shinkai, A. Ohta, and M. Aratono, *J. Incl. Phenom.* 2000, **38**, 163.
72. S. Mized, P. E. Georghiou and M. Ashram, *J. Chem. Soc., Perkin Trans. 2* 2000, 277.
73. M. Yanase, M. Matsuoka, Y. Tatsumi, M. Suzuki, H. Iwamoto, T. Haino and Y. Fukawaza, *Tetrahedron Lett.* 2000, **41**, 493.
74. A. Ikeda, Y. Suzuki, M. Yoshimura and S. Shinkai, *Tetrahedron* 1998, **54**, 2497.
75. (a) G. D. Andreetti, R. Ungaro and A. Pochini, *J. Chem. Soc., Chem. Commun.* 1979, 1005. (b) M. Coruzzi, G. D. Andreetti, V. Bocchi and A. Pochini, *J. Chem. Soc., Perkin Trans. 2* 1982, 1133. (c) G. D. Andreetti, A. Pochini and R. Ungaro, *Ibid.* 1983, 1773. (d) C. Rizzoli, G. D. Andreetti, R. Ungaro and A. Pochini, *J. Mol. Struct.* 1982, **82**, 133.
76. S. Chowdhury, J. N. Bridson and P. E. Georghiou, *J. Org. Chem.* 2000, **65**, 3299.
77. T. M. Letcher, P. B. Crosby, U. Domanska, P. W. Fowler and A. C. Letcher, *South Afr. J. Chem.* 1993, **46**, 41.
78. W. Tao and M. Barra, *J. Chem. Soc., Perkin Trans. 2* 1998, 1957.
79. M. M. Olmstead, F. Jiang and A. L. Balch, *Chem. Commun.* 2000, 483.
80. L. J. Bauer and D. Gutsche, *J. Am. Chem. Soc.* 1985, **107**, 6063.
81. L. Liu and Q.-X. Guo, *Chem. Rev.* 2001, **101** (3), 673.
82. Y. Inoue, T. Hakushi, Y. Liu, L.-H. Tong, B.-J. Shen and D.-S. Jin, *J. Am. Chem.*

- Soc.* 1993, **115**, 457
- 83 Y. Inoue, Y. Liu, L.-H. Tong, B.-J. She and D.-S. Jin, *J. Am. Chem. Soc.* 1993, **115**, 10637
- 84 *Calixarenes 50th Anniversary: Commemorative Issue* (Eds. J. Vicens, Z. Asfari, J. and McB. Harrowfield), Kluwer Academic Publishers, Dordrecht, 1995.
- 85 K. Tsubaki, T. Mormoto, T. Otsubo, T. Kinoshita and K. Fuji, *J. Org. Chem.* 2001, **66**, 4083.
- 86 C. D. Gutsche, B. Dhawan, K. H. No and R. Muthukrishnan, *J. Am. Chem. Soc.* 1981, **103**, 3782
- 87 P. Zerr, M. Mussrabi and J. Vicens, *Tetrahedron Lett.* 1991, **32**, 1879
- 88 P. D. Hampton, Z. Bencze, W. Tong and C. E. Daitch, *J. Org. Chem.* 1994, **59**, 4838
- 89 K. Tsubaki, T. Otsubo, K. Tanaka, K. Fuji and T. Kinoshita, *J. Org. Chem.* 1998, **63**, 3260.
- 90 K. Tsubaki, K. Mukoyoshi, T. Otsubo and K. Fuji, *Chem. Pharm. Bull.* 2000, **48**, 882.
- 91 B. Masci, *Tetrahedron* 2001, **57**, 2841.
- 92 N. Komatsu, *Tetrahedron Lett.* 2001, **42**, 1733
- 93 H. Matsumoto, S. Nishio, M. Takeshita and S. Shinkai, *Tetrahedron* 1995, **51**, 4647
- 94 K. Araki, K. Inada and S. Shinkai, *Angew. Chem., Int. Ed. Engl.* 1996, **35**, 72
- 95 (a) A. Ikeda, H. Udzu, M. Yoshimura and S. Shinkai, *Tetrahedron* 2000, **56**,

- 1825 (b) A. Ikeda, M. Yoshimura, H. Udzu, C. Fukuhara and S. Shinkai *J. Am. Chem. Soc.* 1999, **121**, 4296. (c) A. Ikeda, M. Yoshimura, H. Udzu, C. Fukuhara and S. Shinkai, *Chem. Lett.* 1994, 587.
- 96 M. Ashram, S. Mizyed and P. E. Georghiou, *J. Org. Chem.* 2001, **66**, 1473
- 97 The following names are based upon a "calixarene"-type naming and numbering scheme: *sym*-3,1,3,2,3,3-trihydroxy-2,3,1,2,1,3,2,2,2,3-hexahomo-3,1,3,2,3-trioxacalix[3]naphthalene, for the C_2 -symmetrical compound **26**; 3,1,3,2,3,3-trihydroxy-2,3,1,2,1,3,2,2,2,3-hexahomo-3,1,3,2,3-trioxacalix[3]naphthalene for the unsymmetrical compound **27**; *sym*-8,18,28-tri-*tert*-butyl-3,1,3,2,3,3-trihydroxy-2,3,1,2,1,3,2,2,2,3-hexahomo-3,1,3,2,3-trioxacalix[3]naphthalene for the C_2 -symmetrical compound **26a**. Names based upon the Chemical Abstracts naming system are the following: 16*H*,26*H*,28*H*,-5,29,9,15,19,25-trimetheno-6*H*,8*H*,18*H*-tribenzo[d,1,t][1,9,17]trioxacyclotetracosin-30,31,32-triol for **26**; 16*H*,26*H*,28*H*,-5,29,9,15,19,25-trimetheno-6*H*,8*H*,18*H*-tribenzo[d,1,u][1,9,17]trioxacyclotetracosin-30,31,32-triol for **27**; 10,10'-[[2-(methoxymethoxy)-1,3-naphthalenediyl]bis(methyleneoxymethylene)]bis[[2,2-dimethyl-4*H*-naphtho[2,3-d]-1,3-dioxin for the linear trimer **41**; and 10,10'-[[2-(methoxymethoxy)-1,3-naphthalenediyl]bis(methyleneoxymethylene)]bis[[2,2-dimethyl-7-(1,1-dimethylethyl)-4*H*-naphtho[2,3-d]-1,3-dioxin for the *tert*-butyl linear trimer **41a**
- 98 A. I. Vogel, "*Vogel's Textbook of Practical Organic Chemistry*"; 5th Ed., Longman London, 1989

- 99 P. E. Georghiou, M. Ashram, H. J. Claseand and J. N. Bridson, *J. Org. Chem.* 1998, **63**, 1819.
- 100 P. E. Georghiou and M. Ashram, *unpublished results*.
- 101 (a) K. Araki, N. Hashimoto, H. Otsuka and S. Shinkai, *S. J. Org. Chem* 1993, **58**, 5958. (b) K. Araki, K. Inada, H. Otsuka and S. Shinkai, *Tetrahedron* 1993, **49**, 9465
- 102 L. Mandolini and R. Ungaro, (Eds.) *Calixarenes in Action*. Imperial College Press, London, England 2000.
- 103 K. Tsubaki, K. Tanaka, T. Kinoshita and K. Fuji, *Chem. Commun* 1998, 895
- 104 L. Fielding, *Tetrahedron* 2000, **56**, 6151.
- 105 M. Yanase, T. Haino and Y. Fukuzawa, *Tetrahedron Lett.* 1999, **40**, 2781
- 106 C. Tanford In *The Hydrophobic Effect: Formation of Micelles and Biological Membranes*, 2nd Edn. Wiley, New York, 1980.
- 107 T. V. Chalikian, G. E. Plum, A. P. Sarvazyan and K. J. Breslauer, *Biochemistry* 1994, **33**, 8629.
- 108 E. Vikingstad In *Aggregation Processes in Solution*, S. E. Wyn-Jone, J. Gormally, Eds., Elsevier Scientific Publishing Company, Amsterdam, 1983
- 109 H. Hoiland, J. A. Ringseth and E. Vikingstad, *J. Solution Chem.* 1978, **7**, 515
- 110 H. Hoiland, J. A. Ringseth and T. S. Burn, *J. Solution Chem.* 1979, **8**, 779
- 111 H. Hoiland, L. H. Hald and E. Vikingstad, *J. Solution Chem.* 1981, **10**, 775
- 112 M. S. Bakshi, *J. Solution Chem.* 1996, **25**, 411.
- 113 S. Milito and M. S. Bakshi, *J. Solution Chem.* 1995, **24**, 103.

114. L. D. Wilson and R. E. Verrall, *J. Phys. Chem. B* 1997, **101**, 9270.
115. L. D. Wilson and R. E. Verrall, *J. Phys. Chem. B* 1998, **102**, 480
116. W. Zielenkiewicz, O. Pietraszkiewicz, M. Wszelaka-Rylik, M. Pietraszkiewicz, G. Roux-Desgranges, A. H. Roux and J.-P. E. Grolier, *J. Solution Chem.* 1998, **27**, 121
117. T. M. Letcher and J. D. Mercer-Chalmers, *J. Solution Chem.* 1992, **21**, 489
118. P. Ruelle, A. Farina-Cuendet and U. W. Kesselring, *J. Am. Chem. Soc.* 1996, **118**, 1777
119. N. S. Isaacs and D. J. Young, *Tetrahedron Lett* 1999, **40**, 3953
120. Z. Liron and S. Cohen, *J. Pharm. Sci.* 1983, **72**, 499
121. A. Martin, Z. Liron and S. Cohen, *J. Pharm. Sci.* 1985, **74**, 638
122. For a recent bibliography see F. C. Tucci, D. M. Rudkevich and J. Rebek, Jr., *J. Org. Chem.* 1999, **64**, 4555 and references cited therein
123. F. Daniels, J. W. Williams, P. Bender, R. A. Alberty, C. D. Cornwell and J. E. Harriman, *Experimental Physical Chemistry*, 7th Ed., McGraw Hill, New York, 1970
124. T. F. Young and M. B. Smith, *J. Phys. Chem.* 1954, **58**, 716
125. Y. P. Handa and G. C. Benson, *Fluid Phase Equilib.* 1979, **3**, 185
126. K. Shinoda and J. H. Hildebrand, *J. Phys. Chem.* 1958, **62**, 295
127. W. B. Jepson and J. S. Rowlinson, *J. Chem. Soc.* 1956, 261, 1278
128. E. B. Smith, J. Walkely and J. H. Hildebrand, *J. Phys. Chem.* 1959, **63**, 703
129. K. A. Connors, *Chem. Rev.* 1997, **97**, 1325

- 130 J. Timmermans, *Physico-chemical Constants of Pure Organic Compounds*, Elsevier, New York, 1950.
- 131 Caibin Xiao, Ph.D. Dissertation, Memorial University of Newfoundland, St. John's, Newfoundland, Canada, 1997.
- 132 R. M. Izatt, J. D. Lamb, R. T. Hawkins, P. Brown, S. R. Izatt and J. J. Christensen, *J. Am. Chem. Soc.* 1983, **105**, 1782.
- 133 M. A. McKervey, E. M. Seward, G. Ferguson, B. Ralph and S. J. Harris, *J. Chem. Soc. Chem. Commun.* 1985, 388.
- 134 W. Vogt and A. Wolff, *J. Org. Chem.* 1993, **58**, 4023.

Appendix A.

Table A.1 Experimental values of ΔAbs , as a function of [8] or [9] for the 8 C_{50} and 9 C_{60} complexes at different temperatures (* = no data available). Absorbance data ± 0.005 .

8 C_{50} in toluene						
[8]·10 ⁴ M	15 °C	20 °C	30 °C	35 °C	[8]·10 ⁴ M	25 °C
0.2237	4.62e-3	3.33e-3	1.82e-3	1.92e-3	0.1920	4.20e-3
0.4616	9.20e-3	5.97e-3	3.44e-3	3.67e-3	0.3750	7.90e-3
0.6556	0.012	9.16e-3	4.86e-3	5.37e-3	0.5500	0.017
0.8630	0.015	0.012	5.64e-3	7.40e-3	0.7170	0.022
1.0329	0.016	0.015	7.33e-3	8.84e-3	0.8760	0.031
1.2152	0.019	0.017	9.50e-3	0.010	1.0280	0.035
1.5268	0.022	0.020	*	*	1.1740	0.042
1.8903	0.030	0.021	0.012	0.012	1.3140	*
2.2054	*	0.028	0.017	0.014	1.5770	0.054
2.6063	0.036	0.031	0.019	0.016	1.8200	0.055
2.9405	*	*	*	0.021	2.2530	0.060
					2.6280	0.065
					2.9570	0.069

[C₅₀]=1.043e-4

8 C_{60} in toluene					
[8]·10 ⁴ M	15 °C	20 °C	25 °C	30 °C	35 °C
0.2187	1.85e-3	2.19e-3	3.16e-3	1.1316e-3	0.023
0.4512	3.60e-3	4.15e-3	*	1.8800e-3	4.05e-3
0.6408	5.03e-3	5.98e-3	8.79e-3	2.8900e-3	6.84e-3
0.8435	5.99e-3	7.70e-3	0.012	3.5100e-3	9.07e-3
1.0096	6.50e-3	8.80e-3	0.014	4.8400e-3	0.010
1.1878	8.20e-3	9.75e-3	0.017	6.1800e-3	0.012
1.4923	0.010	0.012	0.021	8.0900e-3	*
1.8476	0.012	0.015	0.023	0.0100	0.015
2.1556	*	0.018	0.026	*	0.017
2.5475	0.014	0.020	0.030	0.0113	0.019
2.8741	0.017	0.022	0.034	0.0133	0.023
3.2334			0.037		

[C₆₀]=1.021e-4

Table A.1. continued

8 C ₆₀ in benzene					
[8]•10 ⁴ M	15 °C	20 °C	25 °C	30 °C	35 °C
0.2389	3.80e-3	4.14e-3	5.24e-3	3.47e-3	3.05e-3
0.4600	6.76e-3	6.89e-3	9.55e-3	6.77e-3	5.54e-3
0.6654	9.57e-3	0.011	0.013	9.09e-3	8.84e-3
0.8566	0.013	0.013	0.018	0.011	0.011
1.0351	0.015	0.015	0.022	0.015	0.014
1.2421	0.017	0.017	0.027	0.018	0.015
1.6102	0.022	0.022	0.035	0.024	0.019
2.0702	0.027	0.026	0.043	0.030	0.023
2.6617	0.033	0.033	0.048	0.033	0.030
3.1053	0.036	0.037	0.053	0.037	0.035

$$[C_{60}] = 1.026e-4$$

8 C ₆₀ in benzene						
[8]•10 ⁴ M	15 °C	20 °C	30 °C	35 °C	[8]•10 ⁴ M	25 °C
0.2599	3.66e-3	3.85e-3	2.68e-3	2.97e-3	0.1866	2.76e-3
0.5006	7.14e-3	7.07e-3	5.35e-3	5.21e-3	0.3640	9.63e-3
0.7241	0.010	0.011	8.13e-3	7.40e-3	0.5330	0.017
0.9322	0.012	0.014	9.94e-3	0.010	0.6950	0.022
1.1264	0.014	0.016	0.011	0.012	0.8502	0.029
1.3517	0.016	0.019	0.013	0.014	0.9981	0.036
1.7522	0.020	0.023	0.017	0.017	1.1397	0.043
2.2528	0.026	0.026	0.021	0.022	1.2753	0.045
2.8965	0.032	0.030	0.025	0.028	1.5304	0.049
3.3792	*	0.034	0.029	0.033	1.7658	0.053
					2.1863	0.065
					2.5507	0.073
					2.8695	0.078
					3.2794	0.087
					3.6246	0.095

$$[C_{60}] = 1.101e-4$$

Table A.1. continued

8:C ₆₀ in CS ₂					
[8]•10 ⁴ M	15 °C	20 °C	25 °C	30 °C	35 °C
0.2268	3.73e-3	3.25e-3	1.90e-3	3.75e-3	2.89e-3
0.4483	5.57e-3	5.68e-3	3.38e-3	6.92e-3	5.42e-3
0.6647	8.33e-3	8.29e-3	4.63e-3	9.84e-3	8.12e-3
0.8761	0.011	0.011	6.43e-3	0.012	9.71e-3
1.0827	0.013	0.013	7.50e-3	0.014	0.011
1.4169	0.015	0.014	9.22e-3	0.018	0.014
2.0494	0.017	0.017	0.010	0.024	0.019
2.6383	0.021	0.020	0.013	*	*
3.7022	0.033	*	0.015	*	0.031
4.6371	0.019	0.025	0.016	0.044	*
5.8174	*	*	*	*	0.048

$$[C_{60}] = 1.032e-4$$

8:C ₆₀ in CS ₂					
[8]•10 ⁴ M	15 °C	20 °C	25 °C	30 °C	35 °C
0.2410	3.54e-3	2.08e-3	4.11e-3	4.31e-3	2.96e-3
0.4764	5.91e-3	3.63e-3	7.43e-3	7.82e-3	5.96e-3
0.7064	8.56e-3	4.95e-3	9.95e-3	0.011	7.94e-3
0.9311	9.89e-3	6.05e-3	0.012	0.014	0.010
1.1506	0.012	7.13e-3	0.014	0.016	0.012
1.5058	0.013	9.16e-3	0.02	0.021	0.016
2.1780	0.017	0.010	0.023	0.025	0.020
2.8039	0.020	0.012	*	0.034	0.027
3.9345	0.022	*	0.036	*	0.028
4.9280	0.024	0.017	0.042	0.053	0.034

Table A.1. continued

9-C ₅₀ in toluene						
[9]·10 ⁴ M	15 °C	20 °C	30 °C	35 °C	[9]·10 ⁴ M	25 °C
0.1726	4.35e-3	2.09-3	2.62e-3	2.21e-3	0.2228	1.04e-3
0.3369	4.62e-3	3.02e-3	4.76e-3	3.25e-3	0.4412	2.09e-3
0.4936	7.12e-3	4.88e-3	5.76e-3	4.50e-3	0.6554	3.77e-3
0.6432	0.010	6.34e-3	7.24e-3	5.44e-3	0.8655	5.22e-3
0.7862	0.014	8.19e-3	9.52e-3	6.94e-3	1.0716	6.69e-3
0.9229	0.016	8.59e-3	0.011	8.09e-3	1.2738	7.82e-3
1.0538	0.019	0.010	0.012	9.44e-3	1.4722	8.88e-3
1.1792	0.022	0.011	0.014	0.010	1.7310	0.011
1.2996	0.028	0.013	0.017	0.013	2.0458	0.012
1.4151	0.033	0.014	0.020	0.015	2.6475	0.015
1.6328	0.043	0.017	0.026	0.019	3.2148	0.017
2.0216	0.051	0.021	0.030	0.022	3.7506	0.019
2.3585	0.058	0.026	0.034	0.025	4.7376	0.025
2.6533	0.067	0.029	0.040	0.029	5.6259	0.029
3.0323	0.077	0.033	0.045	0.033		
3.5377	*	0.040	*	*	[C60]	1.220e-4

[C₆₀]=1.526e-4

9-C ₅₀ in toluene					
[9]·10 ⁴ M	15 °C	20 °C	25 °C	30 °C	35 °C
0.2228	4.35e-3	2.10e-3	1.86e-3	1.37e-3	1.75e-3
0.4412	4.62e-3	3.12e-3	3.71e-3	2.45e-3	3.31e-3
0.6554	7.12e-3	4.75e-3	5.23e-3	3.71e-3	4.50e-3
0.8655	0.010	7.00e-3	6.46e-3	4.58e-3	6.29e-3
1.0716	0.014	9.54e-3	8.38e-3	5.48e-3	8.26e-3
1.2738	0.016	0.010	0.010	6.52e-3	0.010
1.4722	0.019	0.012	0.012	7.86e-3	0.012
1.7310	0.022	0.013	0.014	0.010	0.014
2.0458	0.028	0.015	0.015	0.013	0.016
2.6475	0.033	0.020	0.019	0.018	0.019
3.2148	0.043	0.024	0.022	0.022	0.022
3.7506	0.051	0.028	0.025	0.026	0.025
4.7376	0.058	0.036	0.028	0.032	0.028

[C₆₀]=1.220e-4

Table A.1. continued

9:C ₆₀ in benzene						
[9]·10 ⁴ M	15 °C	25 °C	30 °C	35 °C	[9]·10 ⁴ M	20 °C
0.6186	8.36e-3	6.31e-3	2.52e-3	2.16e-3	0.2767	3.29e-3
0.8168	0.011	8.27e-3	5.33e-3	4.14e-3	0.5445	6.17e-3
1.0113	0.014	9.71e-3	7.20e-3	6.11e-3	0.8037	9.52e-3
1.2021	0.017	0.012	0.010	7.99e-3	1.0549	0.013
1.3894	0.019	0.014	0.013	0.010	1.2983	0.015
1.6337	0.023	0.017	0.015	0.013	1.5344	0.017
1.9307	0.027	0.019	0.017	0.015	1.9857	0.021
2.4986	0.034	0.024	0.019	*	2.4111	0.027
3.0340	0.041	0.029	0.022	0.020	2.8130	0.031
3.5396	0.047	0.032	0.027	0.025	3.5533	0.036
4.4711	0.058	0.038	0.031	*	4.2195	0.039
5.3094	0.068	0.045	0.036	0.034		

9:C ₆₀ in benzene						
[9]·10 ⁴ M	15 °C	20 °C	30 °C	35 °C	[9]·10 ⁴ M	25 °C
0.2767	3.57e-3	3.57e-3	3.19e-3	4.17e-3	0.1795	1.47e-3
0.5445	6.77e-3	6.77e-3	5.78e-3	7.89e-3	0.3505	3.88e-3
0.8037	0.010	0.010	8.12e-3	0.012	0.5135	9.14e-3
1.0549	0.013	0.013	0.011	0.016	0.6691	0.013
1.2983	0.016	0.016	0.014	0.019	0.8178	0.012
1.5344	0.019	0.019	0.016	0.023	0.9600	0.013
1.9857	0.024	0.024	0.021	0.030	1.0962	0.014
2.4111	0.030	0.030	0.024	0.037	1.2267	0.018
2.8130	0.034	0.034	0.029	0.042	1.4720	0.019
3.5533	0.043	0.043	0.035	0.049	1.6985	0.023
4.2195	0.049	0.049	0.040	0.055	2.1029	0.026
					2.4533	0.030
					2.7600	0.032
					3.1543	0.037
					3.4863	0.041
					[C60]	1.060e-4

[C₆₀]=1.049e-4

Table A.1. continued

9-C ₁₀ in CS ₂					
[9]·10 ⁴ M	15 °C	20 °C	25 °C	30 °C	35 °C
0.2037	1.20e-3	1.08e-3	1.03e-3	9.90.e-4	1.33e-3
0.3985	2.44e-3	1.98e-3	1.79e-3	1.69e-3	2.20e-3
0.5850	3.59e-3	2.52e-3	2.29e-3	2.58e-3	3.05e-3
0.7638	3.28e-3	3.17e-3	3.18e-3	3.08e-3	4.01e-3
0.9353	*	*	3.24e-3	3.77e-3	4.88e-3
1.0999	4.57e-3	4.01e-3	3.83e-3	*	5.70e-3
1.4101	5.57e-3	4.68e-3	4.29e-3	4.52e-3	7.25e-3
1.9640	6.05e-3	6.03e-3	5.73e-3	5.55e-3	9.40e-3
2.4441	7.05e-3	*	6.76e-3	*	*
2.8642	7.54e-3	8.45e-3	8.11e-3	*	0.013
3.7157	9.19e-3	*	0.010	0.011	0.015
4.3645	*	0.013	0.012	*	

[C₁₀]=1.041e-4

9-C ₁₀ in CS ₂					
[9]·10 ⁴ M	15 °C	20 °C	25 °C	30 °C	35 °C
0.2029	1.54e-3	1.01e-3	1.03e-3	1.16e-3	1.32e-3
0.3970	2.66e-3	2.05e-3	1.83e-3	2.08e-3	2.04e-3
0.5828	*	2.60e-3	2.77e-3	2.75e-3	2.88e-3
0.7609	4.08e-3	3.58e-3	3.40e-3	3.60e-3	4.13e-3
0.9317	4.52e-3	3.13e-3	3.61e-3	4.24e-3	4.83e-3
1.0956	5.07e-3	3.85e-3	3.98e-3	4.85e-3	5.09e-3
1.4047	6.24e-3	4.14e-3	4.66e-3	5.81e-3	7.40e-3
1.9565	8.04e-3	5.48e-3	6.02e-3	7.25e-3	0.010
2.8532	*	6.57e-3	7.78e-3	9.32e-3	*
3.7015	0.013	7.28e-3	*	*	0.015
4.1086	*	8.17e-3	8.56e-3	0.012	*

[C₁₀]=1.041e-4

Appendix B.

Table B.1. The experimental values of $\Delta\delta_{\text{H}}$ as a function of [26] or [26a] for the complexes **26**: C_{60} and **26a**: C_{60} at 25 °C.

26 : C_{60} in toluene- d_6			
[C_{60}] M	$\Delta\delta_{\text{H}}$ (ppm)	[C_{60}] M	$\Delta\delta_{\text{H}}$ (ppm)
0.0000	0.0000	0.0000	0.0000
170.21e-6	1.0000e-3	308.05e-6	2.0000e-3
791.86e-6	4.0000e-3	462.07e-6	3.0000e-3
1.1508e-3	6.0000e-3	734.04e-6	4.0000e-3
1.4283e-3	7.0000e-3	929.69e-6	5.0000e-3
949.12e-6	5.0000e-3	1.2336e-3	7.0000e-3
1.7058e-3	8.0000e-3	1.4653e-3	9.0000e-3
2.3238e-3	0.0110	1.7331e-3	0.0100
2.6938e-3	0.0120	2.2521e-3	0.0120
3.1933e-3	0.0130	2.4824e-3	0.0130
[26]=1.283e-3 M		[26]=1.013e-3 M	

26a : C_{60} in toluene- d_6			
[C_{60}] M	$\Delta\delta_{\text{H}}$ (ppm)	[C_{60}] M	$\Delta\delta_{\text{H}}$ (ppm)
0.0000	0.0000	0.0000	0.0000
195.65e-6	6.0000e-3	195.65e-6	6.0000e-3
389.92e-6	0.0100	682.70e-6	0.0180
677.15e-6	0.0180	896.39e-6	0.0230
978.26e-6	0.0240	1.1462e-3	0.0270
1.3945e-3	0.0320	1.3834e-3	0.0310
1.8733e-3	0.0410	1.9052e-3	0.0400
2.0731e-3	0.0430	2.3992e-3	0.0470
2.3367e-3	0.0450	2.6545e-3	0.0490
2.7821e-3	0.0510	3.0014e-3	0.0520
3.2248e-3	0.0520	3.2373e-3	0.0530
[26a]=1.637e-3 M		[26a]=1.279 e-3M	

Table B.1. continued

26: C ₆₀ in benzene-d ₆			
[C ₆₀] M	Δδ _{HF} (ppm)	[C ₆₀] M	Δδ _{HF} (ppm)
0.0000	0.0000	0.0000	0.0000
213.69e-6	1.0000e-3	267.81e-6	3.1646e-3
471.79e-6	5.0000e-3	434.32e-6	5.0000e-3
720.17e-6	8.0000e-3	535.61e-6	6.0000e-3
990.75e-6	0.0100	829.79e-6	0.0100
1.3682e-3	0.0130	1.0532e-3	0.0120
1.5486e-3	0.0150	1.3293e-3	0.0140
1.8747e-3	0.0180	1.5236e-3	0.0150
2.0092e-3	0.0180	2.0051e-3	0.0180
[26]= 1.160e-3 M		[26]= 1.124e-3M	

26a: C ₆₀ in benzene-d ₆			
[C ₆₀] M	Δδ _{HF} (ppm)	[C ₆₀] M	Δδ _{HF} (ppm)
0.0000	0.0000	0.0000	0.0000
225.49e-6	0.0205	155.41e-6	0.0130
335.34e-6	0.0290	378.82e-6	0.0290
580.48e-6	0.0470	666.05e-6	0.0440
753.93e-6	0.0590	775.67e-6	0.0540
1.0858e-3	0.0740	994.91e-6	0.0630
1.2882e-3	0.0800	1.1989e-3	0.0720
1.4593e-3	0.0890	1.5666e-3	0.0780
1.9611e-3	0.1010	2.0134e-3	0.0980
[26a]= 1.122e-3 M		[26a]= 9.316e-4 M	

Table B.2. The experimental values of $(X_{26} \cdot \Delta\delta_{\text{H}})$ or $(X_{26a} \cdot \Delta\delta_{\text{H}})$ as a function of $X_{\text{C}_{60}}$ for the complexes **26**:C₆₀ and **26a**:C₆₀ at 25 °C.

26 :C ₆₀ in toluene- <i>d</i> ₆	
$X_{\text{C}_{60}}$	$(X_{26} \cdot \Delta\delta_{\text{H}})$
1.0000	0.0000
0.8000	1.4000e-3
0.7000	1.8000e-3
0.6000	2.0000e-3
0.5000	2.0000e-3
0.4000	1.8000e-3
0.3000	1.4000e-3
0.2000	800.00e-6
0.0000	0.0000
[26] =3.440e-3 M	
26a :C ₆₀ in toluene- <i>d</i> ₆	
$X_{\text{C}_{60}}$	$(X_{26a} \cdot \Delta\delta_{\text{H}})$
0.0000	0.0000
0.2000	0.0100
0.3000	0.0138
0.4000	0.0152
0.5000	0.0150
0.6000	0.0156
0.7000	0.0154
0.8000	0.0104
1.0000	0.0000
[26a] =1.047e-3 M	

Table B.2. continued

26:C ₅₀ in benzene-d ₆	
$X_{C_{50}}$	$(X_{26} * \Delta\delta_H)$
0.0000	0.0000
0.2000	4.0000e-3
0.3000	4.9000e-3
0.4000	4.8000e-3
0.5000	5.0000e-3
0.6000	4.4000e-3
0.7000	3.9000e-3
0.8000	2.8000e-3
1.0000	0.0000

[26]=1.459e-3 M

26a:C ₅₀ in benzene-d ₆	
$X_{C_{50}}$	$(X_{26a} * \Delta\delta_H)$
1.0000	0.0000
0.8000	0.0144
0.7000	0.0192
0.6000	0.0248
0.5000	0.0255
0.4000	0.0234
0.3000	0.0203
0.2000	0.0168
0.0000	0.0000

[26a]=1.459e-3 M

Appendix C.

Table C.1 Relative densities and apparent molar volumes V_a of **8**, **9**, **8:C₆₀** and **9:C₆₀** in different solvents at 25 °C.

$m(\text{mol.kg}^{-1})$	$V_a(\text{ml.mol}^{-1})$	$\rho - \rho^0(\text{g.ml}^{-1})$	$m(\text{mol.kg}^{-1})$	$V_a(\text{ml.mol}^{-1})$	$\rho - \rho^0(\text{g.ml}^{-1})$
C₆₀ in toluene			8 in toluene		
543.68e-6	359.5463	191.46e-6	374.60e-6	505.2744	81.062e-6
649.52e-6	377.6315	201.20e-6	670.40e-6	514.2383	124.80e-6
812.49e-6	354.8044	270.47e-6	821.48e-6	547.7106	127.97e-6
1.0062e-3	370.1644	328.22e-6	1.0833e-3	515.8242	188.03e-6
507.63e-6	350.0498	163.29e-6	348.73e-6	536.8214	48.670e-6
738.87e-6	380.8299	229.87e-6	753.91e-6	519.1693	115.09e-6
824.84e-6	379.6185	259.67e-6	1.0246e-3	572.9381	115.45e-6
1.0062e-3	370.1644	328.22e-6	1.4640e-3	548.5113	191.49e-6
			1.7941e-3	561.0141	217.98e-6
C₆₀ in benzene			8 in benzene		
511.73e-6	359.3647	181.80e-6	513.61e-6	514.0592	78.798e-6
740.30e-6	361.4291	261.81e-6	572.34e-6	594.7808	52.554e-6
1.0734e-3	366.3815	375.52e-6	636.90e-6	552.2768	79.135e-6
1.2365e-3	365.1919	433.68e-6	714.04e-6	575.6437	75.985e-6
155.79e-6	302.9845	62.054e-6	748.01e-6	562.2572	87.239e-6
232.22e-6	402.2702	74.901e-6			
242.04e-6	404.6336	77.633e-6	588.05e-6	518.9483	118.02e-6
338.25e-6	367.6515	118.03e-6	888.69e-6	573.3642	126.10e-6
395.00e-6	342.6084	145.38e-6	1.2020e-3	529.2064	200.45e-6
			1.3499e-3	559.0503	190.68e-6
C₆₀ in CS₂					
226.92e-6	339.1518	83.988e-6			
305.67e-6	336.7632	114.28e-6			
393.02e-6	358.5082	133.46e-6			
220.19e-6	340.1189	81.162e-6			
356.86e-6	348.0135	127.09e-6			
393.02e-6	355.2038	135.51e-6			

Table C.1. continued

$m(\text{mol.kg}^{-1})$	$V_g(\text{ml.mol}^{-1})$	$\rho - \rho^0(\text{g.ml}^{-1})$	$m(\text{mol.kg}^{-1})$	$V_g(\text{ml.mol}^{-1})$	$\rho - \rho^0(\text{g.ml}^{-1})$
	8 in CS₂			9 in CS₂	
966.22e-6	488.7850	13.218e-6	119.02e-6	636.7131	72.515e-6
1.0679e-3	494.2065	5.4827e-6	140.57e-6	654.8661	55.487e-6
1.5114e-3	489.7190	18.444e-6	164.76e-6	609.0557	68.334e-6
1.6550e-3	481.7227	41.046e-6	175.17e-6	618.8984	66.773e-6
1.7497e-3	496.4263	2.8601e-6			
1.8947e-3	492.6553	14.352e-6	773.37e-6	649.3803	36.860e-6
	9 in toluene		956.46e-6	650.0302	44.600e-6
404.88e-6	772.7360	88.922e-6	1.2367e-3	643.4395	70.495e-6
538.60e-6	694.2751	72.999e-6	1.4704e-3	633.7989	106.14e-6
874.78e-6	807.3908	163.20e-6	1.7090e-3	633.9049	123.05e-6
1.2184e-3	738.6868	101.73e-6	1.8142e-3	627.9469	147.64e-6
				8:C₆₀ in toluene	
494.18e-6	742.1904	90.972e-6	376.76e-6	1056.4751	174.54e-6
745.12e-6	724.0376	147.20e-6	499.45e-6	1004.3722	235.87e-6
1.0067e-3	747.9529	180.95e-6	612.32e-6	1048.4788	262.20e-6
1.4594e-3	751.7072	258.17e-6	784.06e-6	1145.5371	264.78e-6
1.7318e-3	766.6453	287.09e-6			
			499.56e-6	1106.9303	211.23e-6
			612.45e-6	1082.3017	260.54e-6
			784.23e-6	1060.7882	215.12e-6
	9 in benzene			8:C₆₀ in benzene	
267.53e-6	802.5936	35.600e-6	102.42e-6	844.7404	86.251e-6
387.00e-6	719.5563	76.014e-6	191.89e-6	836.8139	135.77e-6
534.66e-6	767.3683	85.504e-6	338.41e-6	834.8929	218.75e-6
624.39e-6	820.1853	74.688e-6	447.21e-6	885.9921	257.14e-6
			277.27e-6	884.6852	170.89e-6
466.70e-6	786.2478	67.916e-6			
551.93e-6	784.0451	81.243e-6	155.78e-6	796.6577	121.73e-6
624.39e-6	788.0926	89.976e-6	310.37e-6	820.9030	201.31e-6
			381.66e-6	807.5365	249.00e-6
	9 in CS₂		423.05e-6	882.9009	244.38e-6
149.10e-6	651.6705	5.3974e-6			
171.92e-6	667.7976	3.2049e-6			
193.46e-6	677.5265	638.46e-9			
			44.635e-6	786.5288	70.160e-6
				8:C₆₀ in CS₂	

Table C.1. continued

m(mol.kg ⁻¹)	V _g (ml.mol ⁻¹)	ρ-ρ ^o (g.ml ⁻¹)	m(mol.kg ⁻¹)	V _g (ml.mol ⁻¹)	ρ-ρ ^o (g.ml ⁻¹)
	8:C₆₀ in CS₂			9:C₆₀ in CS₂	
201.49e-6	828.7377	127.26e-6	64.936e-6	1105.1807	67.675e-6
230.82e-6	807.2036	151.20e-6	87.388e-6	1094.1210	66.579e-6
295.56e-6	799.5408	178.14e-6	123.02e-6	1141.8577	86.280e-6
293.48e-6	815.6017	173.85e-6	119.88e-6	1075.0865	100.68e-6
615.40e-6	797.8758	271.52e-6	80.925e-6	1076.1836	72.680e-6
940.10e-6	810.7912	389.93e-6	113.68e-6	1135.1428	71.363e-6
1.1988e-3	818.8185	505.89e-6	164.97e-6	1158.2303	75.294e-6
1.3109e-3	822.0072	526.19e-6	175.92e-6	1091.4865	95.668e-6
	9:C₆₀ in toluene		378.54e-6	1099.7170	181.71e-6
522.58e-6	1147.0483	287.28e-6	515.05e-6	1042.9417	223.57e-6
696.11e-6	1222.5146	344.95e-6	763.24e-6	1107.8466	226.65e-6
833.89e-6	1163.4180	436.12e-6	1.0009e-3	1037.3926	392.51e-6
131.21e-6	1127.5725	82.236e-6	916.57e-6	1098.3054	368.67e-6
216.60e-6	1139.0540	112.27e-6	986.77e-6	1049.0975	403.79e-6
280.92e-6	1169.8126	141.79e-6			
350.37e-6	1119.7978	185.40e-6			
378.62e-6	1137.5115	197.77e-6			
	9:C₆₀ in benzene				
62.198e-6	1167.3638	61.715e-6			
175.49e-6	1231.4297	114.45e-6			
227.84e-6	1195.8297	157.99e-6			
271.01e-6	1167.5237	169.86e-6			
86.320e-6	1177.1883	74.158e-6			
208.05e-6	1184.9452	136.22e-6			
250.45e-6	1219.9420	144.79e-6			
289.60e-6	1203.7578	165.75e-6			

Table C.2. Relative densities and apparent molar volumes V_a of **26**, **26a**, **26:C₆₀** and **26a:C₆₀** in different solvents at 25 °C.

$m(\text{mol.kg}^{-1})$	$V_a(\text{ml.mol}^{-1})$	$\rho - \rho^0(\text{g.ml}^{-1})$	$m(\text{mol.kg}^{-1})$	$V_a(\text{ml.mol}^{-1})$	$\rho - \rho^0(\text{g.ml}^{-1})$
26a in toluene			26 in toluene		
716.97e-6	597.9436	130.62e-6	745.67e-6	386.2423	145.01e-6
888.56e-6	622.4037	145.71e-6	839.79e-6	399.8874	154.79e-6
1.2905e-3	591.5495	241.17e-6	910.81e-6	387.3611	176.36e-6
1.3878e-3	588.3767	262.60e-6	1.1092e-3	409.0657	196.87e-6
1.0962e-3	601.0242	197.15e-6	1.1092e-3	420.0953	187.77e-6
1.2487e-3	584.8495	239.57e-6	995.52e-6	432.6854	159.22e-6
1.3431e-3	603.9733	238.59e-6	1.1888e-3	426.6552	195.44e-6
1.5795e-3	614.0112	268.76e-6	1.3356e-3	421.5000	224.68e-6
1.8749e-3	602.3638	335.20e-6	1.6545e-3	417.0732	283.74e-6
26a in benzene			26 in benzene		
876.07e-6	609.8744	148.50e-6	1.0201e-3	399.2941	186.90e-6
1.0176e-3	623.6328	161.80e-6	1.1778e-3	449.8102	170.38e-6
1.2101e-3	627.2667	189.03e-6	1.2612e-3	442.5844	189.38e-6
1.4754e-3	620.3442	238.22e-6	1.4095e-3	422.5775	233.17e-6
1.8978e-3	615.2480	313.73e-6	1.5371e-3	430.8127	244.60e-6
1.2895e-3	608.7978	219.58e-6	1.6755e-3	424.4675	274.73e-6
1.4152e-3	610.9285	238.68e-6	748.16e-6	403.0369	134.95e-6
1.9982e-3	629.0183	309.33e-6	911.73e-6	421.2439	151.77e-6
2.4104e-3	617.9854	393.33e-6	1.0508e-3	431.2594	166.89e-6
			1.2747e-3	443.5469	190.47e-6
			1.3846e-3	416.3965	235.58e-6
26a in CS₂			26/ in CS₂		
792.71e-6	671.5500	34.163e-6	764.49e-6	440.7029	4.9647e-6
792.67e-6	629.3395	86.901e-6	901.87e-6	436.3106	12.101e-6
1.0077e-3	662.8404	16.606e-6	923.70e-6	439.6141	7.5834e-6
1.0708e-3	655.1472	21.240e-6	1.1914e-3	434.9838	18.474e-6
1.1757e-3	689.7583	55.480e-6			
575.98e-6	630.9323	47.304e-6	860.64e-6	430.9939	18.761e-6
666.47e-6	632.1946	56.058e-6	930.14e-6	443.6300	1.7480e-6
865.67e-6	642.8207	87.299e-6	1.1214e-3	448.4201	6.3591e-6
992.58e-6	635.5719	88.749e-6	1.1614e-3	447.9183	5.6673e-6
			1.4395e-3	438.0126	15.448e-6

Table D.2. continued

m(mol.kg ⁻¹)	V _g (ml.mol ⁻¹)	ρ-ρ ^o (g.ml ⁻¹)	m(mol.kg ⁻¹)	V _g (ml.mol ⁻¹)	ρ-ρ ^o (g.ml ⁻¹)
26a:C₆₀ in toluene			26:C₆₀ in toluene		
274.93e-6	1004.6390	277.99e-6	759.09e-6	905.9533	407.28e-6
323.17e-6	955.0195	341.18e-6	824.60e-6	893.8728	451.47e-6
377.91e-6	949.8239	405.34e-6	903.06e-6	890.5871	488.04e-6
411.61e-6	1021.9519	413.67e-6			
			478.86e-6	910.2876	334.74e-6
467.32e-6	977.3552	250.23e-6	481.64e-6	922.1145	323.19e-6
587.57e-6	920.4285	337.26e-6	539.82e-6	939.2431	351.82e-6
769.74e-6	1015.9172	418.80e-6	598.59e-6	906.3005	378.42e-6
26a:C₆₀ in benzene			26:C₆₀ in benzene		
499.69e-6	974.5580	267.04e-6	650.37e-6	831.1647	323.81e-6
600.13e-6	1006.6157	301.36e-6	726.34e-6	813.8504	363.07e-6
659.45e-6	991.2566	335.35e-6	817.66e-6	827.2247	408.84e-6
670.82e-6	990.9897	360.28e-6			
749.30e-6	1000.8408	387.69e-6	423.86e-6	853.8489	204.52e-6
			530.67e-6	821.5792	269.78e-6
429.25e-6	914.6338	251.92e-6	762.63e-6	881.0823	343.07e-6
566.68e-6	989.6807	289.49e-6	821.61e-6	838.2943	418.63e-6
636.18e-6	1029.3369	305.81e-6			
699.86e-6	1051.6573	327.90e-6			
744.54e-6	1010.3977	374.61e-6			
26a:C₆₀ in CS₂			26:C₆₀ in CS₂		
439.22e-6	1023.3323	90.933e-6	654.69e-6	760.7457	265.91e-6
519.81e-6	985.3408	137.77e-6	740.43e-6	786.9213	269.89e-6
549.64e-6	1052.7760	114.64e-6	774.93e-6	781.4590	289.24e-6
650.84e-6	996.6684	165.42e-6	798.59e-6	788.2288	289.95e-6
703.39e-6	1033.4817	132.15e-6			
708.20e-6	985.4679	187.15e-6	405.96e-6	779.0510	153.30e-6
			496.52e-6	764.0655	198.56e-6
			565.53e-6	800.1949	194.00e-6
			777.32e-6	785.9381	284.68e-6
483.53e-6	987.1462	132.74e-6			
584.57e-6	1020.0009	128.83e-6			
740.25e-6	1024.8211	150.15e-6			
735.63e-6	1058.9087	146.67e-6			

Appendix D.

X-ray Structure Report

For
Complex of C₆₀ with **26a**

Prepared by
David O. Miller

December 7, 2000

Introduction

Collection, solution and refinement all proceeded normally. Hydrogen atoms were introduced in calculated or difference map positions with isotropic thermal parameters set twenty percent greater than those of their bonding partners at the time of their inclusion. They were not refined.

The C₆₀ is either disordered or rotating and as a result the ellipsoids are elongated. Trying to model this disorder would not be practical. However as a result the R values are somewhat higher than usual.

Dr. Bob McDonald, University of Alberta is acknowledged for data collection.

Experimental

Data Collection

A deep red prism crystal of $C_{108}H_{54}O_6$ having approximate dimensions of 0.64 x 0.11 x 0.11 mm was mounted on a glass fiber. All measurements were made on a Bruker P4/CCD system with graphite monochromated Mo-K α radiation and a rotating anode generator.

Cell constants and an orientation matrix for data collection corresponded to an R-centered trigonal cell (laue class: -3) with dimensions:

$$\begin{aligned}a &= 23.136(2) \text{ \AA} \\c &= 17.217(2) \text{ \AA} \\V &= 7981(1) \text{ \AA}^3\end{aligned}$$

For $Z = 6$ and F.W. = 1447.61, the calculated density is 1.81 g/cm³. Based on the systematic absences of:

$$hkil: -h+k+l \pm 3n$$

packing considerations, a statistical analysis of intensity distribution, and the successful solution and refinement of the structure, the space group was determined to be:

R-3 (#148)

The data were collected at a temperature of $-80 \pm 1^\circ\text{C}$. The full hemisphere of data was collected with 30 sec., 0.3 deg. frames to a maximum 2θ value of 53.0°.

Data Reduction

Of the 14183 reflections which were collected, 3647 were unique ($R_{int} = 0.096$). The linear absorption coefficient, μ , for Mo-K α radiation is 1.1 cm^{-1} . The Siemens area detector absorption routine (SADABS) was used to correct the data with maximum and minimum effective transmissions of 0.9879 and 0.9326 respectively. The data were corrected for Lorentz and polarization effects.

Structure Solution and Refinement

The structure was solved by direct methods² and expanded using Fourier techniques³. The non-hydrogen atoms were refined anisotropically. Hydrogen atoms were included but not refined. The final cycle of full-matrix least-squares refinement⁴ on F^2 was based on 1744 observed reflections and 247 variable parameters and converged (largest parameter shift was 0.00 times its esd) with unweighted and weighted agreement factors of:

$$R1 = \sum ||F_o| - |F_c|| / \sum |F_o| = 0.154$$

$$wR2 = [\sum (w (F_o^2 - F_c^2)^2) / \sum w(F_o^2)^2]^{1/2} = 0.462$$

The standard deviation of an observation of unit weight⁵ was 1.47. The weighting scheme was based on counting statistics. The maximum and minimum peaks on the final difference Fourier map corresponded to 1.25 and -0.40 $e^{-}/\text{\AA}^3$, respectively.

Neutral atom scattering factors were taken from Cromer and Waber⁶. Anomalous dispersion effects were included in F_{calc} ⁷; the values for $\Delta f'$ and $\Delta f''$ were those of Creagh and McAuley⁸. The values for the mass attenuation coefficients are those of Creagh and Hubbell⁹. All calculations were performed using the teXsan¹⁰ crystallographic software package of Molecular Structure Corporation except for refinement, which was performed using SHELXL-97¹¹.

References

- (1) CrystalClear: Rigaku Corporation, 1999.
- (2) SIR92: Altomare, A., Cascarano, M., Giacovazzo, C., Guagliardi, A. (1994). J. Appl. Cryst., 26, 343.
- (3) DIRDIF94: Beurskens, P.T., Admiraal, G., Beurskens, G., Bosman, W.P., de Gelder, R., Israel, R. and Smits, J.M.M.(1994). The DIRDIF-94 program system, Technical Report of the Crystallography Laboratory, University of Nijmegen, The Netherlands.

- (4) Least Squares function minimized: (SHELXL97)

$$\sum w(F_o^2 - F_c^2)^2 \text{ where}$$

$$w = 1 / [\sigma^2(F_o^2) + (0.2000 \cdot P)^2 + 0.0000 \cdot P]$$
$$P = (\text{Max}(F_o^2, 0) + 2F_c^2) / 3$$

- (5) Standard deviation of an observation of unit weight:

$$[\sum w(F_o^2 - F_c^2)^2 / (N_o - N_v)]^{1/2}$$

where: N_o = number of observations
 N_v = number of variables

- (6) Cromer, D. T. & Waber, J. T.; "International Tables for X-ray Crystallography", Vol. IV, The Kynoch Press, Birmingham, England, Table 2.2 A (1974).
- (7) Ibers, J. A. & Hamilton, W. C.; Acta Crystallogr., 17, 781 (1964).
- (8) Creagh, D. C. & McAuley, W.J. ; "International Tables for Crystallography", Vol C, (A.J.C. Wilson, ed.), Kluwer Academic Publishers, Boston, Table 4.2.6.8, pages 219-222 (1992).
- (9) Creagh, D. C. & Hubbell, J.H.; "International Tables for Crystallography", Vol C, (A.J.C. Wilson, ed.), Kluwer Academic Publishers, Boston, Table 4.2.4.3, pages 200-206 (1992).

(10) teXsan for Windows version 1.06: Crystal Structure Analysis Package, Molecular Structure Corporation (1997-9).

(11) SHELX97: Sheldrick, G.M. (1997).

EXPERIMENTAL DETAILS

A. Crystal Data

Empirical Formula	C ₁₀₈ H ₅₄ O ₆
Formula Weight	1447.61
Crystal Color, Habit	deep red, prism
Crystal Dimensions	0.64 X 0.11 X 0.11 mm
Crystal System	trigonal
Lattice Type	R-centered
Lattice Parameters	a = 23.136(2) Å c = 17.217(2) Å V = 7981(1) Å ³
Space Group	R-3 (#148)
Z value	6
D _{calc}	1.807 g/cm ³
F ₀₀₀	4500.00
μ(MoKα)	1.10 cm ⁻¹

B. Intensity Measurements

Detector	Bruker P4/CCD
Radiation	MoK α ($\lambda = 0.71073 \text{ \AA}$) graphite monochromated
Temperature	$-80 \pm 1^\circ\text{C}$.
Scan Rate	30s., 0.3 deg. frames
$2\theta_{\text{max}}$	53.0°
No. of Reflections Measured	Total: 14183
	Unique: 3647 ($R_{\text{int}} =$ 0.096)
Corrections	Lorentz-polarization SADABS Correction (trans. Factors: 0.9879 - 0.9326)

C. Structure Solution and Refinement

Structure Solution	Direct Methods (SIR92)
Refinement	Full-matrix least-squares on F^2
Function Minimized	$\sum w (F_o^2 - F_c^2)^2$
Least Squares Weights	$w = 1 / [\sigma^2(F_o^2) + (0.2000 \cdot P)^2 + 0.0000 \cdot P]$ where $P = (\text{Max}(F_o^2, 0) + 2F_c^2)/3$
Anomalous Dispersion	All non-hydrogen atoms
No. Observations ($I > 2.00\sigma(I)$)	1744
No. Variables	247
Reflection/Parameter Ratio	7.06
Residuals: R1; wR2	0.154 ; 0.462
Goodness of Fit Indicator	1.47
Max Shift/Error in Final Cycle	0.00
Maximum peak in Final Diff. Map	1.25 e ⁻ /Å ³
Minimum peak in Final Diff. Map	-0.40 e ⁻ /Å ³

Appendix D. Continued

X-ray Structure Report

For compound **49a**

Prepared by
David O. Miller

September 21, 2000

Introduction

Collection, solution and refinement all proceeded normally. Hydrogens were placed in calculated positions with isotropic thermal parameters set twenty percent greater than those of their bonding partners at the time of their inclusion. They were not refined.

Experimental

Data Collection

A colorless irregular crystal of $C_{48}H_{48}O_{12}$ having approximate dimensions of $0.35 \times 0.20 \times 0.40$ mm was mounted on a glass fiber. All measurements were made on a Rigaku AFC6S diffractometer with graphite monochromated Cu-K α radiation.

Cell constants and an orientation matrix for data collection, obtained from a least-squares refinement using the setting angles of 25 carefully centered reflections in the range $42.32 < 2\theta < 53.60^\circ$ corresponded to a primitive orthorhombic cell with dimensions:

$$\begin{aligned}a &= 17.092(2) \text{ \AA} \\b &= 30.493(3) \text{ \AA} \\c &= 16.382(2) \text{ \AA} \\V &= 8538(2) \text{ \AA}^3\end{aligned}$$

For $Z = 8$ and F.W. = 816.90, the calculated density is 1.27 g/cm^3 . The systematic absenc

$$\begin{aligned}0kl: &k \pm 2n \\h0l: &l \pm 2n \\hk0: &h \pm 2n\end{aligned}$$

uniquely determine the space group to be:

$$\text{Pbca (\#61)}$$

The data were collected at a temperature of $26 \pm 1^\circ\text{C}$ using the ω - 2θ scan technique to a maximum 2θ value of 120.1° . Omega scans of several intense reflections, made prior to data collection, had an average width at half-height of 0.27° with a take-off angle of 6.0° . Scans of $(0.79 + 0.14 \tan \theta)^\circ$ were made at a speed of $4.0^\circ/\text{min}$ (in ω). The weak reflections ($I < 10.0\sigma(I)$) were rescanned (maximum of 3 scans) and the counts were accumulated to ensure good counting statistics. Stationary background counts were recorded on each side of the reflection. The ratio of peak counting time to background counting time was 2:1. The diameter of the incident beam collimator was 1.0 mm, the crystal to detector distance was 400 mm, and the detector aperture was 4.5×3.0 mm (horizontal x vertical).

Data Reduction

A total of 7028 reflections was collected. The intensities of three representative reflections were measured after every 150 reflections. No decay correction was applied.

The linear absorption coefficient, μ , for Cu-K α radiation is 7.5 cm^{-1} . An empirical absorption correction based on azimuthal scans of several reflections was applied which resulted in transmission factors ranging from 0.87 to 1.00. The data were corrected for Lorentz and polarization effects. A correction for secondary extinction was applied (coefficient = $7.68401\text{e-}007$).

Structure Solution and Refinement

The structure was solved by direct methods¹ and expanded using Fourier techniques². The non-hydrogen atoms were refined anisotropically. Hydrogen atoms were included but not refined. The final cycle of full-matrix least-squares refinement³ on F was based on 3274 observed reflections ($I > 1.00\sigma(I)$) and 542 variable parameters and converged (largest parameter shift was 0.00 times its esd) with unweighted and weighted agreement factors of:

$$R = \sum ||F_o| - |F_c|| / \sum |F_o| = 0.087$$

$$R_w = [\sum w (|F_o| - |F_c|)^2 / \sum w F_o^2]^{1/2} = 0.080$$

The standard deviation of an observation of unit weight⁴ was 2.01. The weighting scheme was based on counting statistics and included a factor ($p = 0.028$) to downweight the intense reflections. Plots of $\sum w (|F_o| - |F_c|)^2$ versus $|F_o|$, reflection order in data collection, $\sin \theta/\lambda$, various classes of indices showed no unusual trends. The maximum and minimum peaks in the final difference Fourier map corresponded to 0.33 and -0.29 e⁻/Å³, respectively.

Neutral atom scattering factors were taken from Cromer and Waber⁵. Anomalous dispersion effects were included in F_{calc} ⁶; the values for $\Delta f'$ and $\Delta f''$ were those of Creagh and McAuley⁷. The values for the mass attenuation coefficients are those of Creagh and Hubbard⁸. Calculations were performed using the teXsan⁹ crystallographic software package of Moleculer Structure Corporation.

References

(1) SIR92: Altomare, A., Cascarano, M., Giacovazzo, C., Guagliardi, A. (1994). *J. Appl. Cryst.*, 26, 343.

(2) DIRDIF94: Beurskens, P.T., Admiraal, G., Beurskens, G., Bosman, W.P., de Gelder, R., Israel, R. and Smits, J.M.M. (1994). The DIRDIF-94 program system, Technical Report of the Crystallography Laboratory, University of Nijmegen, The Netherlands.

(3) Least Squares function minimized:

$$\sum w(|F_o| - |F_c|)^2 \text{ where}$$

$$w = 1/[\sigma^2(F_o)] = [\sigma_c^2(F_o) + p^2 F_o^2/4]^{-1}$$

$\sigma_c(F_o)$ = e. s. d. based on counting statistics

p = p-factor

(4) Standard deviation of an observation of unit weight:

$$[\sum w(|F_o| - |F_c|)^2 / (N_o - N_v)]^{1/2}$$

where N_o = number of observations

N_v = number of variables

(5) Cromer, D. T. & Waber, J. T.: "International Tables for X-ray Crystallography". Vol. IV. Kynoch Press, Birmingham, England, Table 2.2 A (1974).

(6) Ibers, J. A. & Hamilton, W. C.; *Acta Crystallogr.*, 17, 781 (1964).

(7) Creagh, D. C. & McAuley, W. J. ; "International Tables for Crystallography", Vol C. (A.J. Wilson, ed.), Kluwer Academic Publishers, Boston, Table 4.2.6.8, pages 219-222 (1992).

(8) Creagh, D. C. & Hubbell, J.H.; "International Tables for Crystallography", Vol C. (A.J.C Wilson, ed.), Kluwer Academic Publishers, Boston, Table 4.2.4.3, pages 200-206 (1992).

(9) teXsan for Windows version 1.06: Crystal Structure Analysis Package, Molecular Struct Corporation (1997-9).

EXPERIMENTAL DETAILS

A. Crystal Data

Empirical Formula	C ₄₈ H ₄₈ O ₁₂
Formula Weight	816.90
Crystal Color, Habit	colorless, irregular
Crystal Dimensions	0.35 X 0.20 X 0.40 mm
Crystal System	orthorhombic
Lattice Type	Primitive
No. of Reflections Used for Unit Cell Determination (2 θ range)	25 (42.3 - 53.6 $^{\circ}$)
Omega Scan Peak Width at Half-height	0.27 $^{\circ}$
Lattice Parameters	a = 17.092(2) Å b = 30.493(3) Å c = 16.382(2) Å V = 8538(2) Å ³
Space Group	Pbca (#61)
Z value	8
D _{calc}	1.271 g/cm ³
F ₀₀₀	3456.00
μ (CuK α)	7.51 cm ⁻¹

B. Intensity Measurements

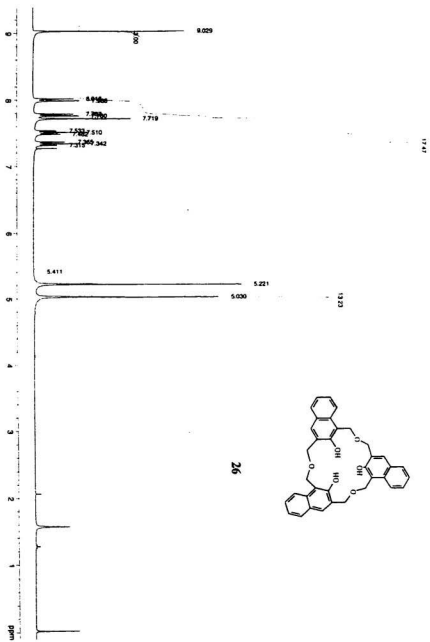
Diffractometer	Rigaku AFC6S
Radiation	CuK α ($\lambda = 1.54178 \text{ \AA}$) graphite monochromated
Take-off Angle	6.0 $^{\circ}$
Detector Aperture	6.0 mm horizontal 3.0 mm vertical
Crystal to Detector Distance	400 mm
Voltage, Current	50kV, 27.5mA
Temperature	26.0 $^{\circ}$ C
Scan Type	ω -2 θ
Scan Rate	4.0 $^{\circ}$ /min (in ω) (up to 3 scans)
Scan Width	(0.79 + 0.14 tan θ) $^{\circ}$
2 θ _{max}	120.1 $^{\circ}$
No. of Reflections Measured	Total: 7028
Corrections	Lorentz-polarization Absorption (trans. factors: 0.8691 - 1.0000) Secondary Extinction (coefficient: 7.68401e-007)

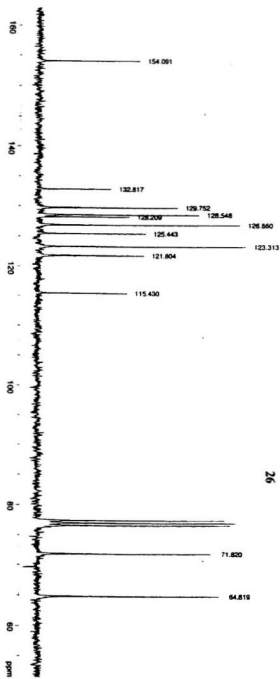
C. Structure Solution and Refinement

Structure Solution	Direct Methods (SIR92)
Refinement	Full-matrix least-squares on F
Function Minimized	$\sum w (F_o - F_c)^2$
Least Squares Weights	$1/\sigma^2(F_o) = 4F_o^2/\sigma^2(F_o^2)$
p-factor	0.0276
Anomalous Dispersion	All non-hydrogen atoms
No. Observations ($ I > 1.00\sigma(I)$)	3274
No. Variables	542
Reflection/Parameter Ratio	6.04
Residuals: R; R _w	0.087 ; 0.080
Goodness of Fit Indicator	2.01
Max Shift/Error in Final Cycle	0.00
Maximum peak in Final Diff. Map	0.33 e ⁻ /Å ³
Minimum peak in Final Diff. Map	-0.29 e ⁻ /Å ³

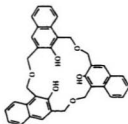
Appendix E.

^1H NMR, ^{13}C spectra

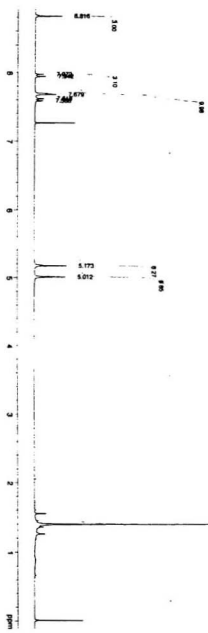
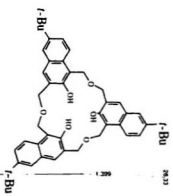


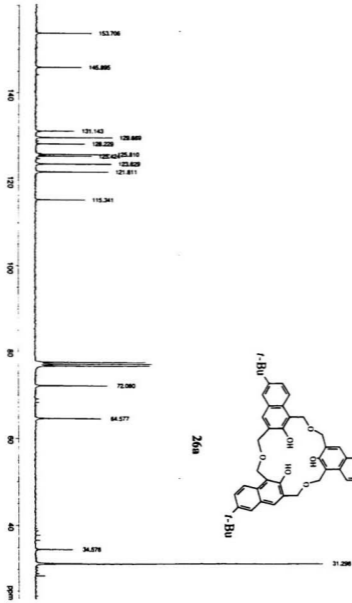


26

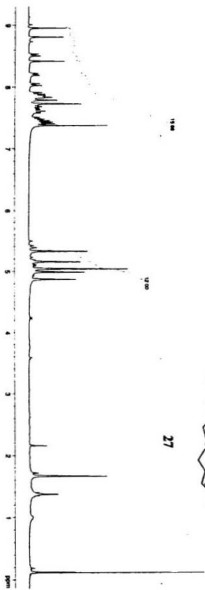
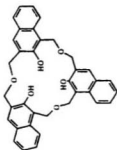


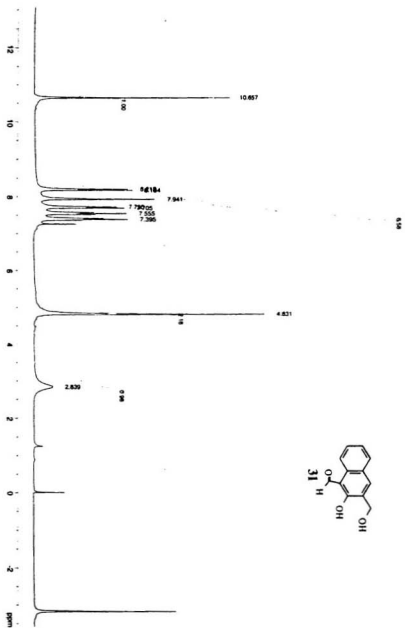
26a

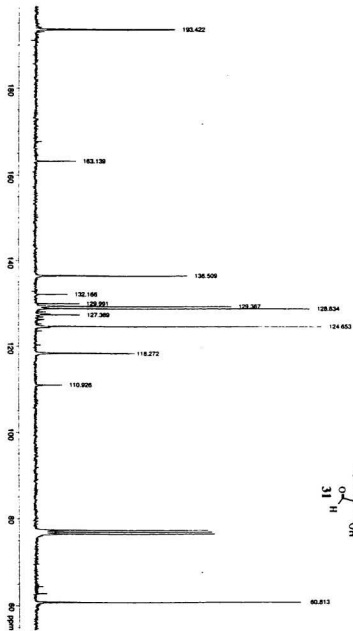


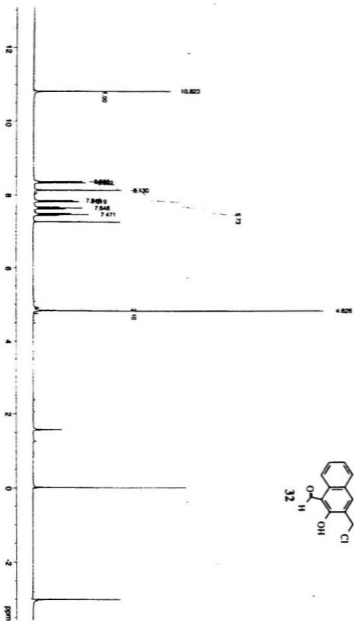


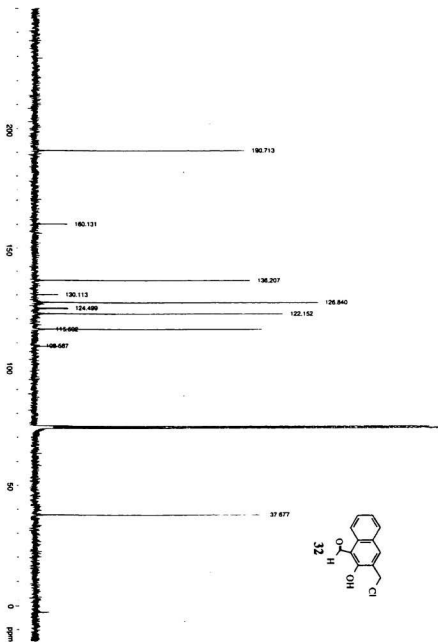
27

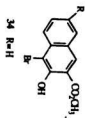
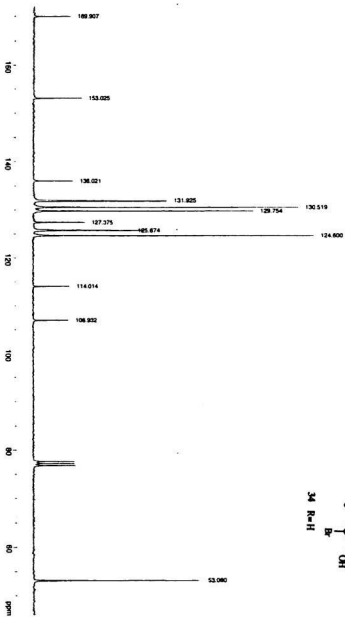


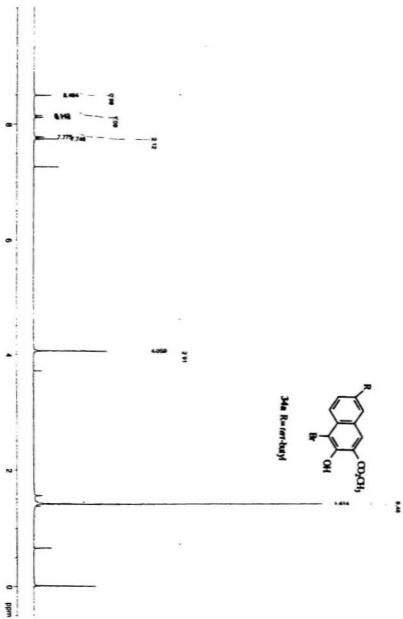


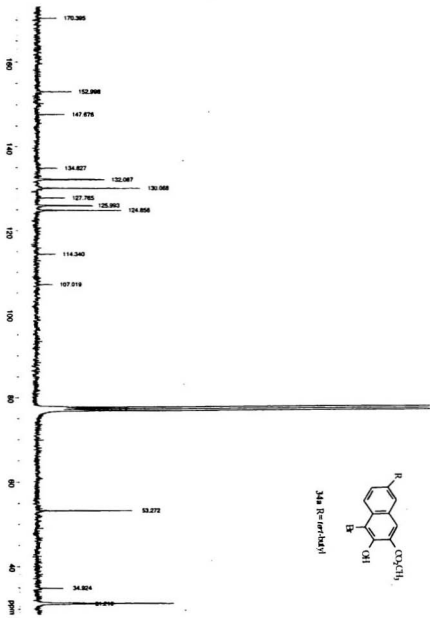


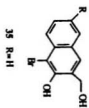
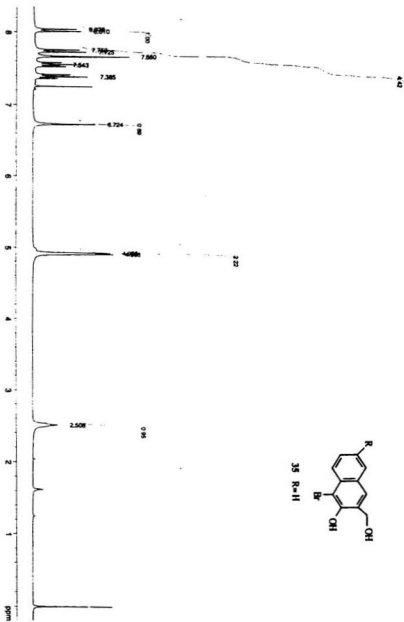


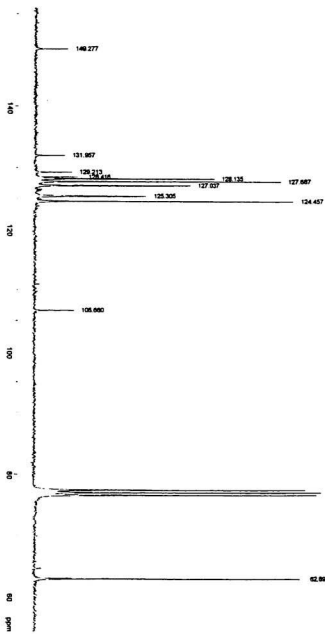




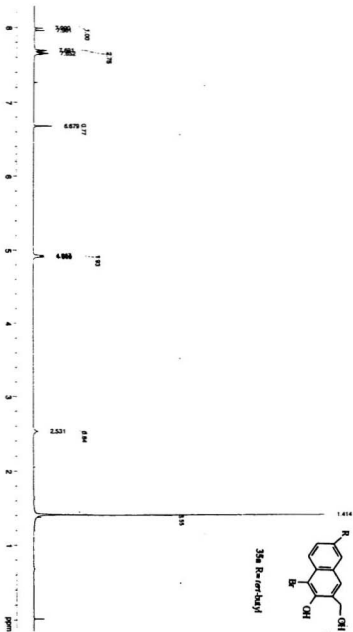
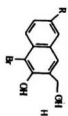


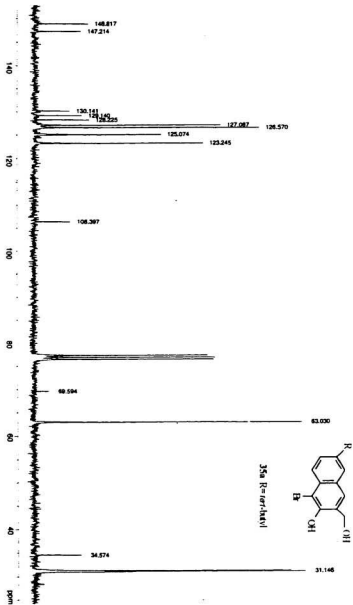


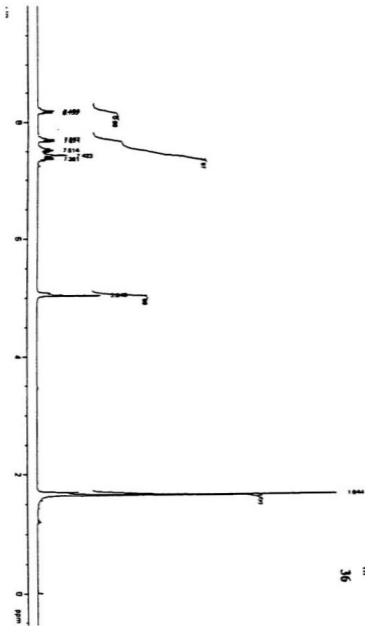


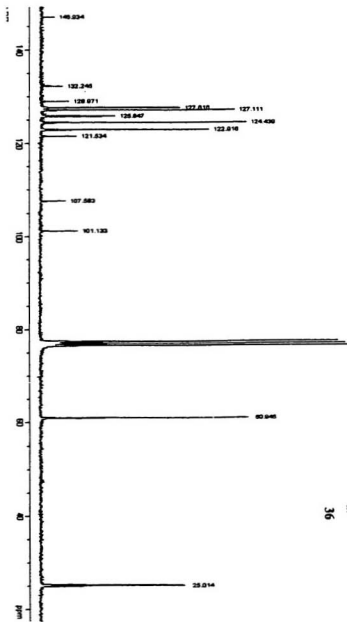


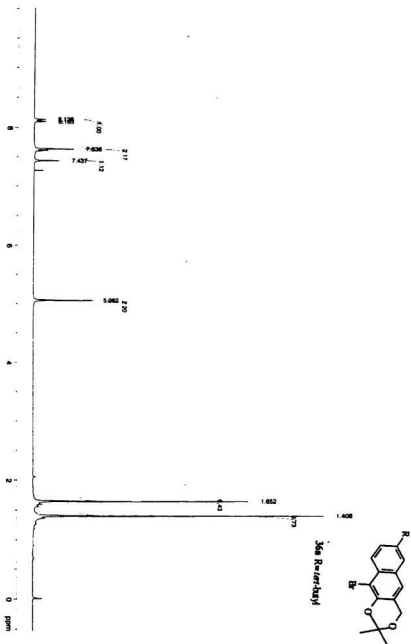
35a R=tert-butyl

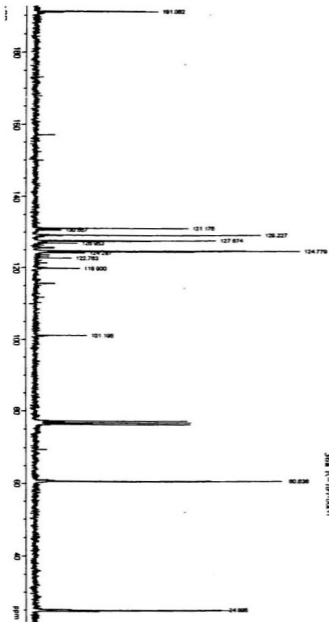




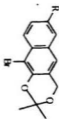


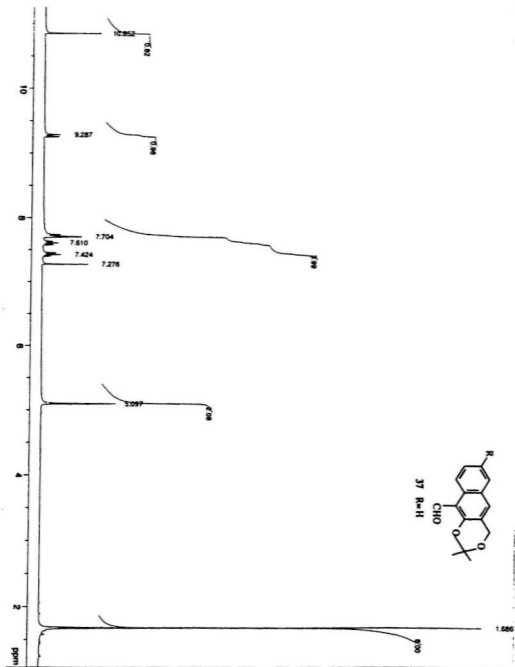


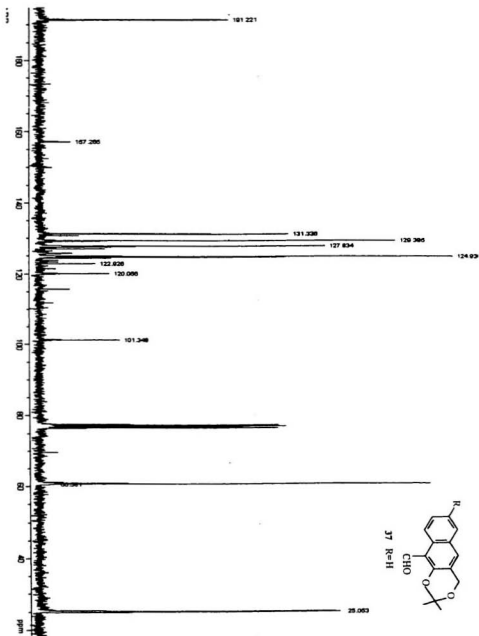


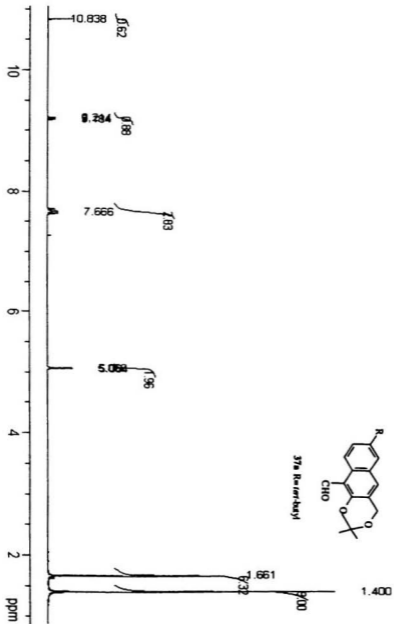


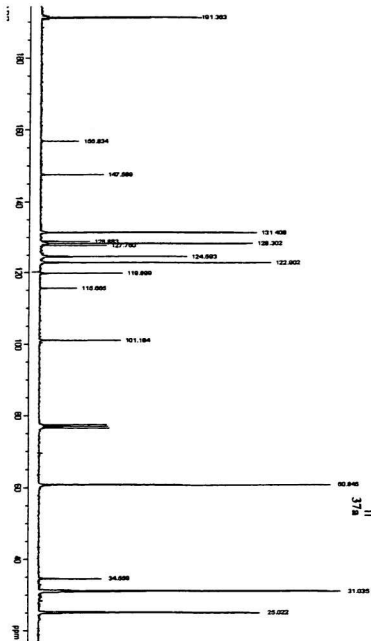
36a R=tert-butyl

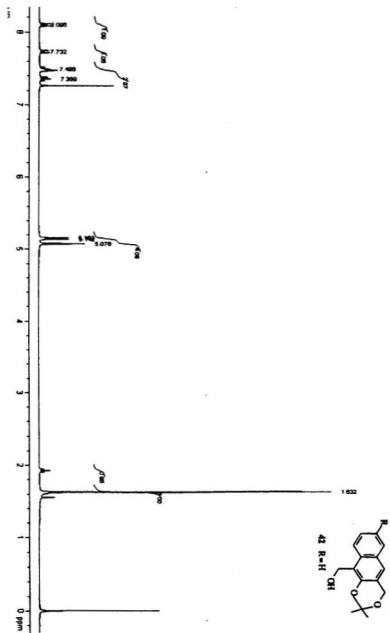


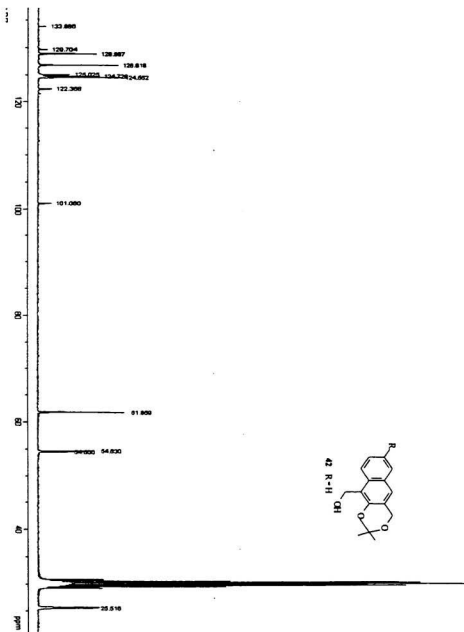


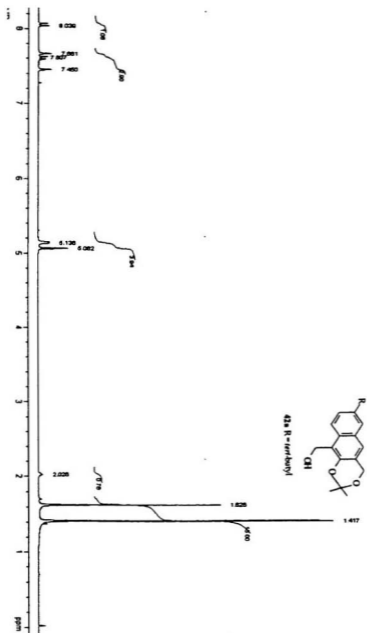


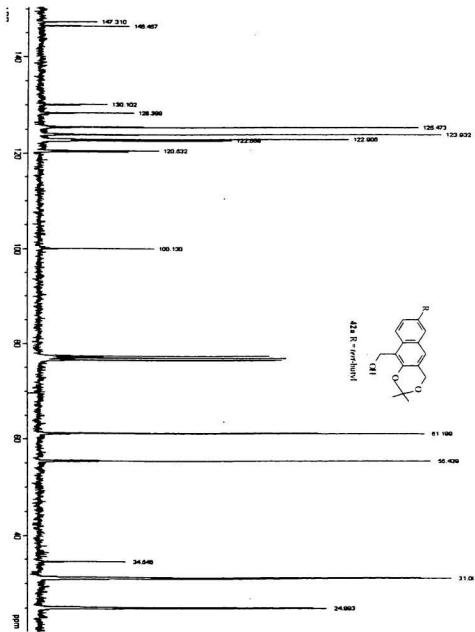


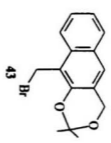
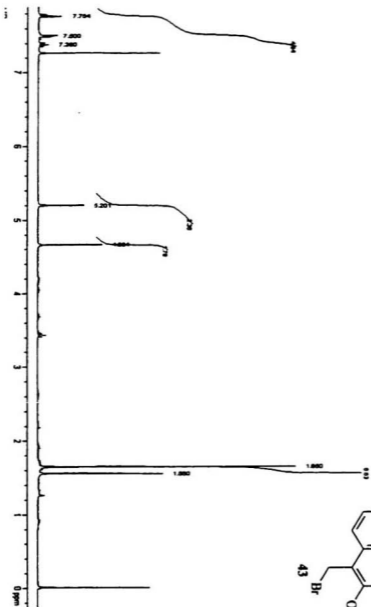


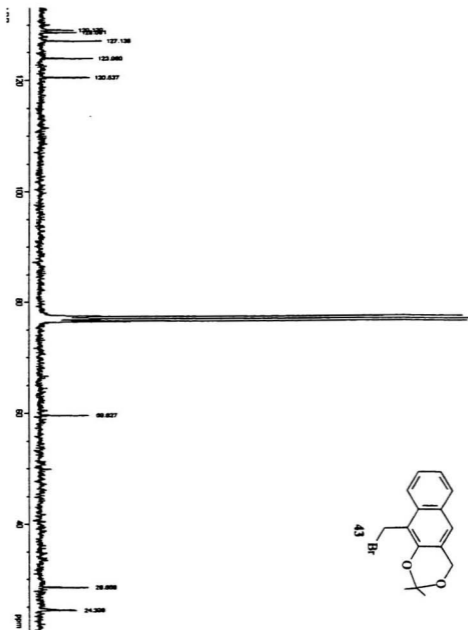


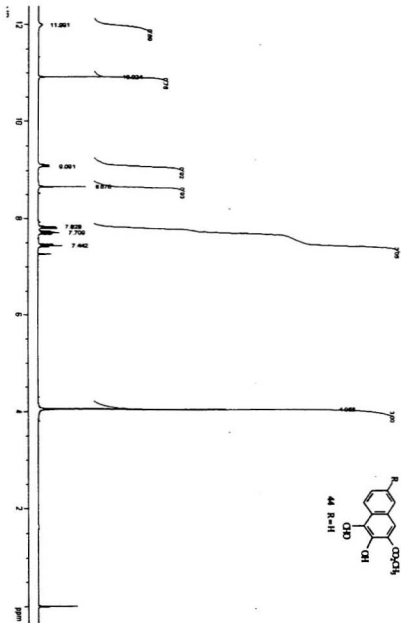


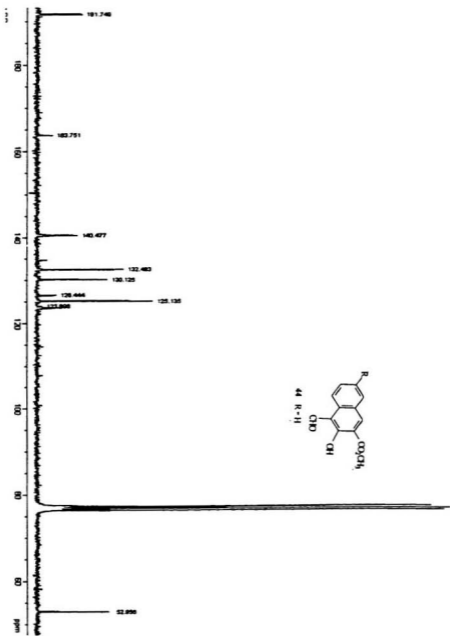


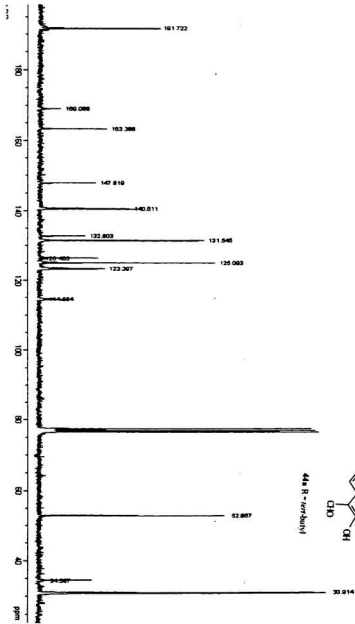


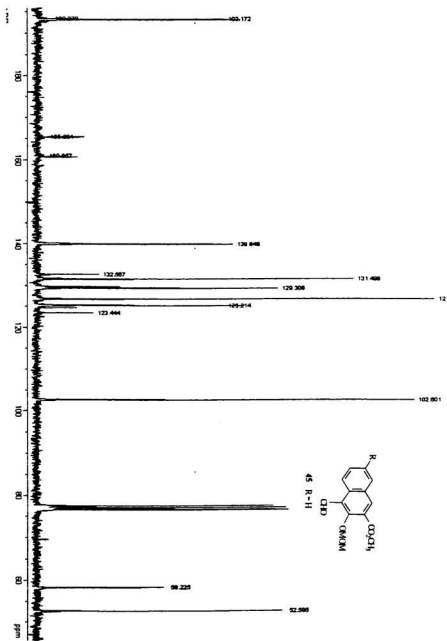


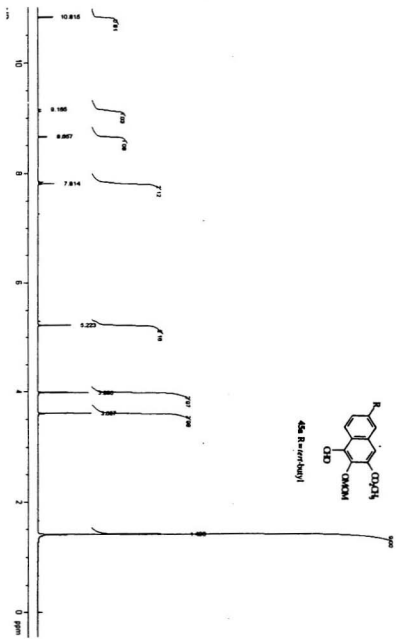


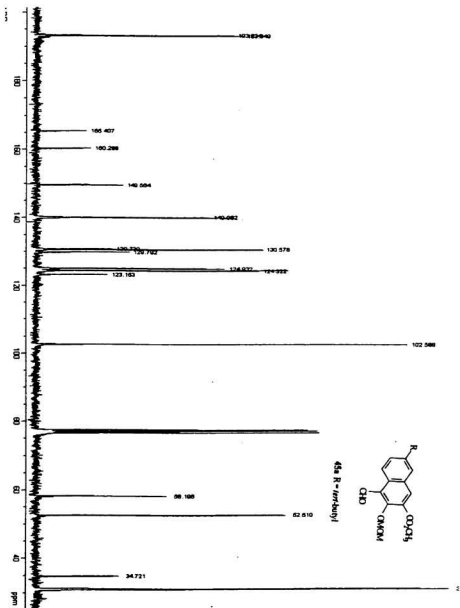


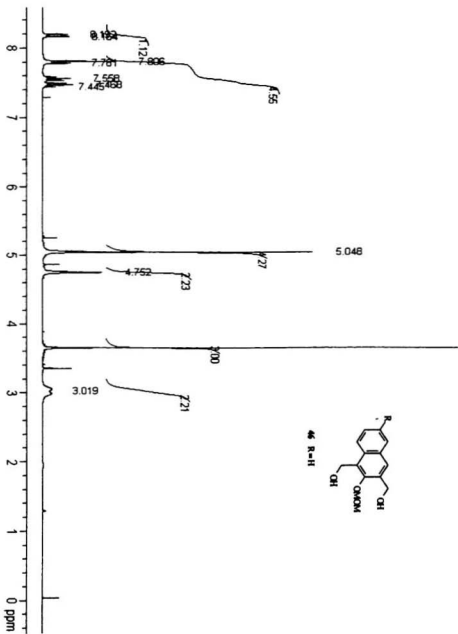


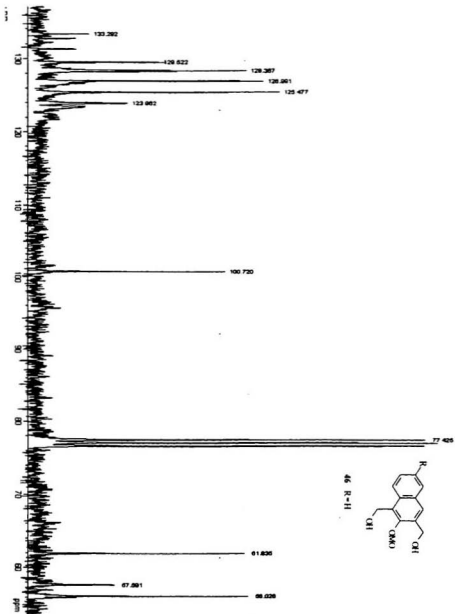


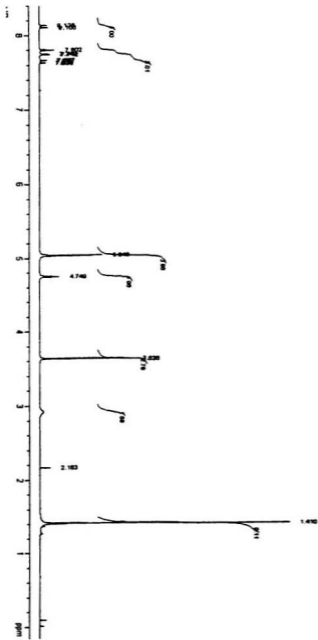




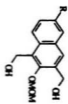


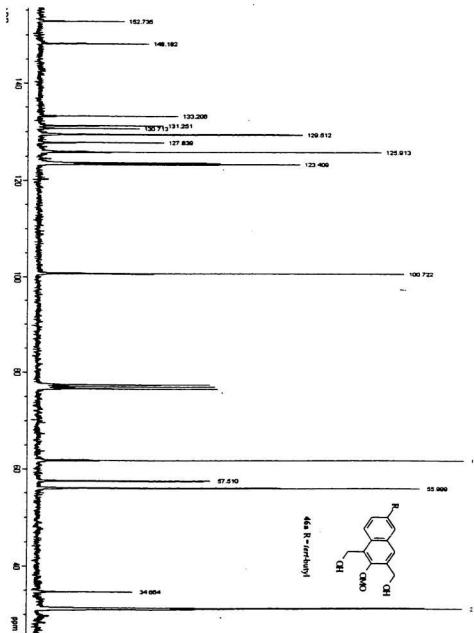


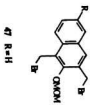
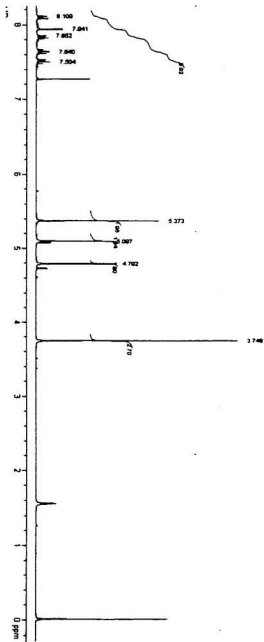


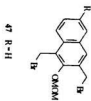
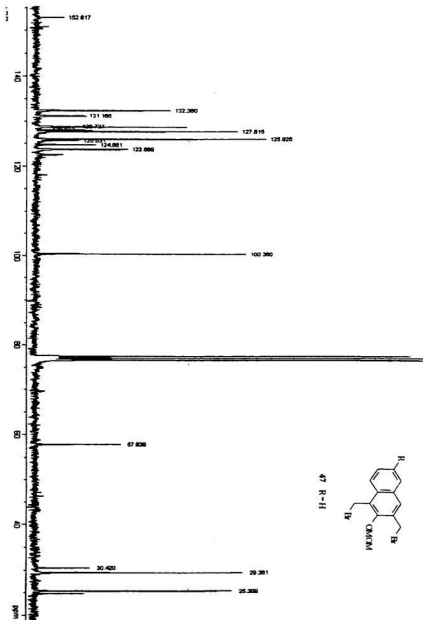


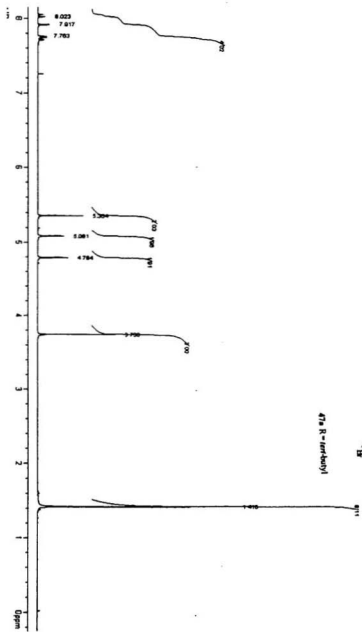
4-Me R-erubonyl



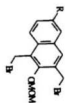


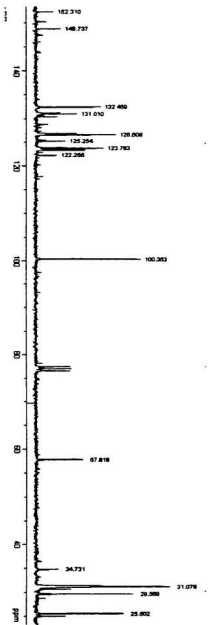




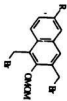


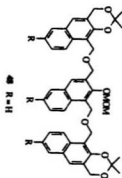
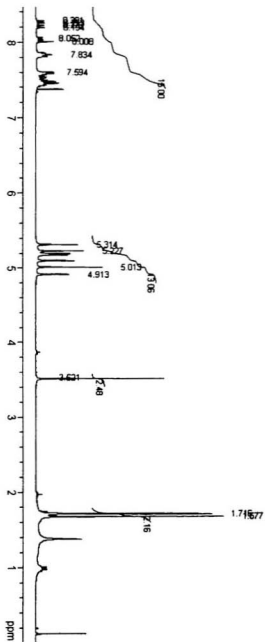
475 (R = tert-butyl)

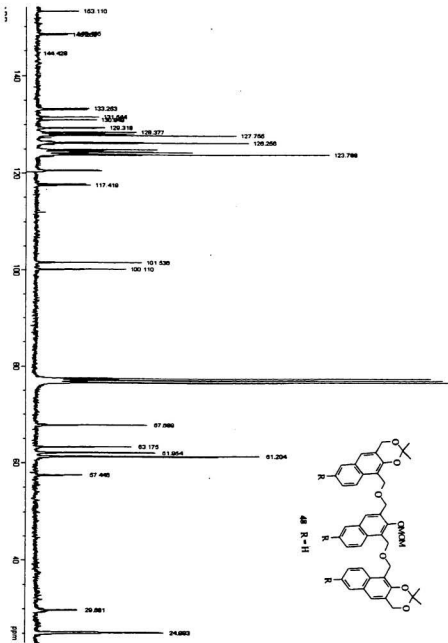


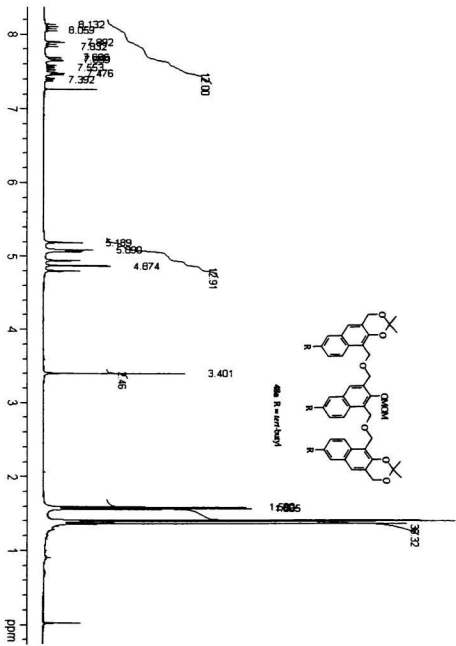


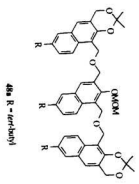
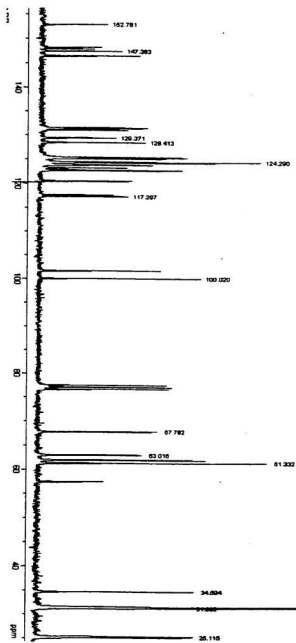
47a R = *tert*-butyl

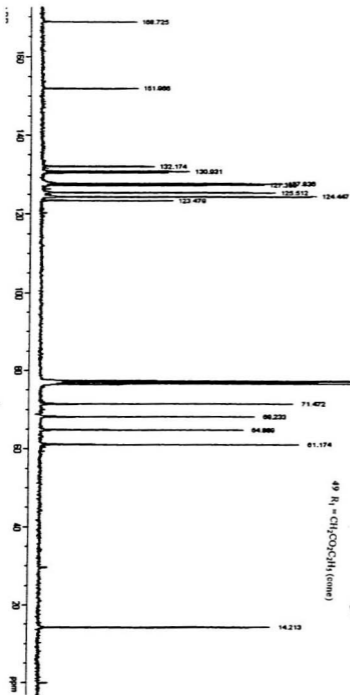




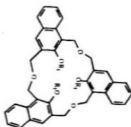


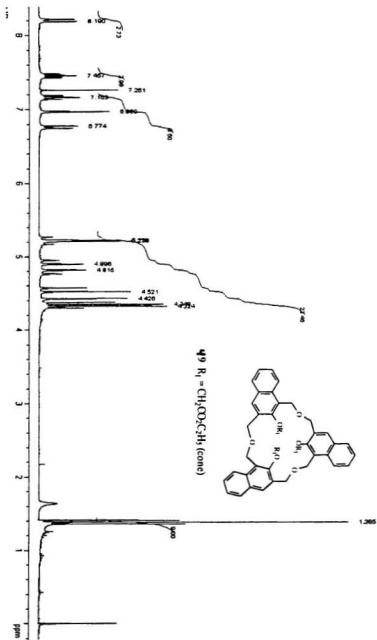


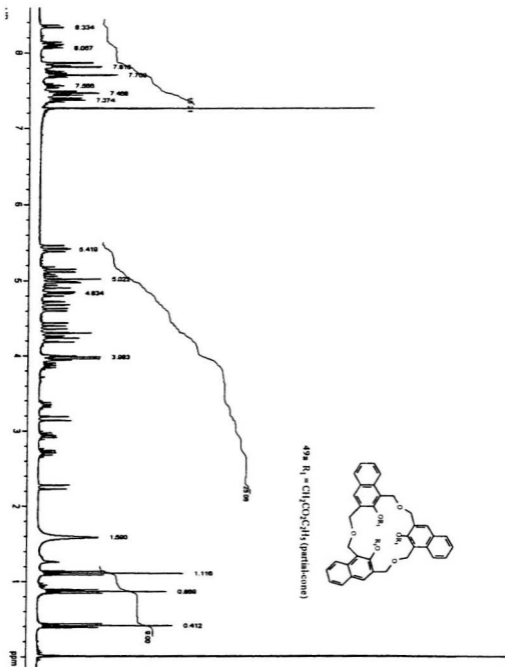


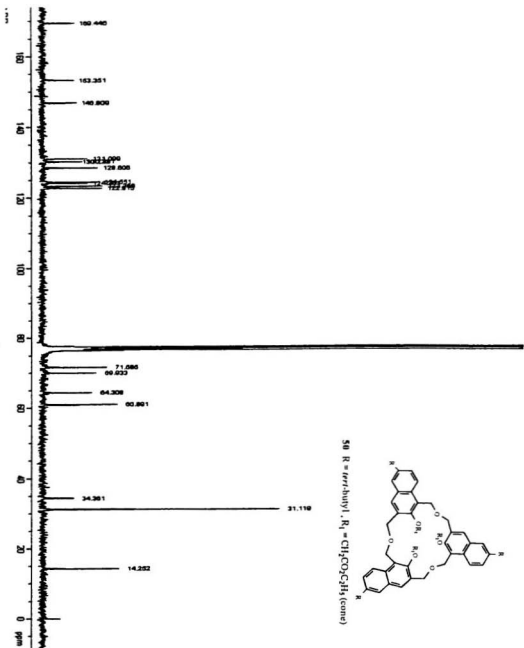


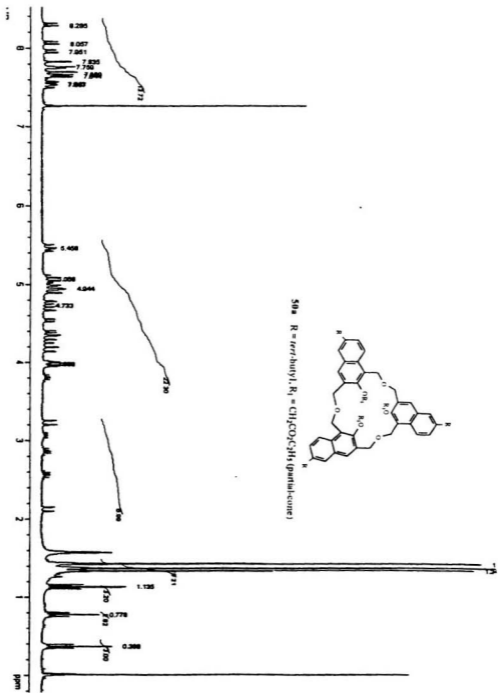
49 $R_1 = \text{CH}_2\text{CO}_2\text{C}_2\text{H}_5$ (cone)

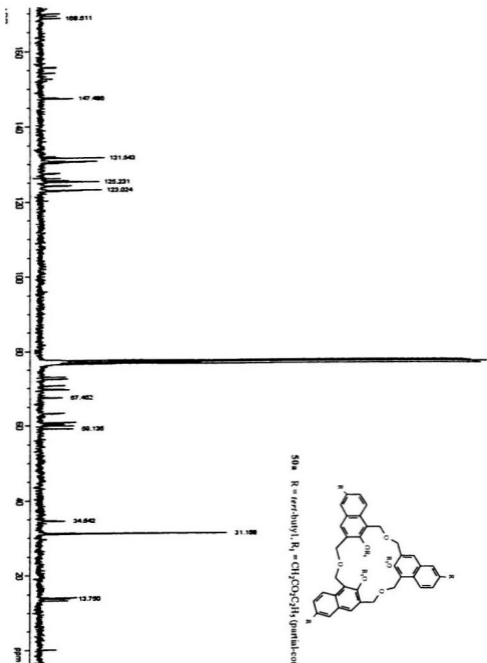












50a R = *tert*-butyl, R₁ = CH₂CO₂C₂H₅ (partial-cone)

